NAVAL POSTGRADUATE SCHOOL

MONTEREY, CALIFORNIA

THESIS

SMART CLIMATOLOGY APPLICATIONS FOR UNDERSEA WARFARE

by

Allon Turek

September 2008

Thesis Advisor: Tom Murphree
Second Reader: Rebecca Stone

Approved for public release; distribution is unlimited.

THIS PAGE INTENTIONALLY LEFT BLANK

REPORT DOCUMENTATION PAGE		Form Approved OMB No. 0704-0188

1. AGENCY USE ONLY *(Leave blank)*	2. REPORT DATE September 2008	3. REPORT TYPE AND DATES COVERED Master's Thesis

4. TITLE AND SUBTITLE Smart Climatology Applications for Undersea Warfare	5. FUNDING NUMBERS
6. AUTHOR(S) Allon G. Turek	
7. PERFORMING ORGANIZATION NAME(S) AND ADDRESS(ES) Naval Postgraduate School Monterey, CA 93943-5000	8. PERFORMING ORGANIZATION REPORT NUMBER
9. SPONSORING /MONITORING AGENCY NAME(S) AND ADDRESS(ES) N/A	10. SPONSORING/MONITORING AGENCY REPORT NUMBER

11. SUPPLEMENTARY NOTES The views expressed in this thesis are those of the author and do not reflect the official policy or position of the Department of Defense or the U.S. Government.

12a. DISTRIBUTION / AVAILABILITY STATEMENT Approved for public release; distribution is unlimited.	12b. DISTRIBUTION CODE

13. ABSTRACT (maximum 200 words)

Undersea warfare operations, especially sound navigation and ranging (SONAR), are sensitive to small changes in the ocean environment. Variations in both atmospheric and oceanic conditions on monthly to decadal scales can have significant impacts on U.S. Navy operations in the undersea environment. Climate databases presently used in U.S. Navy tactical decision aids (TDAs) are based on less than optimal data sets and long term mean (LTM) climatologies that are unable to represent climatic trends or variations. Thus, existing Navy climatologies are likely to provide inadequate representations of the actual dynamic ocean environment. We have used the Naval Postgraduate School smart climatology process, including state-of-the-science atmospheric and oceanic re-analysis data sets, to create smart ocean climatologies. Comparisons of these climatologies with existing Navy climatologies based on the Generalized Digital Environmental Model (GDEM) reveal differences in sonic layer depth (SLD) and sound speed. These differences lead, in turn, to tactically significant differences in the results from Navy TDAs that support undersea warfare.

14. SUBJECT TERMS antisubmarine warfare, climate variations, climatology, GDEM, ocean, re-analysis, smart climatology, SODA, tactical decision aid, undersea warfare, western North Pacific	15. NUMBER OF PAGES 117
	16. PRICE CODE

17. SECURITY CLASSIFICATION OF REPORT	18. SECURITY CLASSIFICATION OF THIS PAGE	19. SECURITY CLASSIFICATION OF ABSTRACT	20. LIMITATION OF ABSTRACT
Unclassified	Unclassified	Unclassified	UU

NSN 7540-01-280-5500

Standard Form 298 (Rev. 8-98)
Prescribed by ANSI Std. Z39.18

THIS PAGE INTENTIONALLY LEFT BLANK

Approved for public release; distribution is unlimited

SMART CLIMATOLOGY APPLICATIONS FOR UNDERSEA WARFARE

Allon G. Turek
Lieutenant Commander, United States Navy
B.S., Maine Maritime Academy, 1996

Submitted in partial fulfillment of the
requirements for the degree of

MASTER OF SCIENCE IN METEOROLOGY AND PHYSICAL OCEANOGRAPHY

from the

NAVAL POSTGRADUATE SCHOOL
SEPTEMBER 2008

Author: Allon Turek

Approved by: Tom Murphree
Thesis Advisor

Rebecca E. Stone
Second Reader

Philip A. Durkee
Chairman, Department of Meteorology

THIS PAGE INTENTIONALLY LEFT BLANK

ABSTRACT

Undersea warfare operations, especially sound navigation and ranging (SONAR), are sensitive to small changes in the ocean environment. Thus, variations in both atmospheric and oceanic conditions on monthly, seasonal, yearly, and decadal scales can have significant impacts on U.S. Navy operations in the undersea environment. Climate databases presently used in U.S. Navy tactical decision aids (TDAs) are based on long term mean (LTM) climatologies that provide a single value representing the average of a 40-year or greater period. These LTM climatologies are unable to represent climatic trends or variations that occur on scales of months to years. Thus, existing Navy climatologies are likely to provide inadequate representations of the actual ocean environment.

We have used the Naval Postgraduate School smart climatology process, including state-of-the-science atmospheric and oceanic re-analysis data sets, to create smart ocean climatologies. Comparisons of existing Navy ocean climatologies based on the Generalized Digital Environmental Model (GDEM) to our smart ocean climatologies reveal a number of differences. The relationships between these differences and physical processes in the ocean, along with the methods used to construct each climatology, indicate that our smart climatologies provide more realistic characterizations of the ocean environment.

The smart ocean climatologies we have produced for the western north Pacific are based on: (a) long term means of re-analysis data; and (b) conditional composites representing ocean variations due to fluctuations in wind forcing of the ocean. The wind fluctuations describe extremes in the timing and intensity of Asian monsoon winds over the western North Pacific in October, during the fall transition. These wind fluctuations lead to variations in temperature, salinity, evaporative cooling, turbulent mixing, Ekman transport, Ekman pumping, and coastal upwelling and downwelling. These variations lead, in turn, to variations in ocean structure and circulation. The dynamically consistency between the wind

forcing fluctuations and the corresponding ocean structure and circulation variations indicates that a smart climatology approach to developing ocean climatologies can lead to significant improvements over existing Navy climatologies in describing the dynamic environment of the actual ocean.

We also compared tactically significant ocean parameters, such as sonic layer depth (SLD) and sound speed, derived from our climatologies and from existing Navy climatologies. These comparisons show significant differences over large regions and within tactically significant sub-regions of the western north Pacific. These differences highlight the ocean variability overlooked by LTM climatologies, and by climatologies based on less than optimal data sets. Finally, we investigated the tactical implications of these differences by forcing Navy TDAs with existing Navy climatologies and our smart climatologies. The resulting outputs from the TDAs support the conclusion that smart climatologies can produce tactically important improvements in climatological support for undersea warfare.

The results of this study indicate that smart ocean climatologies using state-of-the-science data sets and methods offer significant tactical advantages over using present Navy climatologies.

TABLE OF CONTENTS

LIST OF FIGURES

LIST OF TABLES

THIS PAGE INTENTIONALLY LEFT BLANK

LIST OF ACRONYMS

AXBT	Airborne expendable bathythermograph
AVHRR	Advanced very high resolution radiometer
COADS	Comprehensive Ocean-Atmosphere Data Set
CPC	Climate Prediction Center
ECMWF	European Center for Medium-range Weather Forecasts
ENSEMBLES	Ensemble based predictions of climate changes and their impacts
ERA-40	ECMWF re-analysis of the atmosphere
GDEM	Generalized Digital Environmental Model
LTM	Long-term mean
MODAS	Master Ocean Data Assimilations System
MOODS	Master Oceanographic Observation Data Set
NASA	National Aeronautics and Space Administration
NAVO	Naval Oceanographic Office
NCAR	National Center for Atmospheric Research
NCEP	National Centers for Environmental Prediction
NOAA	National Oceanic and Atmospheric Administration
NODC	National Oceanographic Data Center
NOP	Naval Oceanography Program
NWS	National Weather Service
PC-IMAT	Personalized Curriculum for Interactive Multisensor Analysis Training
PHC	Polar Science Center Hydrographic Climatology
POP	Parallel Ocean Program
RAS	Refueling at sea
RMS	Root mean square
SODA	Simple Ocean Data Assimilation
SONAR	Sound navigation and ranging
SST	sea surface temperature
SURTASS	Surveillance towed array sensor system
TAO	Tropical atmosphere-ocean
TDA	Tactical decision aid
TRITON	Triangle Trans-Ocean Buoy Network
UNREP	Underway replenishment
U.S.	United States
USW	Undersea warfare
WESTPAC	western North Pacific
WOA	World Ocean Atlas
WOCE	World Ocean Circulation Experiment
XBT	Expendable bathythermograph

ACKNOWLEDGMENTS

This thesis would not have been possible without the help and support of many individuals. In particular, I would like to thank Dr. Tom Murphree for his patience, thoughtful insights, scholarly advice, and the countless hours of his time spent discussing this project and smart climatology. I owe many thanks to CDR Rebecca Stone, for her thought-provoking questions and comments that consistently improved the final product. I would also like to thank Bruce Ford of Clear Science Inc., for his generosity in providing the SODA and GDEM data sets and advice on programming in MATLAB, Mike Carnes for information on GDEM and the explanation of its development, Mike Cook for answering endless MATLAB questions, and believing that I could learn to program, and all the people who answered the tough PC-IMAT questions including Scott Ferguson, Steve Loveall, Joseph Osborne, and Laurie Gainey.

I also owe a large debt of gratitude to my parents, for always believing in me, and all their children, and to my big sister for instilling in me a love for science and a belief that anything is possible. Finally, I would like to dedicate this work to my wonderful wife Hiroko and our three beautiful children Joshua, Jacob, and Marissa. Thank you from the bottom of my heart for all your love and support, and creating the opportunities for us to accomplish so much together.

I. INTRODUCTION

A. BACKGROUND

The United States (U.S.) Naval Oceanography Program (NOP) mission is to provide naval and joint forces with an increased understanding of the battle space physical environment, in order to drive down uncertainty and achieve a competitive advantage across the full spectrum of naval warfare (Gove, 2008). This mission is especially relevant than in undersea warfare (USW) and particularly in the employment of sound navigation and ranging (SONAR), as the ocean is a medium in which small changes in the environment can have large impacts on sensor performance.

Correctly forecasting the atmosphere and ocean (i.e., getting the atmosphere and ocean right) is another mission of the Navy's oceanographic community. Doing so on time scales of months, seasons, and years is the goal of climate scale analysis and forecasting. Improved forecasts at these lead times could significantly improve long lead planning of operations in undersea warfare and other warfare areas, and lead to greater tactical advantage.

To maximize their tactical advantage, the NOP presently employs ocean climate databases in its USW tactical decision aids (TDAs). The combination of these ocean databases and TDAs allows for characterization of the undersea environment, even when in situ or remote sensing observations are not available. These ocean climatologies also allow for forecasts of the ocean environment, which in turn enable long range operational planning. The problem is that these ocean climatologies are generally long term means (LTMs) based only on relatively limited numbers of in situ temperature and salinity observations. This severely limits the usefulness of these climatologies.

B. TRADITIONAL CLIMATOLOGY AND LONG-TERM MEANS

1. Traditional Climatology

For the purpose of this paper, it is important to briefly discuss climatology and highlight the differences between traditional climatologies and smart climatologies. This section will primarily be concerned with the discussion of the former whilst the discussion of smart climatology occurs in the following section.

Climatology, as defined by the Climate Prediction Center, (CPC) is "The description and scientific study of climate" (CPC 2008). On the other hand, a climatology is defined as "A quantitative description of climate showing the characteristic values of climate variables over a region (CPC 2008)." The first definition refers to the study of climate, and the second refers to a collection of values representing the climate of a region.

Murphree (2008) defines traditional climatology as: "Climatology that focuses on long term means, especially the description of long term mean (LTM) seasonal cycles. Traditional climatology deals little, or not at all, with variations from the long term."

2. Long-Term Mean

A long-term mean, in the context of climatology, refers to the arithmetic average of a variable taken over a period of usually 30 years or more. The long-term mean thus provides a single value that represents the entire period. A problem arises when we attempt to characterize variations from the long-term mean, such as El Nino and La Nina (ENLN) events. These variations are responsible for large fluctuations in atmospheric and oceanic temperature, as well as changes in winds, currents, precipitation, and other variables. As depicted in Figure 1, such variations are not represented by long-term means. Thus, LTM based climatologies cannot account for variations and can lead to problems in long range operational planning in regions and periods in which such variations occur.

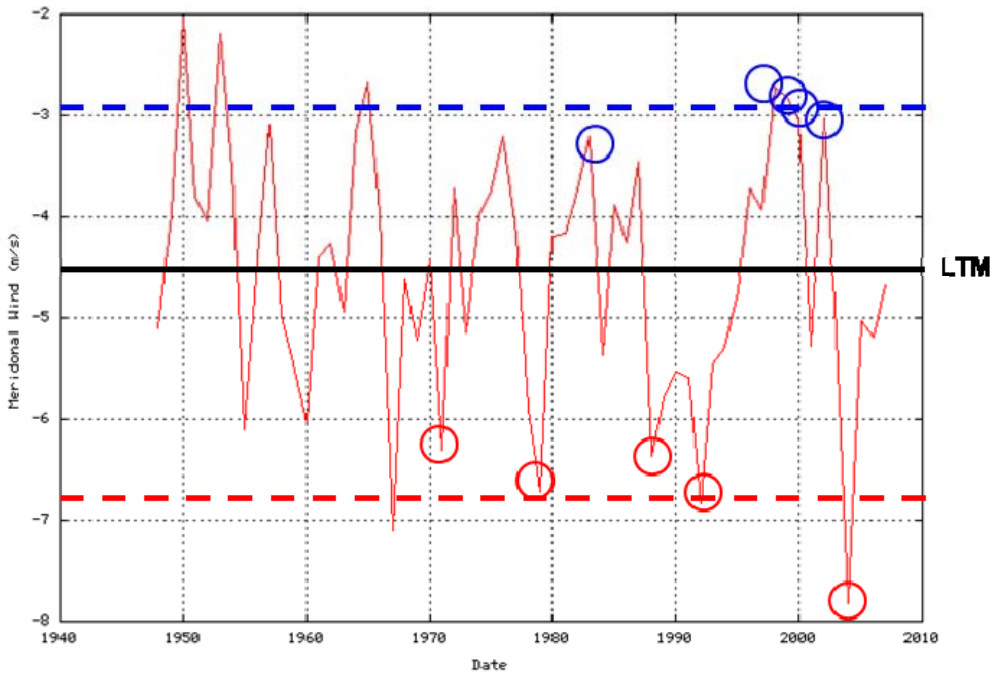

Figure 1. Surface meridional wind speed (m/s) during October of 1948-2007 averaged over the area 20N-28N, 122E-126E of the western North Pacific. Note that all the winds speeds shown are negative, corresponding to the northeasterly monsoon winds typical of this region during October. The highest (lowest) meridional wind speeds are at the bottom (top) of the figure. The red (blue) circles indicate the five Octobers with the highest (lowest) meridional wind speeds during 1970-2007. The horizontal lines delineate the long-term mean for all years shown (bold, black), the mean of the 5 highest wind speed years (dashed, red), and the mean of the 5 lowest wind speed years (dashed, blue). Data from National Centers for Environmental Prediction (NCEP) re-analysis. The high and low wind speeds during 1970-2007 are emphasized because of the relatively large amounts of data, especially satellite, available during this period from which to create the re-analysis fields. Figure created using NOAA/ESRL Physical Sciences Division web site at http://www.cdc.noaa.gov/Timeseries/ (accessed September 2008).

C. SMART CLIMATOLOGY

The preceding section illustrates how long-term mean climatologies obscure important climate variations. Modern or smart climatology is an alternative to traditional climatology that allows these variations to be clearly represented.

Smart climatology is a climatology that uses state-of-the-science data sets and methods to characterize climate system patterns and processes, and to provide operational climate analyses and forecasts (Murphree 2008). So, for example, smart climatology uses re-analysis data sets with high temporal resolution (e.g., individual monthly means from multiple years instead of 30-year long-term monthly means) to describe characteristic climate variations in a region (e.g., the wind speed variations shown in Figure 1), and to relate them to larger scale variations and trends.

A smart climatology approach to providing climatological support is used by the Climate Prediction Center (CPC) and other branches of the National Oceanic and Atmospheric Administration (NOAA). However, this approach is very rarely used by climate support organizations with the US Department of Defense (DoD; e.g., Navy and Air Force organizations) which take a traditional climatological approach in developing almost all of their operational products (Murphree, 2008). However, researchers at the Naval Postgraduate School (NPS) have developed and tested a smart climatology approach for use by DoD in using state of the science climatology data sets and methods for operational support of war fighters (e.g., Ford 2000; Feldmeier 2005; LaJoie 2006; Vorhees 2006; Hanson 2007; Moss 2007; Murphree and Ford 2007; Murphree 2008; Heidt 2008). We will hereafter refer to this approach as the NPS smart climatology process.

The NPS smart climatology process utilizes a systematic and flexible approach for creating and tailoring climate products that enable military decision making. An outline of the smart climatology process is presented in Figure 2. This process has already resulted in the development of several prototype products for the military including: long-range operational forecasts for Iraq (Hanson 2007), long-range operational forecasts for Afghanistan (Moss 2007), impacts of climate variations on military operations in the Horn of Africa (LaJoie 2006), and impacts of global scale climate variations on Southwest Asia (Vorhees 2006). The goal of this thesis is to apply the NPS smart climatology

process to undersea warfare operations, and in so doing provide a more realistic characterization of the ocean environment than is available from a traditional climatology approach.

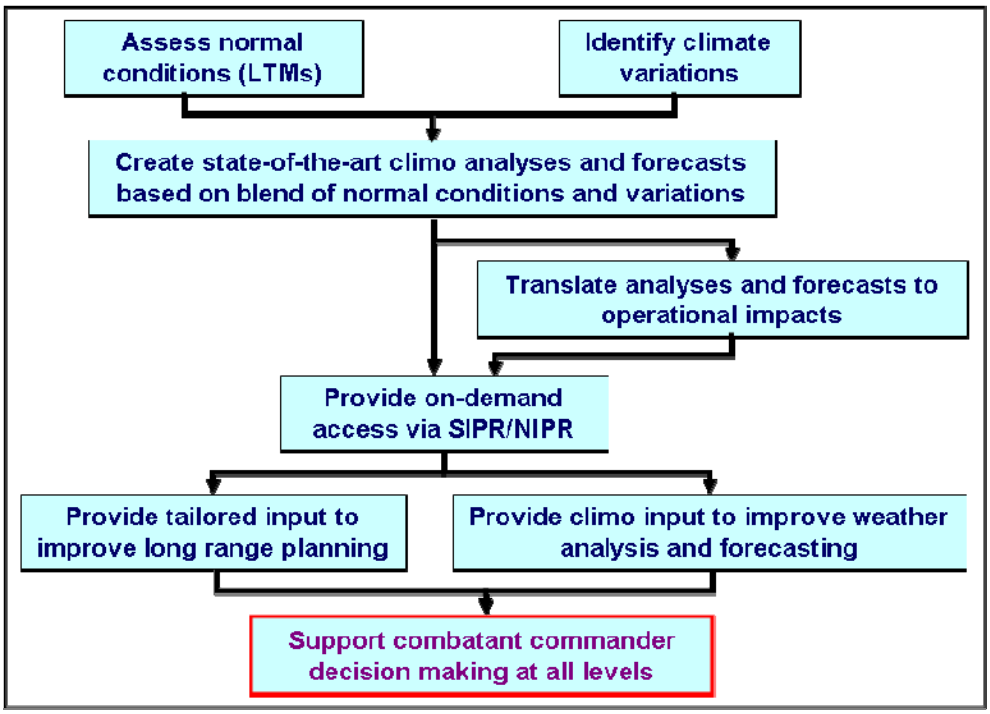

Figure 2. Flow diagram for providing smart climatology support for warfighters. From Murphree (2007a).

D. TACTICAL DECISION AIDS AND CLIMATE DATA SETS

In this study, we tested the hypothesis that the NPS smart climatology process provides a more representative characterization of the ocean environment, and its impacts on undersea warfare operations, than traditional long-term mean climatologies. To do so, we analyzed the differences between ocean structure and outputs from tactical decision aids (TDAs) used in USW when using data from the U.S. Navy's GDEM climatology data set and from the civilian Simple Ocean Data Assimilation (SODA) re-analysis data set.

1. PC-IMAT

The U.S. Navy employs high performance computer software in the form of TDAs to help war fighters involved in USW to visualize and exploit sound propagation within the ocean for tactical advantage. The main TDA used in USW and anti-submarine warfare (ASW) is the U.S. Navy's Personalized Curriculum for Interactive Multisensor Analysis Training (PC-IMAT) software. This TDA uses the Generalized Digital Environmental Model (GDEM) data set as input data to provide climatological descriptions of ocean sound propagation. The resulting descriptions provide long lead tactical outlooks of the ocean environment for use by USW operators and decision makers.

Anecdotal evidence gathered from PC-IMAT users and trainers indicate that predicted acoustic sensor ranges based on GDEM data are excessive. Many users also hold a general belief that the depiction of the environment created by GDEM often does not match in situ observations. In fairness, comparing a long-term mean climatology value to an observed in situ value is not a good practice and will rarely result in an exact match. However, these anecdotal observations regarding the performance of GDEM warrant further investigation, given that war fighters routinely rely on this information for daily operations, and could very possibly be using inaccurate data in a critical situation. Thus, in this study, we also tested the hypothesis that smart climatology can provide more realistic acoustic sensor ranges from PC-IMAT than those available when using GDEM.

2. Climatology for Tactical Decision Aids

a. Traditional Climatology Employed by the Navy

There are many well-regarded and often-used ocean climatologies, such as the NOAA World Ocean Atlas (WOA) (Levitus 1982; Levitus and Boyer 1994), the Hydrobase climatology (Lozier et al. 1995), and the World Ocean Circulation Experiment (WOCE) climatology. The U.S. Navy developed its own

ocean climatology based on the desire for higher horizontal and vertical resolution that was available in most civilian climatologies, as well as to allow for the inclusion of classified temperature and salinity profiles (e.g., those from expendable bathythermograph (XBT) measurements) (Carnes 2003). These desires resulted in the development of the GDEM climatology.

The current version of GDEM (V3.0) is based on temperature and salinity profiles contained in the Modular Ocean Data System (MODAS) climatology, which is derived from in situ temperature and salinity profiles extracted from the Master Oceanographic Observational Data Set (MOODS) in 1995 (Carnes 2003). GDEM has a 0.25 x 0.25 degree grid resolution and contains 78 depths from the surface to 6600 meters (NAVO, 2003). Table 1. provides a detailed description of GDEM properties. Additional information on GDEM properties can be found in Carnes (2003) and Teague, et al. (1990).

Past comparisons of GDEM to in situ observations (Daubin and Hashimoto 1981) and other climatologies (Teague et al. 1990) analyzed older versions of GDEM that are now obsolete. As noted by Carnes (2003), significant changes and improvements occurred in the last two revisions of GDEM since 1994. GDEM V 3.0, the newest version of GDEM and the one used in this study, contains over a million more profiles and has roughly twice the vertical and horizontal resolution of the GDEM versions used in past comparisons of GDEM to in situ observations. Therefore, the comparisons of Duabin and Hashimoto (1981) and Teague et al. (1990) may no longer be relevant, which highlights the need for new comparisons of GDEM to observations and state of the science civilian climatologies.

To compare GDEM to other climatologies it is important to note the methods used to construct the GDEM data set. GDEM uses in situ temperature and salinity profiles to create a gridded global ocean climatology. Like most other climatologies, GDEM faces the challenge of sparse data, both spatially and temporally, in certain areas. To overcome this problem GDEM, uses statistical methods, in particular, minimum curvature interpolation, to fill in spatial and

temporal gaps in the observational data (Carnes 2003). GDEM has a monthly temporal resolution, yet the monthly means are based on three-month averages near the surface and yearly averages at depths from 1000 meters to the bottom. This type of reduction in temporal resolution further obscures climate signals already smoothed by GDEM's long-term mean format.

Table 1. Properties of the GDEM ocean climatology and the SODA ocean re-analysis data set.

	GDEM	SODA
Type:	Ocean Climatology	Ocean Reanalysis
Data Sources:	*Hydrography:* MODAS climatology (based on MODUS dataset)	*Hydrography:* World Ocean Atlas, XBT archive from NODC, Coupled modeling project (NCEP), temperature data from (TOGA) *Satellite Altimetry:* Pathfinder Project2.1 (includes Geosat, ERS/1, TOPEX/Poseidon
Period:	Representing period: 1900-1995	Representing period: 1958-200*
Breakdown:	12 Monthly periods (LTM)	552 monthly averages *(5 day periods available)
Temporal resolution:	* Monthly data is computed from a three month mean centered on analysis month	Individual monthly mean
Interpolation:	Modified Minimum curvature method (using slope minimization and data error minimization and neglecting curvature minimization) Performed at each of 78 levels seperately, then vertical smoothing applied, and static stability	Optimal Interpolation with extensions (including Kalman filter)
Ship Observations:	Classified and unclassified	Unclassified only

GDEM does include estimates of standard deviation of temperature and standard deviation of salinity, thus providing some indication of variability. However, no standard method has been provided to Navy personnel to help them make use of the standard deviation information or assess the impact of the potential error on acoustic propagation predictions. Therefore, we consider GDEM to be an example of a traditional climatology based on long-term means.

b. State of the Science Ocean Re-analysis

Understanding variability in the ocean is dependent on observations of the ocean. Unfortunately, ocean observations are sparse and not uniformly distributed in space or time. One method of resolving this issue is through interpolation, as done by GDEM. Another method, that we feel provides superior results, is to reconstruct a continuous and spatially uniform record of past conditions. This reconstruction is accomplished by integrating observations obtained from numerous data sources together within a numerical prediction model through a process called data assimilation (CCSP 2008). When this data assimilation is done in a consistent manner, using all available observations for multiple years (e.g., 30 years or more), the results are a reconstructed analysis, or re-analysis, data set.

There are a number of well-developed ocean re-analysis projects (see Table 2). The SODA ocean re-analysis is unique in that it provides one of the highest global resolutions (0.5 x 0.5 degrees), for a relatively long temporal scale of nearly 50 years, and for a global domain. SODA also assimilates not only hydrologic data from sources such as the WOA, but also includes ocean data from satellite remote sensing instruments. The assimilation and analysis of diverse data using a dynamic ocean model, allows gaps in observational data to be resolved in a dynamically consistent and relatively realistic manner (cf. Carton and Giese 2008; Carton et al. 2000a, b).

Table 2. Ocean re-analysis project specifications. Green shading indicates resolution finer than 1 degree, global domain, and at least a 30-year period. Table from World Climate Research Program, CLIVAR website, http://www.clivar.org/data/ synthesis/directory.php (accessed July 2008).

Project Name	Sponsors	Vertical	Horizontal Resolution	Domain	Period
BLUELink	BoM, Bureau Australian Navy	47 levels	0.1°x0.1°	Global	1992-2008
CERFACS	Météo France, CERFACS	31 levels	2°x2° (~0.5° meridional at the tropics)	Global	1962-2001
DePreSys	DEFRA	20 levels	1.25°x1.25°	Global	1950-present
ECMWF ORA-S3	ECMWF		1°x1° (equatorial)	Global	1959-2006
ECCO-GODAE (JPL/MIT)	MOPP (NASA, NOAA, NSF)	43 level,	v4: 1°x1° (1/3° equator)	Quasi-global	1992-2001
ECCO_JPL		50 levels	1°x1°	Quasi-global	1993-present
ECCO_NEC	MOPP (NASA, NOAA, NSF)		1°		1992-2002
ECCO2	NASA (JPL)	50 levels	18 x 18 km	Global	1992-present
ENACT	ENACT consort., ENES		1°	Global	1962-2006
ENSEMBLE	ENES/BMBF, UK Met Office	31 levels	1°x1°	Global	1950-2006
ESTOC/GODAE				Quasi-global	
FOAM	Bekish Royal Navy	20 levels	1°x1°	Global	2001-present
GECCO-50 years		23 levels	1°x1°	Quasi-global	1958-2000
GFDL				Global	1960-2006
Global	ENES, UK Met	31 levels	1°x1°	Global	1962-1998
GMAO			1/3° meridional 5/8° zonal	Quasi-global	1993-present
HYCOM				Global	1993-present
IMOW		31 levels	2°x2°	Global	1962-present
K-7	MOST	36 levels	1°x1°	Quasi-global	1993-2000
MERCATOR-2	CNES, IFREMER, Météo FR, IRD SHOM, CNRS,	31 levels	2°x2° (~0.5° meridional at the tropics)	Global	1993-2001
MERCATOR-3	CNES, IFREMER, Météo FR, IRD SHOM, CNRS,	31 levels	2°x2° (~0.5° meridional at the tropics)	Global	1993-2001
MOVE/MRI.COM	JMA		1°	Quasi-global	1949-2005
NCEP/GODAS	NOAA	40 levels	1°x1° (1/3° meridional at the tropics)	Quasi-global	1980-present
POAMA	BoM, CSIRO	27 levels	2°	Global	1980-2006
SODA 2.0.2		27 levels	0.25° (0.25°x0.4° tropics)	Global	1958-2004

E. REGION OF FOCUS

The western North Pacific (WESTPAC), shown in Figure 3, was the focus region for this analysis. There were two reasons for this choice. First, the WESTPAC is a region with large climate variations in both the atmosphere and ocean. The southwest and northeast monsoon wind regimes provided are relatively consistent features of the climate in this region, but they can vary significantly both temporally and spatially. The WESTPAC is a well-researched area with large amounts of in situ ocean observations, particularly along its western boundary. Moreover, the WESTPAC is a region of high tactical and strategic interest to the U.S.

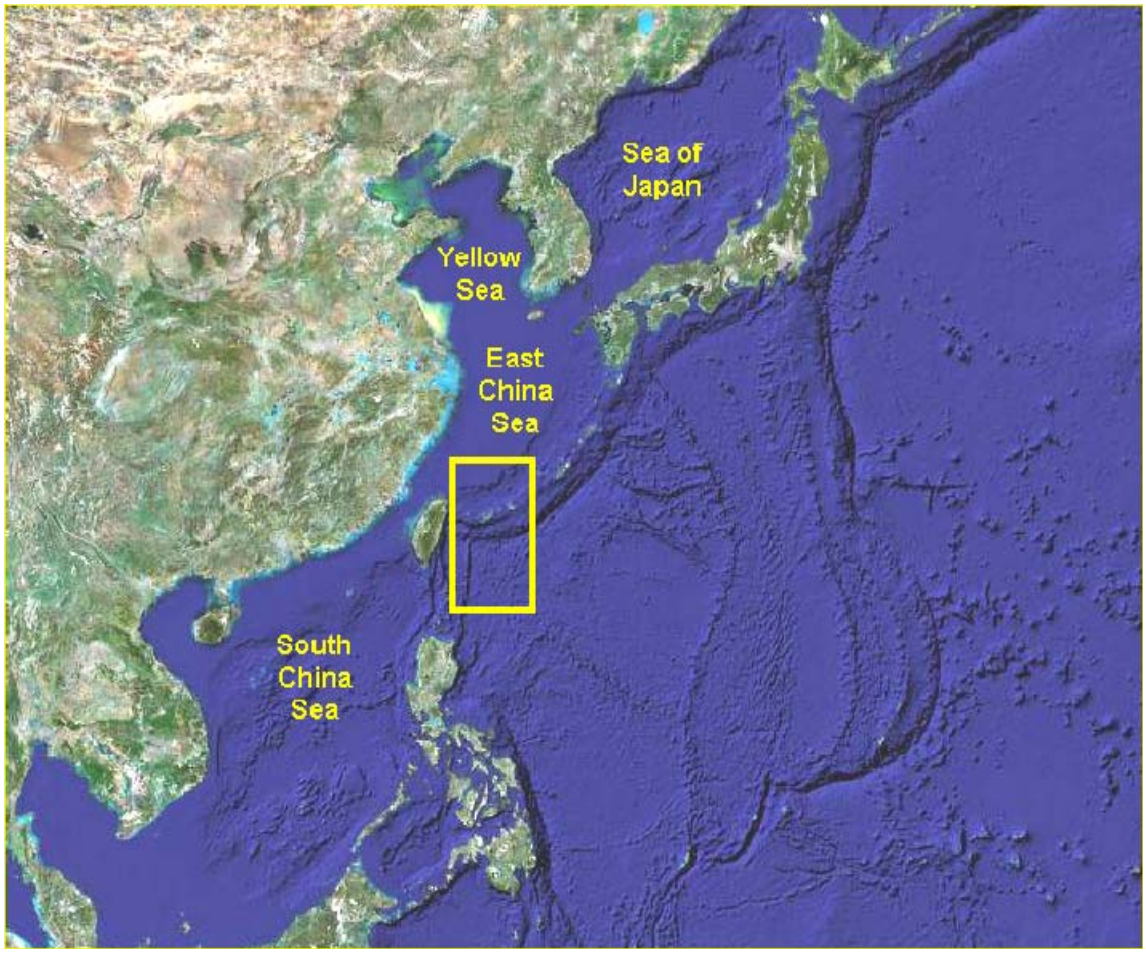

Figure 3. Map of the northern west Pacific including the area 20N-28N, 122E-126E (yellow box) used to construct conditional climatologies. Background map from http://maps.google.com/maps (accessed September 2008).

F. MOTIVATION

> The Navy requires Naval Oceanography to provide a competitive edge in war fighting ability. Commanders require the ability to understand, use, and exploit the changes and structure of the predicted environment just as land forces use terrain to their maximum advantage. (Titley 2008)

These words not only make good sense but also provide the impetus for our research. We believe that the NPS smart climatology process can be applied to ocean re-analysis data sets and provide more realistic characterizations of the ocean environment than existing operational Navy climatologies.

Smart climatology provides the framework, which allows us to turn a request for climatological support into a discrete set of tasks that culminate in a an environmental prediction that supports decision makers. Unlike LTM based climatologies, smart climatologies exploit state-of-the-science data sets (e.g., re-analysis data sets) to obtain the temporal resolution needed to discern variations in the ocean environment. The application of smart climatology analysis and prediction techniques to these variations help indentify predictable patterns and processes in the ocean and atmosphere, leading to improved medium and long-range forecasts (e.g., lead times of one week to one year).

1. Characterization of the Future Environment

Knowledge of the future environment allows commanders and operators to know when and where warfighting advantages exist. These advantages can be defensive or offensive, and based on environmental effects on either friendly or enemy sensors or platforms. Some examples are:

- identifying homogeneous and non-homogeneous water masses within an operating area, which allows smart placement of sensors, such as airborne XBTs (AXBTs) and sea gliders, so that maximum sampling occurs in regions of highest environmental variability
- plotting the future positions of ocean fronts, currents, eddies, and other environmental features so that planners can identify positions

for carrier operating areas (CVOAs), underway replenishment (UNREP) and refueling at sea (RAS) rendezvous points, and ship transit lanes that have favorable environmental conditions and provide a tactical advantages to friendly forces

- using environmental predicted to produce predictions of sensor performance for an area of operations so that commanders can evaluate the best platforms, sensors, positioning, and search methods for maximizing target probability of detection

- creating long range outlooks for specific environmental parameters necessary for optimizing the strategic and tactical placement of platforms, such as SURTASS ships

2. Validation of Short Range Forecasts

Although smart climatology is an excellent approach for creating long range outlooks, it is also very useful in validation of short range forecasts of both atmospheric and ocean models. Sampling of the ocean over large areas is time consuming and costly to conduct. Therefore, it is often difficult to validate the output of an ocean model. Short-range predictions of the ocean environment from a smart ocean climatology offer a quick and inexpensive means of providing a sanity check on ocean model outputs. In situations where in situ sampling is not, possible this may be the only method of preventing large model errors from going undetected.

3. Model Initialization and Boundary Conditions

Atmospheric models rely on initial conditions and boundary conditions to provide the frame of reference for the model's initial calculations. These conditions require countless atmospheric observations that are processed and quality checked. As noted many times already, it is time consuming, costly, and often impractical, if not impossible to sample large areas of the ocean. Environmental data from smart ocean climatologies can provide a quick and inexpensive method for establishing a background state for model initialization.

Recent work by the European ensemble based predictions of climate changes and their impacts (ENSEMBLES) project has shown that assimilation of ocean climate re-analysis data into ECMWF seasonal forecasts significantly reduces root mean square (RMS) forecast error (ENSEMBLES 2008).

II. DATA AND METHODS

A. CLIMATE DATA SETS

The climate data used in this analysis comes from three distinct data sets, one atmospheric and two oceanic. Although our focus is the comparison of the two ocean data sets, the atmospheric climatology facilitates implementation of the NPS smart climatology process and the creation of smart ocean climatologies for comparison to traditional LTM ocean climatologies.

1. Generalized Digital Environmental Model Ocean Climatology

Over 100 years worth of ocean observations are available in the form of various ocean data sets. These data are often stored in condensed and analyzed forms presented as ocean climatologies. Although the amount of data is great, and the number of data sets maintained by various organizations is modest, relatively few ocean climatologies exist. This leaves oceanographers with few choices, especially if high spatial and temporal resolution is needed.

Tactical requirements led the Naval Oceanography Program to create a Navy specific ocean climatology with relatively high horizontal resolution that also included classified ship observations and high resolution bathymetry. The result was GDEM global ocean climatology, which in its most recent version has a 0.25 x 0.25 degree horizontal resolution and 78 vertical levels from 0 - 6600 meters. GDEM provides five gridded variables including temperature, salinity, temperature standard deviation, salinity standard deviation, and bottom depth (NAVO 2003).

The data used in creating GDEM came primarily from the Master Ocean Data Assimilations System (MODAS), but is supplemented by data from the Polar Science Center Hydrographic Climatology (PHC). The 2.7 million temperature and salinity profiles contained in MODAS (see Figure 4) are a small

selection from the nearly 8 million profiles contained in the Navy's Master Oceanographic Observation Data Set (Carnes 2003). The smaller number of profiles included in GDEM is due to a rigorous quality control procedure that excluded anomalous profiles based on range, static stability, erroneous time or location, and duplication (Teague et al., 1990).

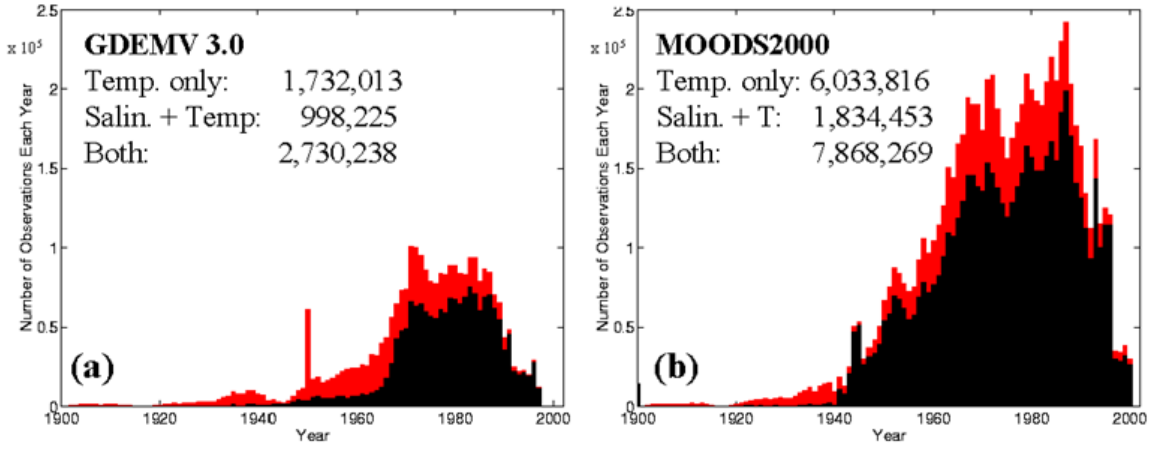

Figure 4. The number of profiles each year in (a) the profile database used to construct the MODAS and GDEM3 climatologies, and (b) the number of profiles in MOODS. Values on the vertical axes are divided by 100,000. From Carnes (2003).

GDEM is based on fitting a non-linear analytical function to the data points for each temperature and salinity profile. Each profile is then represented by the set of coefficients determined in the curve fitting process. By averaging the coefficients of all profiles, for a grid point, GDEM produces an analytical profile representing the mean vertical distributions of temperature or salinity at that location. The model uses three overlapping depth ranges to reduce errors induced by the variations in profile length. The upper layer is from the surface to 200 meters depth. The middle layer is from 200 meters to 1000 meters depth. Finally, the deep layer extends from 1000 meters to the bottom. Each of the three overlapping depth ranges has a separate analytical profile. The three layers are then spliced into a single profile for each grid point, which is then adjusted iteratively to produce a statically stable profile (Carnes 2003).

GDEM uses a modified minimum curvature Interpolation scheme to fill data sparse regions of the global grid. The interpolation scheme fills in missing data by first interpolating each horizontal layer separately, then smoothing to obtain vertical alignment of the data at each grid point. A minimum slope gridding algorithm also prevents interpolation across land boundaries.

The interpolation schemes previously mentioned mitigate the problem of spatially sparse data. However, additional methods are needed to mitigate the temporal gaps in observations. Observational data are most frequent near the surface and become sparser temporally as depth increases. To remedy this problem, GDEM uses annual averages for each grid point in the deep layer, and the average of three months of observations centered on the analysis month at the middle and upper levels (Carnes 2003). Unfortunately, this reduces the temporal resolution of GDEM from the stated value of a monthly LTM to a running seasonal (three-month) mean for the middle and upper levels, and a yearly mean for the deep level.

The use of low-pass filters on the raw data also damps out evidence of climate variations within GDEM. An example is the smoothing of surface temperature fields, using a Martin filter, to remove fluctuations with periods of less than 3 months (Teague et al. 1990).

2. Simple Ocean Data Assimilation Re-analysis

SODA is a 47-year retrospective analysis (re-analysis) of the temperature, salinity, and circulation of the ocean (Carton et al. 2000). This description highlights an important and distinct difference between GDEM and SODA: SODA is an ocean re-analysis, whereas GDEM is an ocean climatology. Our goal was to create smart ocean climatologies using SODA and then compare them with traditional climatologies in the form of GDEM. We present these comparisons in Chapter III.

For this study, we used output from version 1.4.3 of the SODA re-analysis. This output is available at a temporal resolution of five days, and on a global domain with 40 vertical levels from 5 to 5374 meters depth, and at a horizontal resolution ranging from 28 km x 48 km at the equator to 25 km x 25 km in the extratropics. For the purposes of this study, we determined that individual monthly mean data extending from January 1958 through December 2004 and at a horizontal resolution of 0.5 x 0.5 degrees global grid was sufficient. The SODA output variables are temperature, salinity, zonal velocity, meridional velocity, zonal wind stress, meridional wind stress, and sea surface height.

The SODA ocean re-analysis uses a numerical model to provide a first guess of the environment, then at the assimilation update time a set of error estimation equations are used to correct the first guess (Carton and Giese, 2008). The general circulation model used in the SODA re-analysis is based on Parallel Ocean Program (POP) numerics with a displaced pole, which allows resolution of Arctic processes. The model also operates using 1/30 degree bathymetry analysis, and K-profile parameterization for diffusion of momentum, heat, and salt. Information on daily surface winds and freshwater fluxes came from the ECMWF ERA-40 re-analysis and the Global Precipitation Climatology Project, respectively.

Observational data used in SODA is of two basic types: in situ temperature and salinity observations, and remote sensing data from satellites. The approximately 7 million in situ observations (Figure 5) come from a variety of sources, including the World Ocean Database 2001, National Oceanographic Data Center temperature archive, the Tropical Atmosphere-Ocean/Triangle Trans-Ocean Buoy Network (TAO/TRITON) mooring thermistor array, Argo drifting buoys, and ship intake temperatures from the Comprehensive Ocean-Atmosphere Data Set (COADS). The data undergoes a series of quality control filters including location checks, local stability checks, and buddy checks. Additionally, observations are rejected if the value differs from the background by as much as three times the standard deviation of the variable.

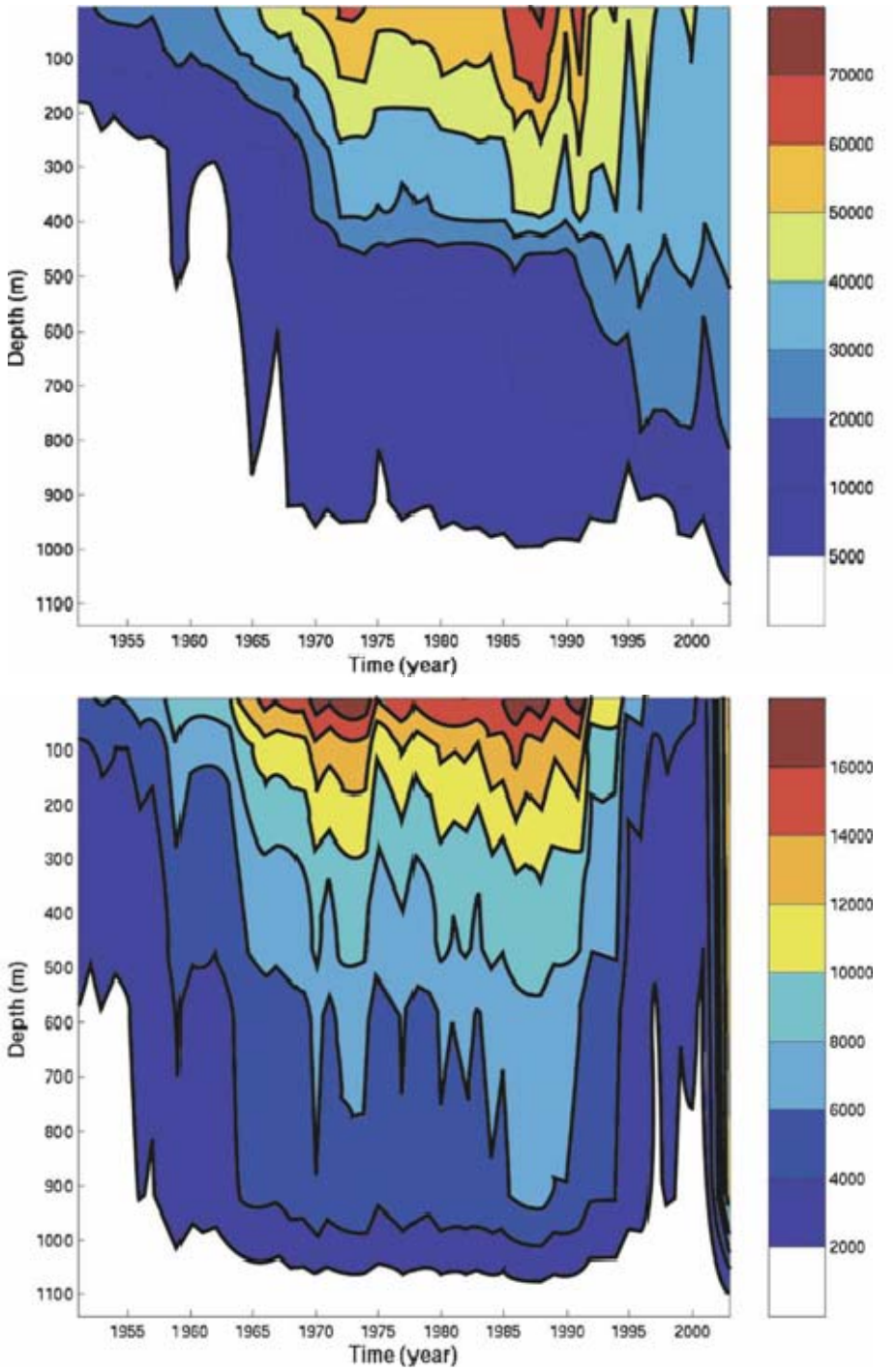

Figure 5. Number of observations used in SODA per year vs. depth for the upper 1000 m of the ocean: (top) temperature; (bottom) salinity used in SODA. Note that the temperature and salinity color scales are different. From Carton and Giese (2008).

Remote sensing data comes from NOAA/National Aeronautics and Space Administration (NASA) Advanced Very High Resolution Radiometer (AVHRR) operational SST data set. Collection of data primarily occurs at night to avoid errors relating to ocean skin temperature on clear calm days. An average of 25,000 samples was collected weekly, starting in 1981. QuikSCAT wind data is used for the 2000-2004 period. Satellite altimetry data is used in more recent versions of SODA (e.g., version 1.4.4) but not in version 1.4.3 that we used for this study.

The primary difference between SODA and GDEM output data is that the SODA data is based on a dynamical ocean re-analysis of temperature, salinity, and other variables, while GDEM is based on interpolated LTMs of temperature and salinity observations. SODA employs complex model dynamics and physics, such as diffusion, advection, fluxes, and wind stresses to create a dynamically balanced depiction of ocean structure and circulation at high temporal resolution (individual monthly means). GDEM uses statistical processing to depict ocean structure at low temporal resolution (long term seasonal means). The spatial resolutions of each are similar (approximately 0.3 degrees for SODA, 0.25 degrees for GDEM).

3. NCEP/NCAR Atmospheric Re-analysis

The construction of our smart ocean climatologies required time series and composite analyses of atmospheric data for our area of interest, in the western North Pacific. For these analyses, we used data from the National Centers for Environmental Prediction (NCEP) atmospheric and sea surface temperature (SST) re-analysis, (Kalnay et al. 1996; Kistler et al. 2001). In particular, we were concerned with surface winds and SST. Data was acquired from the Physical Science Division, Earth System Research Laboratory, National Oceanic and Atmospheric Administration, Boulder, Colorado, from their web site at http://www.esrl.noaa.gov/psd/ (accessed September 2008).

Data was downloaded from the ESRL website in a T62 global Gaussian grid format with 94 x 192 grid points from 88.543°N to 88.543°S, providing roughly 1.9 degree horizontal resolution. Vector wind and SST data were then processed using MATLAB (Mathworks 2005) to form composite mean and composite anomaly maps for our western North Pacific region of interest. Initial investigations of the data were also conducted using the ESRL time series website at http://www.esrl.noaa.gov/ psd/timeseries (accessed September 2008).

4. Study Period

SODA reanalysis output data was available for this study for 1958-2004, and NCEP re-analysis data is available for 1948-2007. Our study period needed to fit within the overlap between these periods, 1958-2004. However, significant amounts of satellite data for these re-analyses were only available starting in the 1970s. To maximize the positive impacts of satellite data, and to work with at least several decades of re-analyses output data, we chose a study period of 1970-2004. This 35-year period allowed us to capture intraseasonal to interannual climate variations, including, for example, a relatively even mix of El Nino and La Nina years as well as some representation of decadal variations (cf. Ford 2000; Vorhees 2006).

B. METHODS OF ANALYSIS

1. Application of NPS Smart Climatology Process

The goal of this study was to determine if the NPS smart climatology process could improve support of USW operations in the western North Pacific (WESTPAC). We answered this question by comparing depictions of the ocean and of sonar performance derived from state-of-the-science smart ocean climatologies to those from existing Navy climatologies.

Developed with military knowledge and experience, the NPS smart climatology process (Figure 6), lends itself to tactical applications. Feldmeier (2005) demonstrated how smart climatology could provide a more representative characterization of the actual ocean environment than traditional climatology. The results from Feldmeier's ocean smart climatology work also showed the potential tactical implications for naval operations. Additional results from LaJoie (2006), Vorhees (2006), Moss (2007), Montgomery (2008) and others support this conclusion.

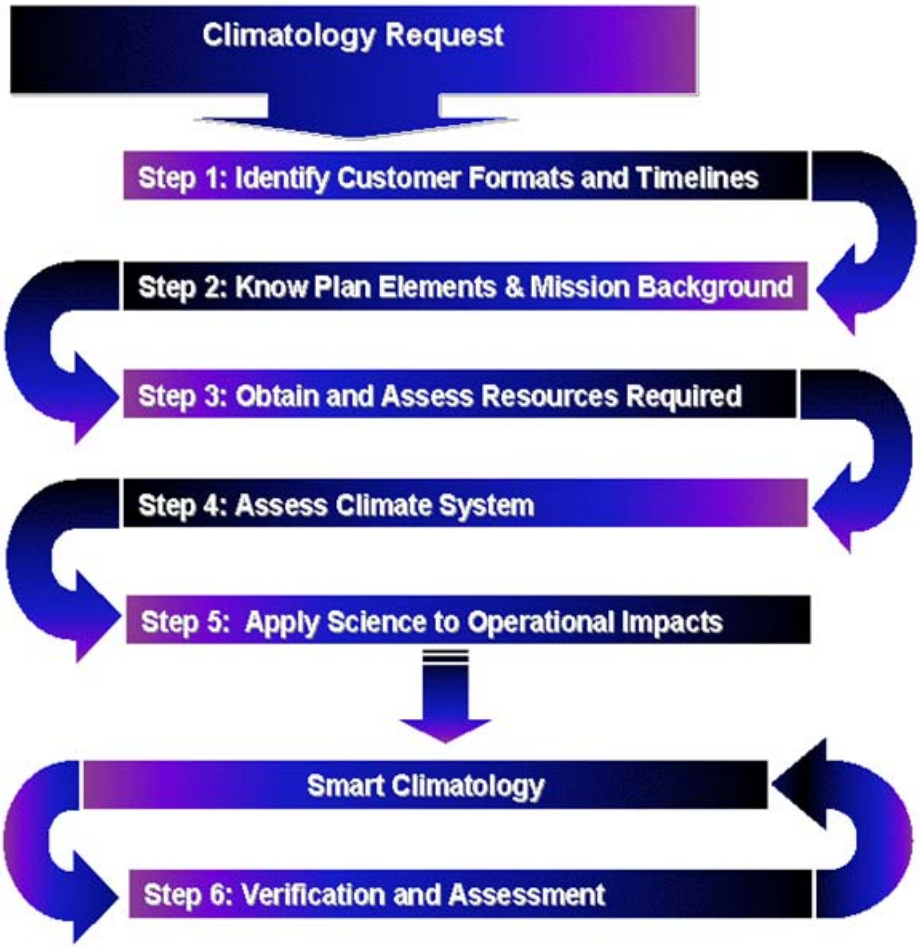

Figure 6. Naval Postgraduate School smart climatology process flow diagram showing the main steps in the process. From LaJoie (2006).

Our study applies the smart climatology process by first assuming the climatology request is mandated by the goals and intentions as delineated in by Gove (2008). For our study, step 1 was completed by assuming a USW customer needed climate scale information on ocean structure, sound speed, and sonar performance at intraseasonal or longer lead times in the format of existing environmental support products (e.g., map displays of SLD, PC-IMAT predictions). Step 2 was completed by assuming long lead planning of all the major elements of USW (e.g., general uses of active and passive sonar). Step 3 required the collection of all necessary data from GDEM, SODA, and the NCEP atmospheric re-analysis, as well as ensuring the availability and applicability of software such as MATLAB, PC-IMAT, and tools on the ESRL website. Steps 4 through 6 are more complicated and require a more detailed explanation. Subsections 2 through 7 of this section provide additional details on these steps in the smart climatology process.

2. Time Series Analysis

Assessing the climate system is step 4 of the smart climatology process. Our assessment of the climate system centered on ocean variability and atmospheric parameters that may force this variability. Because of the strong variations in our study region and study period (see Figure 1), we investigated the effects of wind speed variations on ocean structure, circulation, sound speed, and sonar performance.

A review of long-term mean winds and wind variations in our study area revealed that meridional winds had greater variability, and potentially greater predictability, than zonal winds. This is due in large part to the dominant wind patterns of the southwesterly and northeasterly monsoon wind regimes. The highest wind speeds existed in the area around Taiwan, indicating a high potential for large variations in wind speeds impacts on the upper ocean. Consequently, we chose an area east of Taiwan that possessed both climatological and tactical significance. This box is enclosed by the lines 20N,

28N, 122E, and 126E, as shown in Figure 3. We then created a time series, of meridional wind for the study period. 1970-2004, using the web based climatology analysis tools at: http://www.cdc.noaa.gov/Timeseries/ (accessed September 2008). From this time series, we identified the five years of highest meridional wind speed and the 5 years of lowest meridional wind speed during 1970-2004 (Table 3.)

5 highest wind years	
year	**speed (m/s)**
1971	-6.31
1979	-6.72
1988	-6.37
1992	-6.83
2004	-7.81

5 lowest wind years	
year	**speed (m/s)**
1983	-3.20
1987	-3.46
1998	-2.72
1999	-2.82
2000	-3.04

Table 3. Years of highest and lowest meridional surface wind speed in October during 1970-2004 averaged over area east of Taiwan (box enclosed by 20N-28N, 122E-126E, shown in Figure 3). Negative values indicate northerly (i.e., southward) winds.

3. Conditional Climatologies

Results from the meridional wind time series provided the years used to create our conditional composites. We extracted data from the SODA re-analysis based on the five years of highest wind speed and the five years of lowest wind speed. We then compiled the data for each conditional composite and calculated the mean, which resulted in a conditional climatology for the five lowest and five highest wind years. These high and low wind conditional climatologies were computed for surface winds and a number of oceanic variables.

4. Analysis of Anomalies

We used the high and low wind conditional climatologies to compute atmospheric and oceanic composite anomaly fields. An anomaly as defined by the CPC (2008) as, “the deviation of a measurable unit, (e.g., temperature or

precipitation) in a given region over a specified period from the long-term average, often the thirty year mean, for the same region." We calculated climate anomalies subtracted the long-term mean values of each variable of interest (e.g., LTM ocean temperature at 5 m depth) from the conditional composite mean values of that variable (e.g., high wind ocean temperature at 5 m depth). The LTM values were computed using a base period of 1970-2004. The benefit of an anomaly field is that it highlights climate variations and the dynamical processes that create those variations. By clarifying those variations and processes, anomaly analyses improves the analysis and prediction of the climate system.

We created anomaly fields of vector winds, SST, subsurface temperature and salinity, sound speed, and sonic layer depths to help explore the atmospheric and oceanic patterns and processes that characterize high and low wind periods, and the tactical significance of these patterns and processes. We also created anomaly maps of ocean temperature at various levels in the ocean to identify areas of large differences as well as the patterns and processes associated with these differences. Chapter III contains the detailed results of our anomaly analyses.

5. Comparisons of Climatologies

We compared GDEM LTM climatologies of temperature, salinity, and sound speed to SODA LTM climatologies and SODA conditional climatologies.. We first explored the similarities and differences between the SODA and GDEM LTM climatologies by analyzing maps of temperature at various levels, as well as ocean vertical cross sections and profiles, and maps of derived variables such as sonic layer depth. To facilitate a better comparison, we compared SODA and GDEM on the same grid resolution of 0.5 x 0.5 degrees. Although this reduced the resolution of GDEM, our focus was on the differences between variables at the same grid point and not small scale horizontal features in ocean structure.

6. Extraction of T/S and Sound Speed Profiles

Calculating and plotting the differences between smart and LTM climatologies were rather straightforward and demonstrated that the differences were often substantial (e.g., fifty percent differences in SLD). Determining the tactical significance of our results required further processing of the data. We therefore computed profiles of temperature, salinity, and sound speed for GDEM LTM, SODA LTM, and the SODA high and low wind conditional composites. This part of our analysis is the beginning of step 5 of the NPS smart climatology process (Figure 6), application of climate science to operational impacts.

The anomaly maps helped us to identify grid points at which differences between climatologies were substantial. At these grid points, we extracted profiles from each climatology and plotted them together for comparative analysis. Values of sound speed at each depth and for each climatology, were saved for later use in analyzing environmental impacts on acoustic performance.

7. Analysis of the Impacts of Different Climatologies on Sonar Performance

The final step of our analysis involved computing sonar propagation loss based on oceanic sound speeds from each climatology. We selected five environmentally and tactically significant locations from our larger area of interest in the western North Pacific and used the Navy tactical decision aid, PC-IMAT, to produce propagation loss computations and graphics.

Sound speed profiles were generated in MATLAB using depth, temperature, and salinity data from each of the climatologies. We chose to compute sound speed using the nine-term Mackenzie equation (Mackenzie 1981), because of its simplicity compared to the other more complex equations such as the Del Grosso and Mader equation (Del Grosso 1974) and the Chen and Millero equation (Chen and Millero 1977). The Mackenzie equation is actually a simplification of the Del Grosso and Mader equation. For our sonar analyses, we computed sound speed for a single location instead of over a long

distance. Thus, errors using the nine-term Mackenzie equation should be minimal. For each grid point at which we computed propagation loss, we assumed a homogeneous ocean based on the temperature, salinity, and depth at the grid point obtained from each climatology.

The user interface of PC-IMAT is structured such that all sound speed profiles had to be entered by hand. To reduce data entry time, the depth range for the different sound speed profiles that we used 5-500 m. For each location with deeper depths, PC-IMAT was used to merge to the 5-500 m profiles a LTM GDEM climatological profile for depths greater than 500 m. This merging of profiles had no noticeable impact on sound propagation in numerous tests, probably due to the small differences in temperature between the climatologies at depths greater than 500 m. The results of our propagation loss comparisons are presented in Chapter III.

THIS PAGE INTENTIONALLY LEFT BLANK

III. RESULTS

A. COMPARISONS AND ASSESSMENTS OF LTM CLIMATOLOGIES

1. Patterns in the WESTPAC Region

The LTM climatologies of both SODA and GDEM have similar general patterns that are representative of the actual environment. For example, they are both warm in the tropics and cool in the extratropics, and generally depict similar temperature gradients from south to north. The depiction of SST gradients across the western boundary currents is also similar in both SODA and GDEM LTM climatologies (see for example Figure 7).

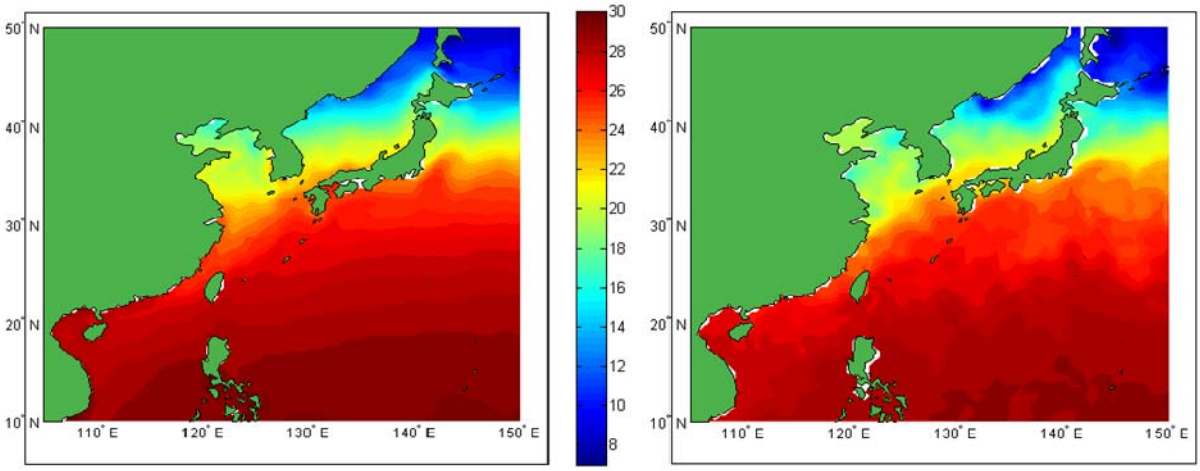

Figure 7. Long term mean sea surface temperature (SST, deg C) for October for: (left) SODA, (right) GDEM.

The similarities between GDEM and SODA LTM climatologies are evident not only in sea surface temperature (SST), but in ocean temperature at a variety of depths (Figure 8). Regional characteristics, such as cooler temperatures in the Yellow Sea, and the strong north-south temperature gradients in the Sea of Japan are also captured by both climatologies. Even the subsurface (70m) pool of relatively cooler water located in the South China Sea, off the coast of Vietnam, can be seen in both SODA and GDEM (Figure 8).

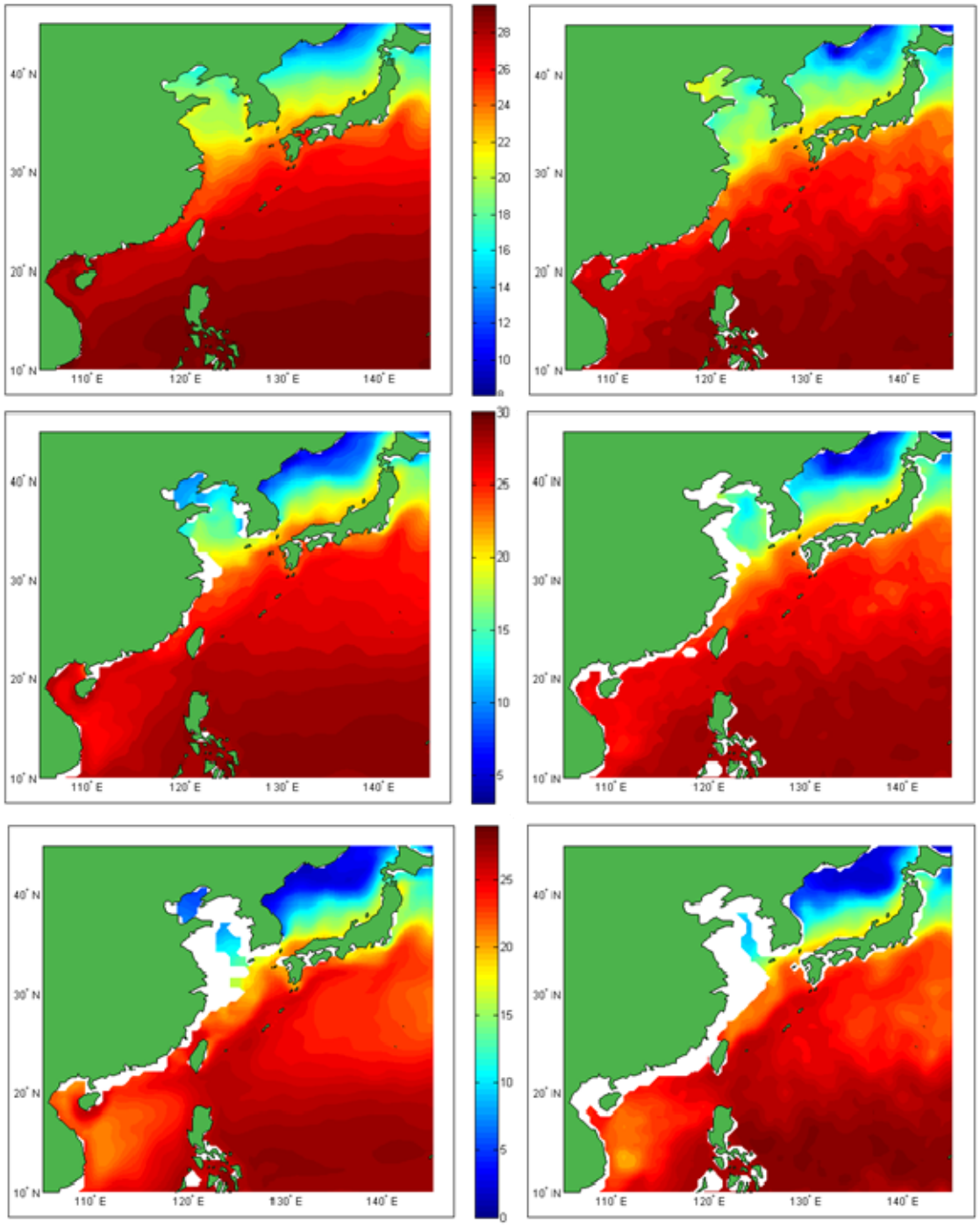

Figure 8. Long term mean ocean temperature (deg C) for October for: (top, left) SODA at 5 m, (top, right) GDEM at 5 m, (middle, left) SODA at 35 m, (middle, right) GDEM at 35 m, (bottom, left) SODA at 70 m, (bottom, right) GDEM at 70m.

However, there are also important differences between the LTM climatologies of GDEM and SODA. Most significant are: (1) the generally cooler temperatures in GDEM, especially near the surface (e.g., upper 50 m); and (2) the relatively high degree of small scale structure in temperature and salinity in GDEM compared to SODA (see Figure 8, note the large undulations in temperature contours in GDEM). The small scale structures in GDEM may appear to be indicative of small scale variability in the environment. However, this explanation seems implausible given that GDEM is a LTM climatology with a representing data from over 50 years. Small scale variability would tend to be smoothed out by LTM averaging, especially in deep water where topographic forcing is weak but where GDEM small scale structure is most pronounced. It is more likely that these undulations are artifacts of the interpolation process used by GDEM to fill in missing profiles in data sparse locations.

Maps of sonic layer depth (SLD) for the LTMs of both SODA and GDEM (see Figure 9) also show significant differences between the two climatologies. For SLD, the small scale structures in GDEM appear as bull's eye patterns. SLD is the depth of maximum sound speed in the near surface waters. Since sound speed has a large dependence on temperature, it is not surprising that irregularities in the GDEM temperature fields are manifest in maps of SLD. It is important to note that the overall patterns of SLD are similar in both SODA and GDEM, but GDEM clearly tends to have has deeper SLD values than SODA, particularly east of the Philippines (Figure 9).

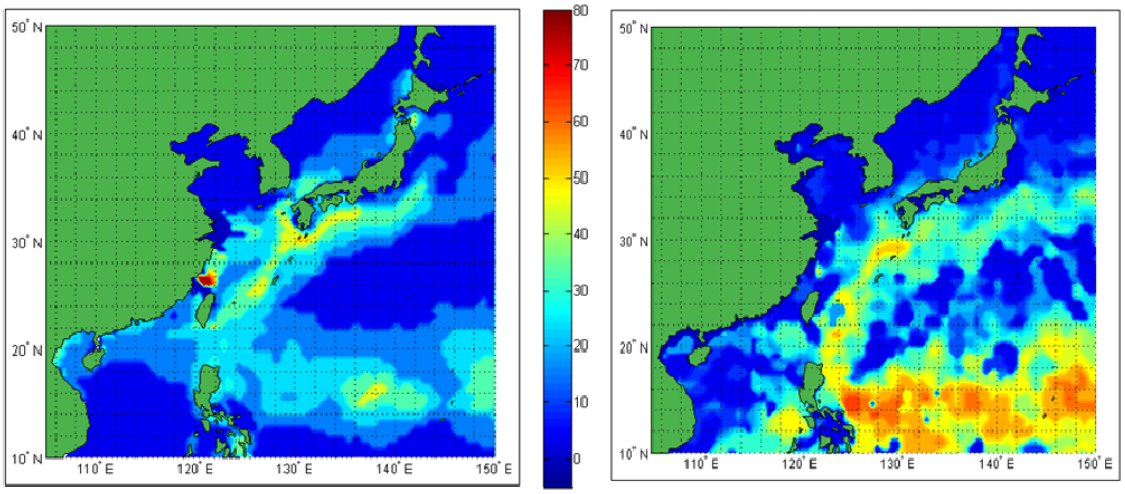

Figure 9. LTM sonic layer depth (m) for October for: (left) SODA, (right) GDEM.

2. Patterns in WESTPAC Sub-regions

As we shift our focus to sub-regions of the WESTPAC and examine the GDEM and SODA LTM climatologies in more detail, the differences between these climatologies become more apparent. On sub-regional scales, large variability is often associated with strong temperature gradients, especially perpendicular to strong western boundary currents, such as the Kuroshio (Figure 10).

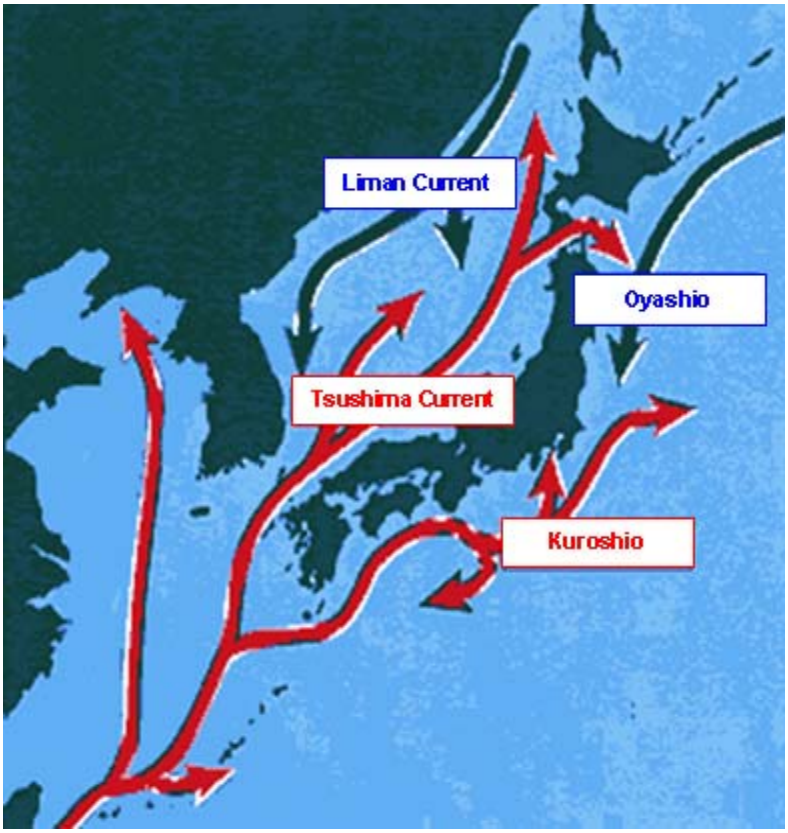

Figure 10. Currents of the western North Pacific: (red) southerly warm currents, and (black) northerly cold currents. Image from Japan Agency for the Marine-Earth Science and Technology website: http://www.jamstec.go.jp/jamstec-e/earth/p2/p2-1.html accessed September 2008.

SODA and GDEM LTM climatologies both depict a large number of the significant small scale features, including strong temperature gradients associated with the major currents and the polar front that marks the division between warm and cold water masses (Figure 11). Looking more closely at the Kuroshio where it separates from the east coast of Japan, we observe that there are small but distinct differences in how GDEM and SODA represent this current. SODA depicts a strong temperature gradient parallel to the coast until the current abruptly separates from land and turns eastward. At this point, the Kuroshio develops a zonal wave like pattern with a pronounced ridge and trough at about 35N (Figure 11). GDEM depicts a weaker gradient that separates from the coast

at an oblique angle and extends eastward with only a slight hint of the zonal wave pattern shown by SODA (Figure 11) and described by Tomczak and Godfrey (1994; Figure 12).

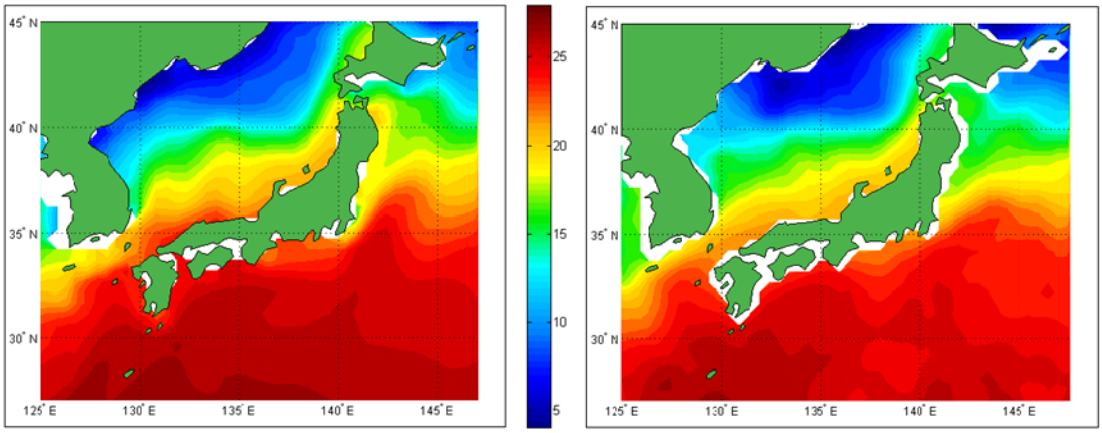

Figure 11. LTM ocean temperature (deg C) for October at 35 m for: (left) SODA; and (right) GDEM.

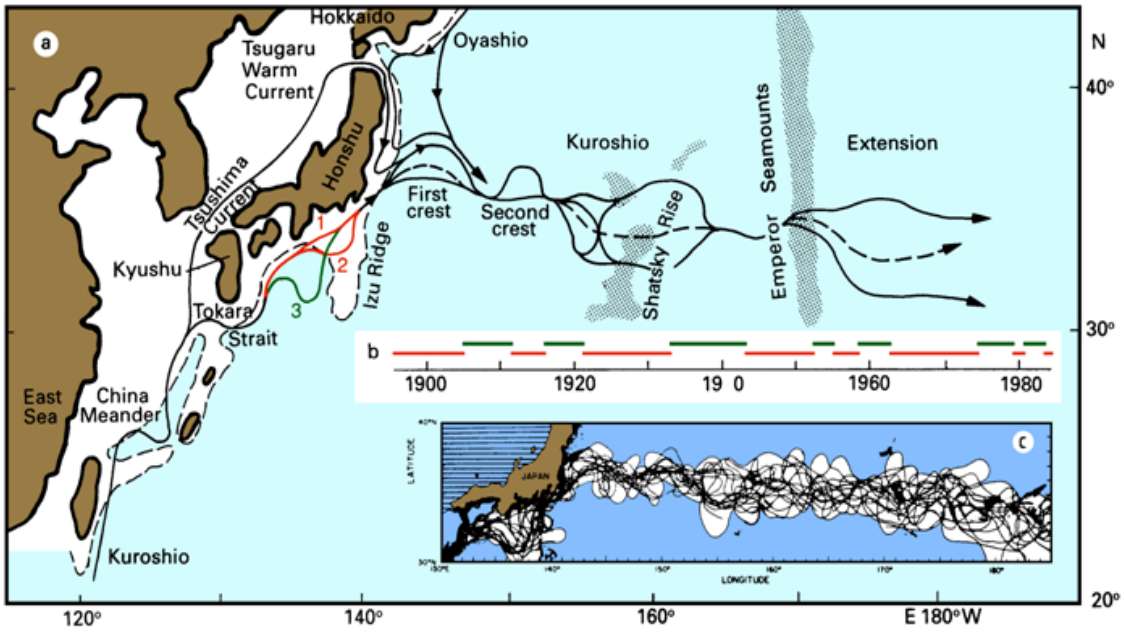

Figure 12. Schematic depictions of the Kuroshio and Oyashio. From Tomczak and Godfrey (1994).

These results suggest that SODA may provide a more realistic depiction of the Kuroshio than GDEM. If so, this be because SODA assimilates satellite SST data, which supplements its hydrographic data. Vertical cross-sections, of SODA and GDEM LTM ocean temperature show that SODA has more pronounced vertical and horizontal gradients in the Kuroshio region (Figure 13 and Figure 14). Thus, the LTM Kuroshio for October that can be inferred from ocean temperature structure is stronger and more sharply defined in SODA than GDEM.

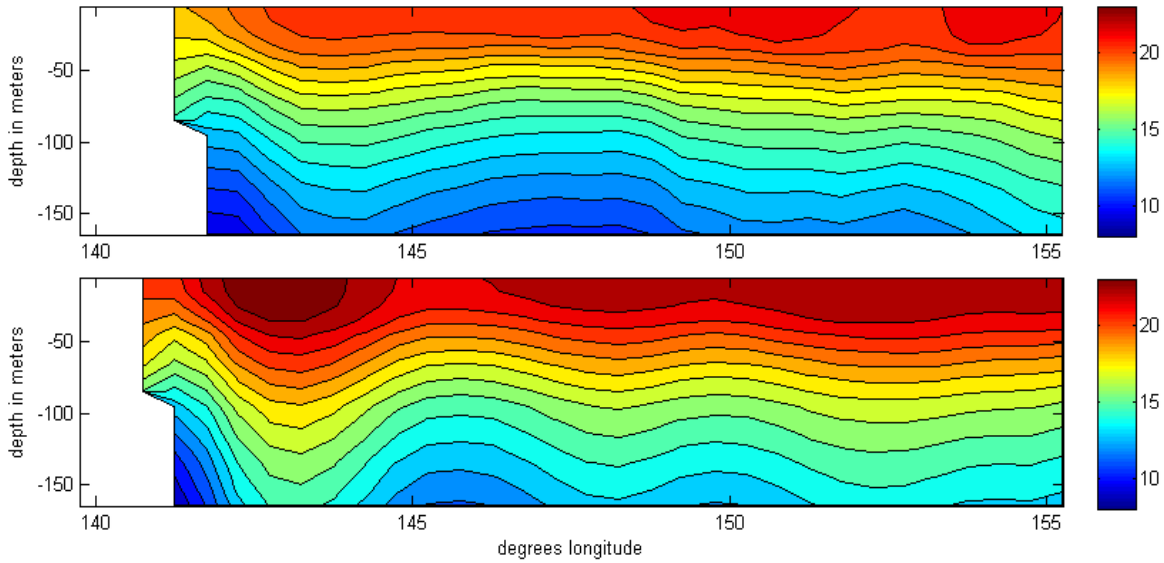

Figure 13. Vertical cross section of ocean temperature (deg C) in October for: (top) GDEM LTM, (bottom) SODA LTM. Cross section taken across Kuroshio east of Tokyo, Japan, along 36.75N, 139.75E-155.25E.

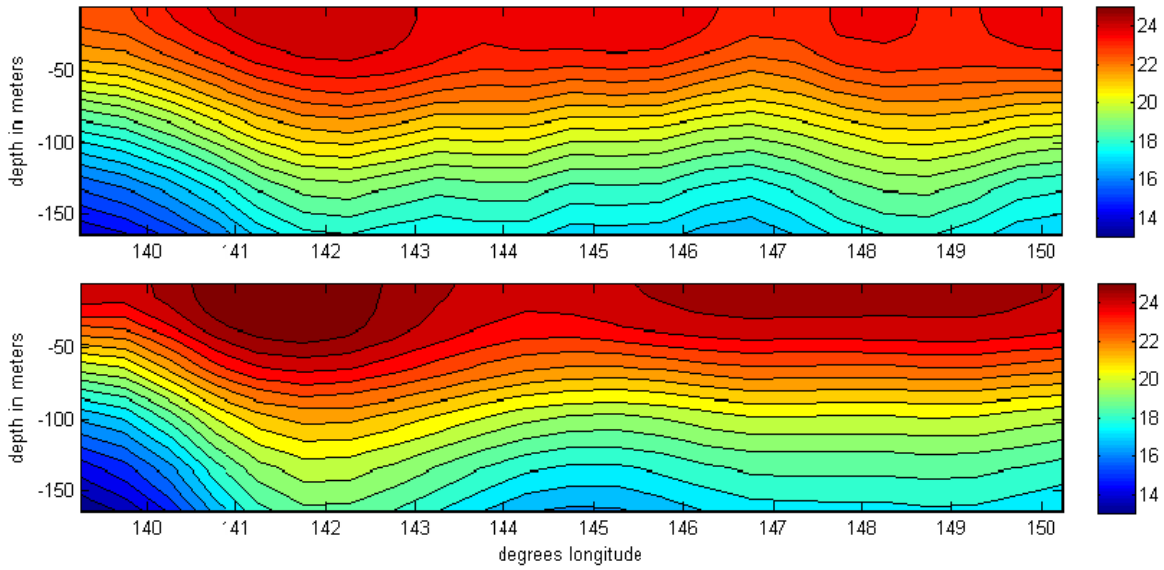

Figure 14. Vertical cross section of ocean temperature (deg C) in October for: (top) GDEM LTM, (bottom) SODA LTM. Cross section taken across Kuroshio east of Tokyo, Japan, along 34.25N, 139.25E-150.25E.

Another good point of comparison is the central Sea of Japan where an oceanic front separates the warm water mass flowing in from the Tsushima Strait along the eastern boundary and the cold water mass flowing south from the Sea of Okhotsk along the western boundary (Figure 10). The position of the front both vertically and horizontally appears to be very similar in both the SODA and GDEM LTM climatologies (Figure 15). The SODA and GDEM thermal gradients along the frontal boundary are also similar. This similarity in such a complex and dynamic environment is may be due to the high number of observations in this region available for use in both SODA and GDEM.

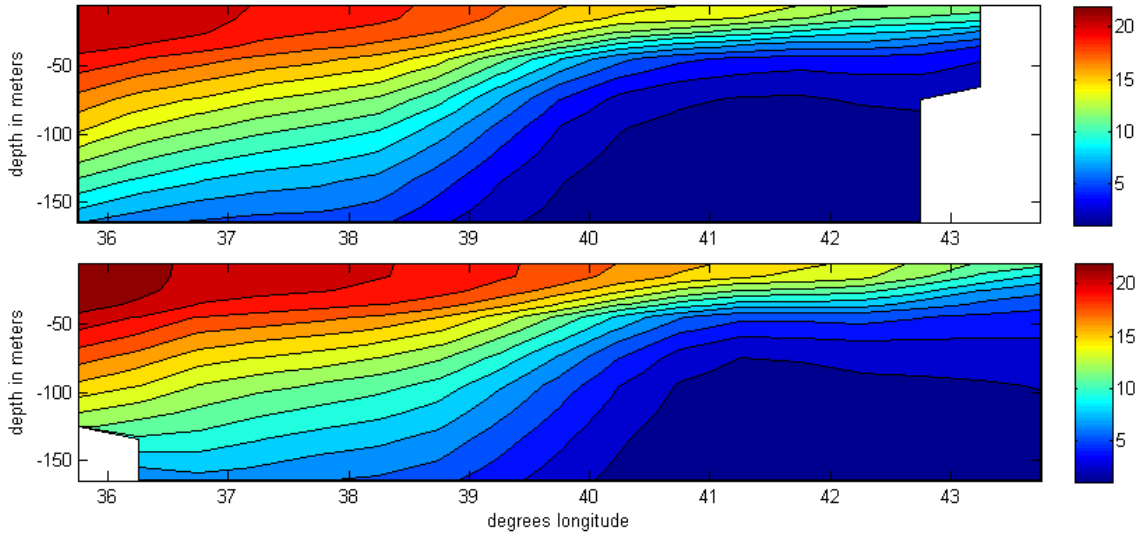

Figure 15. Vertical cross section of ocean temperature (deg C) in October for: (top) GDEM LTM, (bottom) SODA LTM. Cross section taken across the central Sea of Japan, along 135.25N, 35.75E-43.75E.

There are however cases when the SODA and GDEM LTM climatologies disagree. Maps of SLD, a tactically significant ocean parameter, shown in Figure 16 provide a good example of this disagreement. The smooth contours and relatively weak gradients in the SODA SLD map are what we would expect from a LTM mean climatology. The SLD map for GDEM, however, reveals sharp gradients and small isolated areas representing large SLD differences that appear as bull's eyes. It is unlikely that these locations represent actual environmental features, as natural variation in the environment would obscure such features through the averaging process inherent in a LTM.

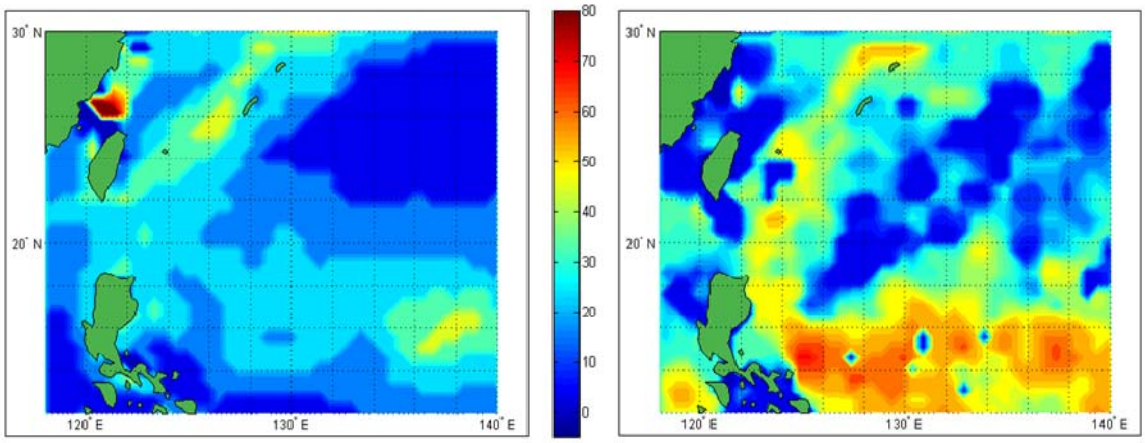

Figure 16. October LTM sonic layer depth (m) for: (left) SODA LTM; (right) GDEM

B. SODA UNIQUE FIELDS

The SODA output fields include several that are not available from GDEM. These include sea surface heights and ocean currents (Figure 17 and Figure 18). Sea surface heights have a wide range of applications and are of particular value in ocean climatology. Sea surface heights are useful in inferring upper ocean thermal energy content, temperature structure, and currents. Such information has tactical applications in undersea warfare. Other applications for sea surface height include tropical cyclone forecasting, climate forecasting, fisheries management, marine mammal research, and spill tracking (JPL, 2008).

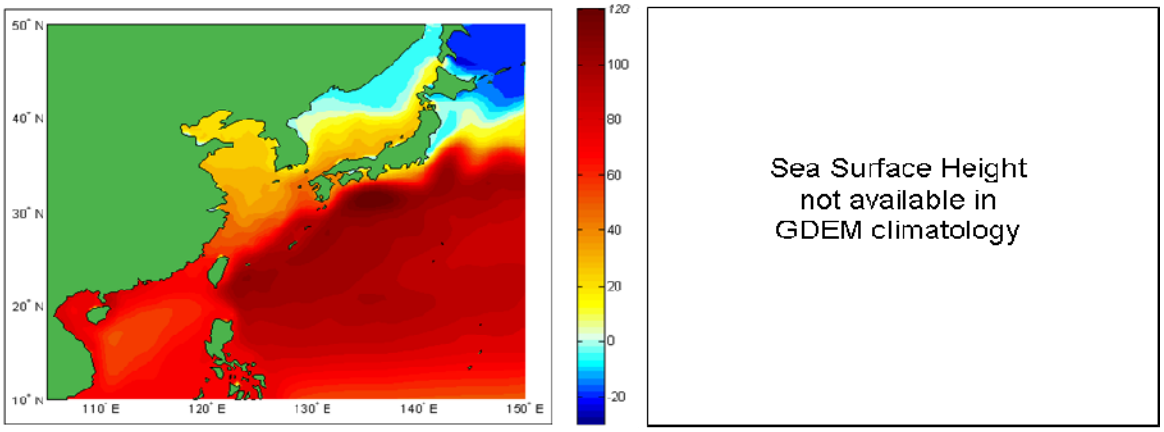

Figure 17. LTM sea surface heights (cm) for October for: (left) SODA; (right) GDEM.

Tomczak and Godfrey (1994) observed that seasonal wind variations in the western North Pacific are in phase with the Kuroshio Current flow, suggesting that a major portion of the Kuroshio mass transport is generated by wind forcing over and near the Kuroshio. This is consistent with one of the hypotheses for this study that variations in wind speed directly affect the ocean's structure and circulation.

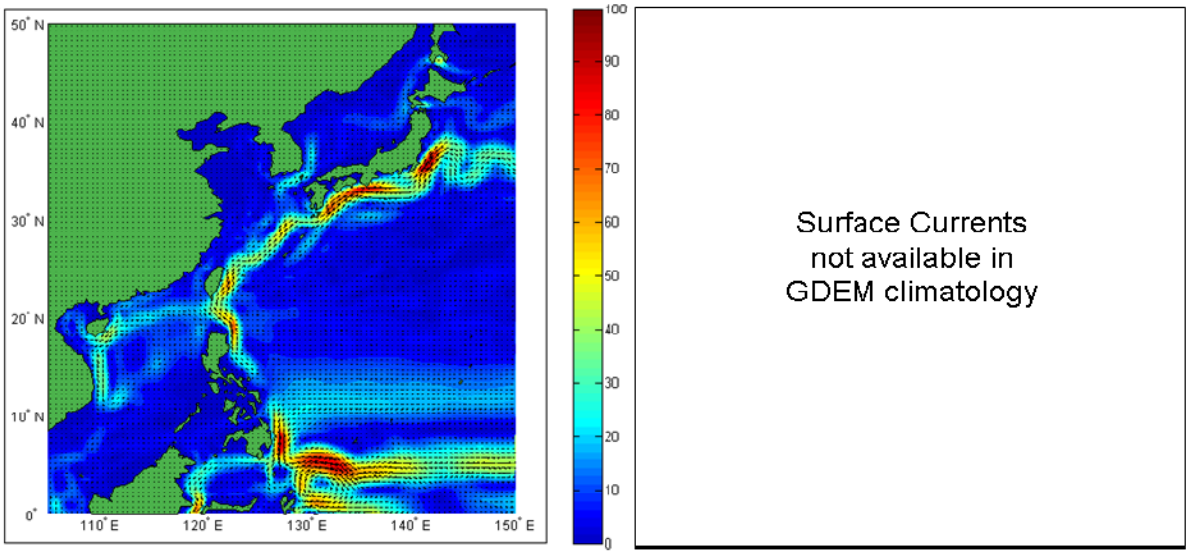

Figure 18. LTM of upper 25 m ocean currents (cm/s) for October: (left) SODA; (right) GDEM.

C. COMPARISONS AND ASSESSMENTS OF CONDITIONAL CLIMATOLOGIES DERIVED FROM SODA

1. Meridional Winds and Conditional Climatologies

a. LTM

The predominant seasonal variations of winds in the western North Pacific are part of the Asian monsoon cycle. Our study period, October, occurs at the beginning of the winter phase of the monsoon cycle, known as the northeast monsoon phase. From September to October, the, mean winds over the East China Sea and South China Sea shift from southwesterly to northeasterly (see Figure 19).

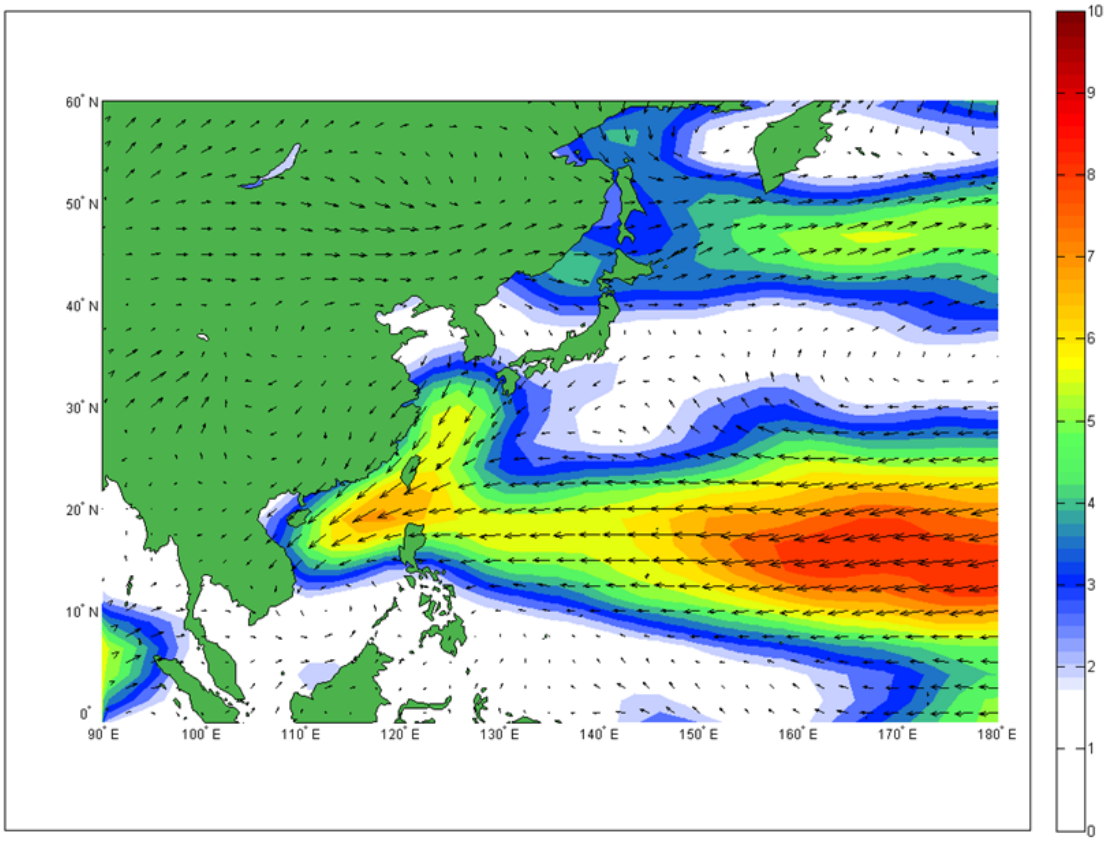

Figure 19. October long-term mean surface vector winds (m/s).

b. Conditional Composites: High and Low Wind Speed

A particularly early (late) onset of the northeast monsoon can mean that the southwesterly to northeasterly transition takes place prior (during) October. This variability in the onset of the northeast monsoon can lead to large interannual variations in wind forcing of the ocean in the western North Pacific. In this study, we examined these atmospheric and oceanic variations to assess how well they and their tactical USW impacts can be described.

To do so, we created and assessed conditional composites based on periods of high and low meridional wind speeds during October (see chapter 2). Composites of the surface winds for five highest surface meridional wind Octobers and five lowest surface meridional wind Octobers are shown in Figure 20. The high wind composite shows enhanced northeasterly flow over the East

China Sea and South China Sea, yet a weakening of the easterly trades and midlatitude westerlies. The opposite pattern is seen in the low wind composite. These patterns indicate that upper ocean structure in high wind periods is likely to be significantly from the structure in low wind periods.

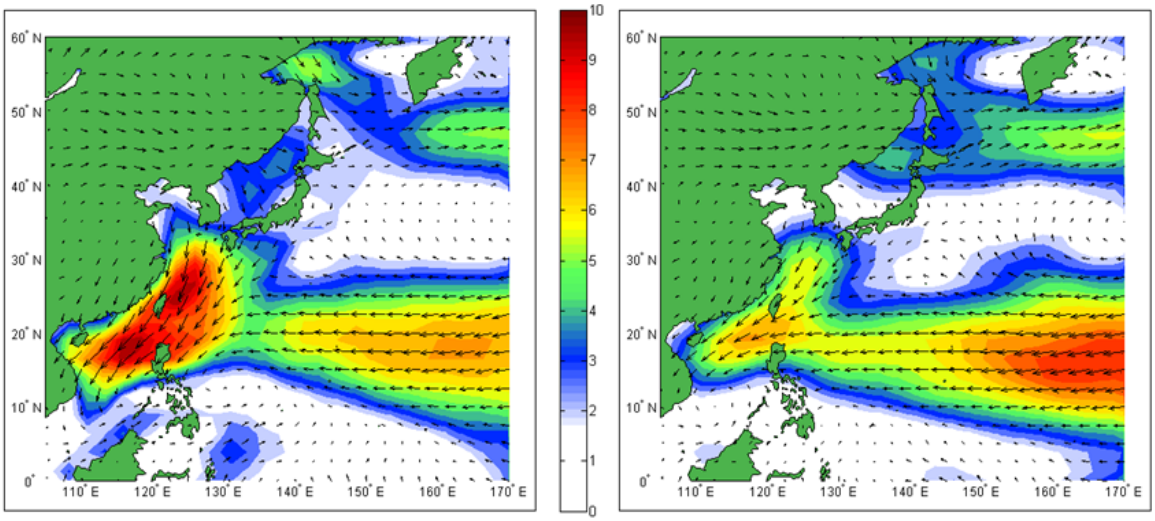

Figure 20. October mean surface vector wind (m/s) conditional composites: (left) 5 years of highest meridional wind speeds, (right) 5 years lowest meridional wind speeds. See Chapter II, Section B, for details on how these composites were constructed.

c. Composite Anomalies

The composite vector wind anomaly maps for the high and low wind composites (Figure 21) clearly show marked differences, and indicate the value of anomalies in analyzing climate variations.

An anomalous cyclonic (anticyclonic) circulation pattern occurs at about 20N over much of the western North Pacific in the high (low) wind composite. Note that the high (low) wind anomalies indicate an anomalous strengthening (weakening) of the northeasterlies, consistent with an early (late) onset of winter conditions.

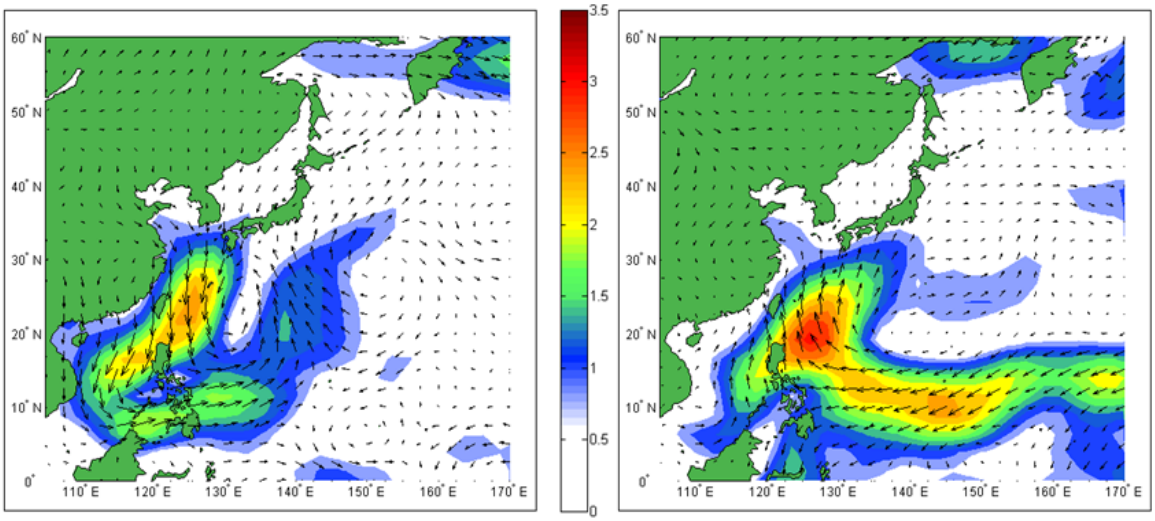

Figure 21. October surface vector winds anomalies (m/s) for conditional composites of: (left) 5 years of highest meridional wind speeds, (right) 5 years lowest meridional wind speeds. See Chapter II, Section B, for details on how these composites were constructed.

2. Ocean Temperature and Conditional Climatologies

Wind drives many of the physical processes that occur in near surface waters of the ocean, including latent heat fluxes, turbulent mixing, Ekman pumping, Ekman transport, upwelling, and downwelling. Each of these processes affects the temperature structure of the ocean to varying degrees. Therefore, by comparing maps of ocean temperatures from our conditional climatologies we can observe the impact of these processes on ocean structure.

SST anomaly maps provide a method for assessing the impact of surface winds on the ocean. In general, an increase (decrease) in surface wind speeds over the ocean should increase (decrease) latent and sensible heat fluxes from the ocean, and increase (decrease) turbulent mixing. Thus, in the vicinity of the largest wind anomalies (Figure 21), we would expect negative (positive) upper ocean temperature anomalies for the high (low) wind composite case. The SST anomalies shown in Figure 22 support this expectation. However, there are also large SST anomalies outside the regions of large wind anomalies (e.g., to east of northern Japan). This suggests that other factors besides surface wind

anomalies need to be considered to explain all aspects of upper ocean temperature variability (e.g., differences in long distance oceanic temperature advection and surface radiative forcing, pre-existing temperature anomalies).

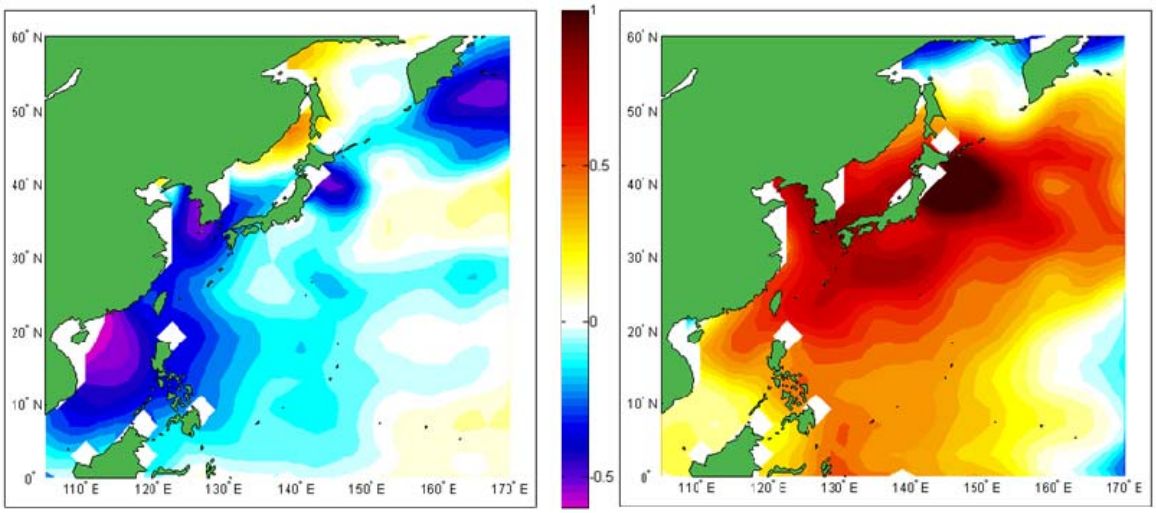

Figure 22. October sea surface temperature anomalies (deg C) for conditional composites of: (left) 5 years of highest meridional wind speeds, (right) 5 years lowest meridional wind speeds. SST data from NCEP re-analysis data set. White areas indicate relatively coarse horizontal resolution of this data set. See Chapter II, section B, for details on how these composites were constructed.

Comparing the SODA LTM ocean temperatures at 5 m (Figure 23) with ocean temperatures at 5 m from the SODA high and low wind conditional climatologies (Figure 24), we see a pattern of generally warmer than average temperatures in the low wind composite, and cooler than normal temperatures in the high wind composite. Additionally, there are indications of increased (decreased) southward advection of cooler ocean waters along the coast of China and into the South China Sea in the high (low) wind periods.

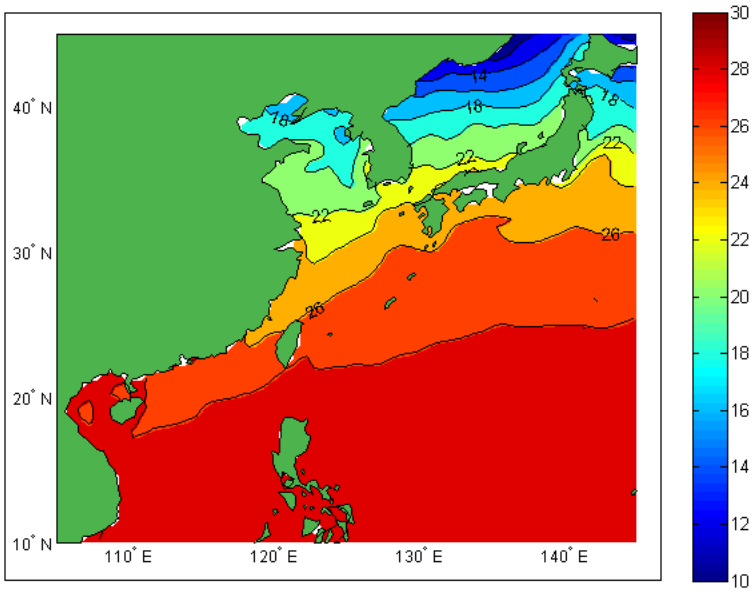

Figure 23. SODA LTM ocean temperatures (deg C) in October at 5 meters depth. White shading indicate land or areas in which sea floor depth is 5 meters or less.

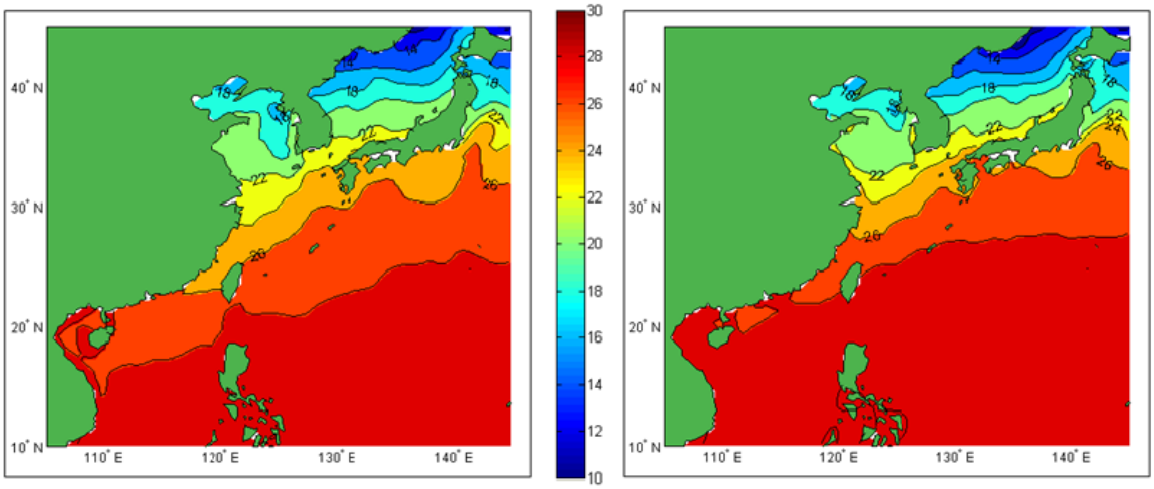

Figure 24. SODA ocean temperatures (deg C) at 5 meters depth for: (left) composites of five highest meridional wind speed Octobers, and (right) five lowest meridional wind speed Octobers. See Chapter II, section B, for details on how these composites were constructed. White shading indicates areas in which sea floor depth is 5 meters or less.

Anomalies in ocean temperature at 5 m for the conditional composites show a dipole pattern of temperature differences in our area of interest, with opposite anomalies in most of the western North Pacific (Figure 25). If we

compare these results to the wind anomalies shown in Figure 21, we see that areas with relatively small wind anomalies (e.g., the Sea of Japan, northern Yellow Sea, and Pacific Ocean southeast of Japan) do not exhibit the dipole differences in temperature. These results provide further evidence that climate scale variations in surface winds lead to significant climate scale variations in upper ocean structure.

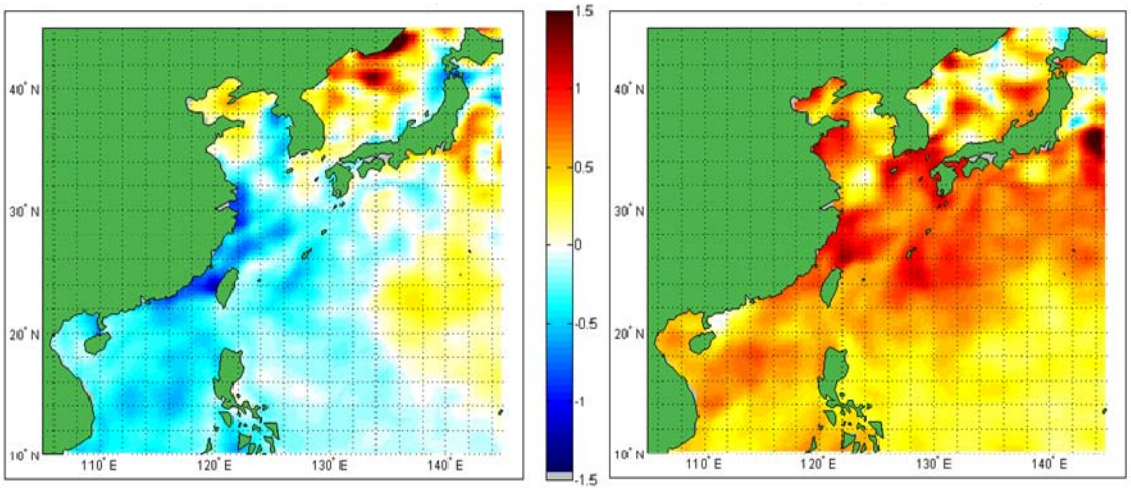

Figure 25. SODA ocean temperature anomalies (deg C) at 5 meters depth for: (left) composites of five highest meridional wind speed Octobers, and (right) five lowest meridional wind speed Octobers. See Chapter II, section B, for details on how these composites were constructed. Grey shading indicates areas in which sea floor depth is 5 meters or less.

If we look deeper into the ocean, at 35 m depth, and continue comparing the SODA LTM ocean temperatures (Figure 26) with ocean temperatures from the SODA conditional climatologies (Figure 27), we see patterns similar to those at the surface and 5 m. The dipole pattern in the East China Sea and South China Sea at 5 m is still evident. However, a stronger anomaly dipole pattern is evident in the Yellow Sea and Sea of Japan (Figure 28). The Yellow Sea and Sea of Japan warm (cool) anomalies at 35 m in the high (low) wind composite may be due to positive (negative) anomalies in the strength of turbulent mixing, that then leads to positive (negative) anomalies in the mixing downward of warm surface waters. The Sea of Japan anomalies may also be due in part to anomalies in temperature advection. Tomczak and Godfrey (1994) discuss how

the Tsushima Current (Figure 12) transports large volumes of warmer and less saline Yellow Sea water into the Sea of Japan during summer. It is possible that the surface wind anomalies alter the ocean structure in a way that changes the strength of this temperature advection (e.g., high winds strengthen the positive zonal temperature gradient at the south end of the Tsushima Current, leading to enhanced poleward flow and warm water advection by the current).

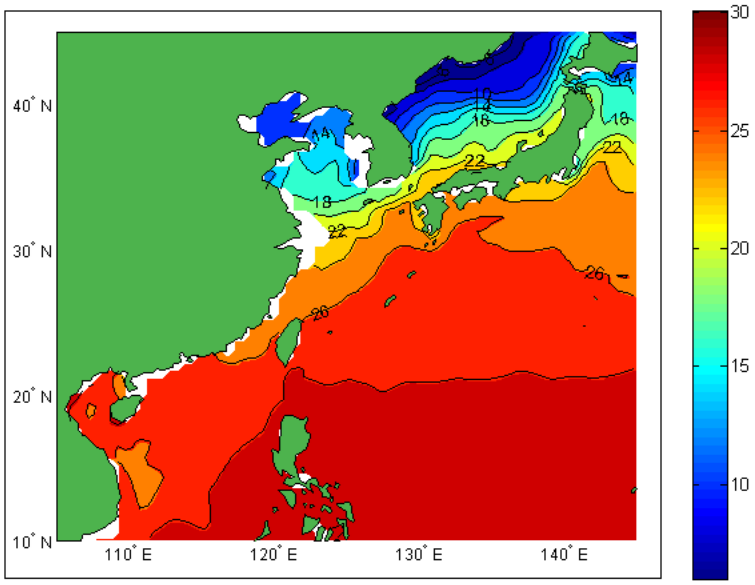

Figure 26. SODA LTM ocean temperatures (deg C) in October at 35 meters depth. White shading indicates land or areas in which sea floor depth is 35 meters or less.

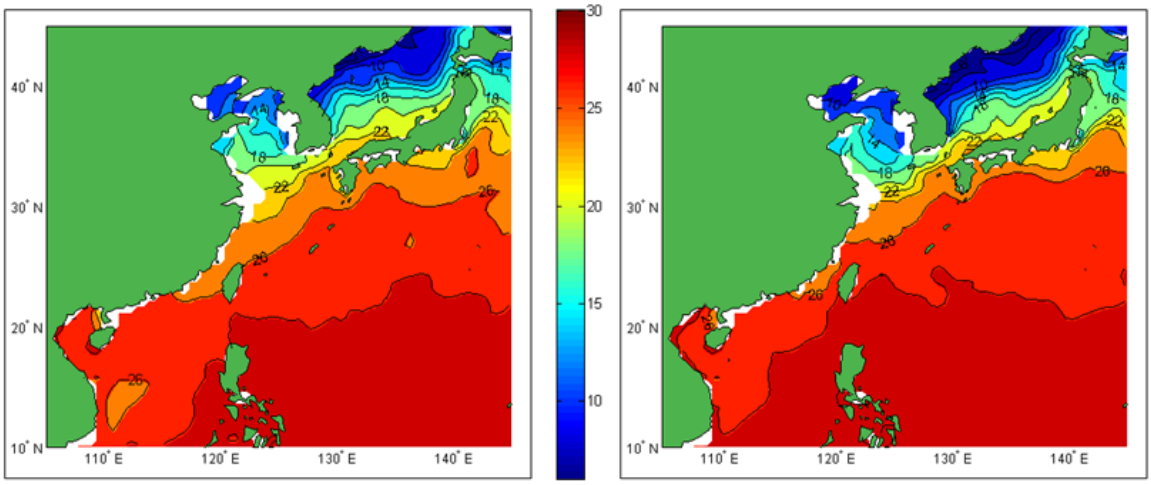

Figure 27. SODA ocean temperatures (deg C) at 35 meters depth for: (left) composites of five highest meridional wind speed Octobers, and (right) five lowest meridional wind speed Octobers. See Chapter II, section B, for details on how these composites were constructed. White shading indicates areas in which sea floor depth is 35 meters or less.

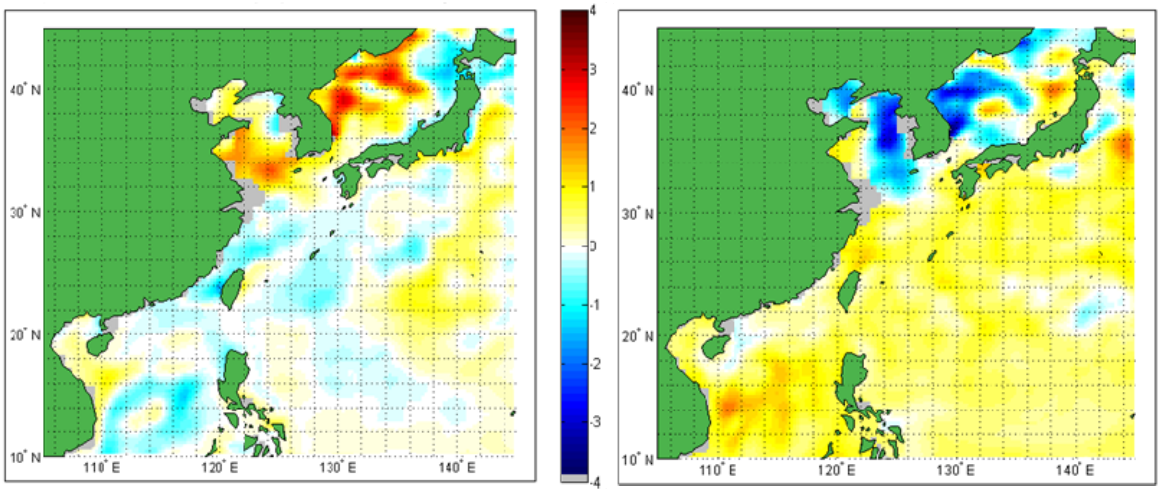

Figure 28. SODA ocean temperature anomalies (deg C) at 35 meters depth for: (left) composites of five highest meridional wind speed Octobers, and (right) five lowest meridional wind speed Octobers. See Chapter II, section B, for details on how these composites were constructed. Grey shading indicates areas in which sea floor depth is 35 meters or less.

At a depth of 70m, the effects of surface wind variations are less obvious over most of the WESTPAC. The patterns visible in SODA LTM ocean temperatures shown in Figure 29 are very similar to the patterns in ocean

temperature for the SODA conditional climatologies seen in Figure 30. However, the ocean temperature anomalies of the conditional composites (Figure 31) show some clear differences. There remain significant temperature anomaly differences in the western Sea of Japan, perhaps associated with variations in the position of the front driven by differences in temperature advection. A weaker temperature anomaly difference than that seen at shallower depths also exists in the South China Sea.

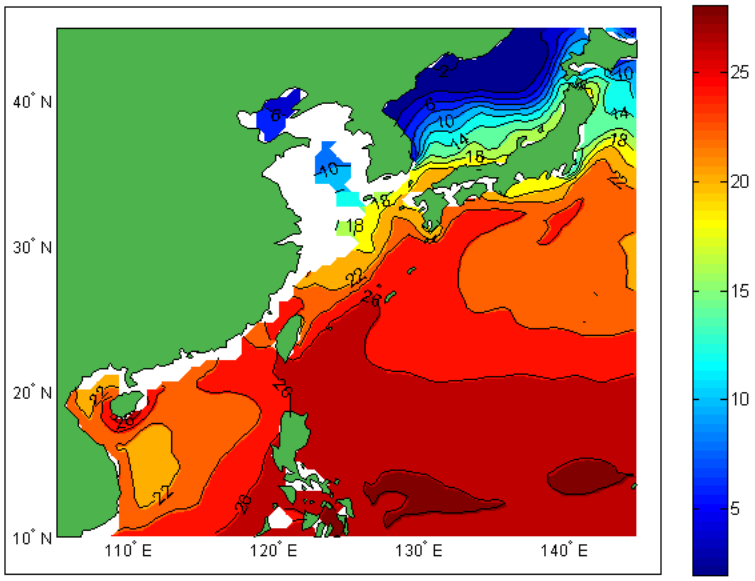

Figure 29. SODA LTM ocean temperatures (deg C) in October at 70 meters depth. White shading indicates land or areas in which sea floor depth is 70 meters or less.

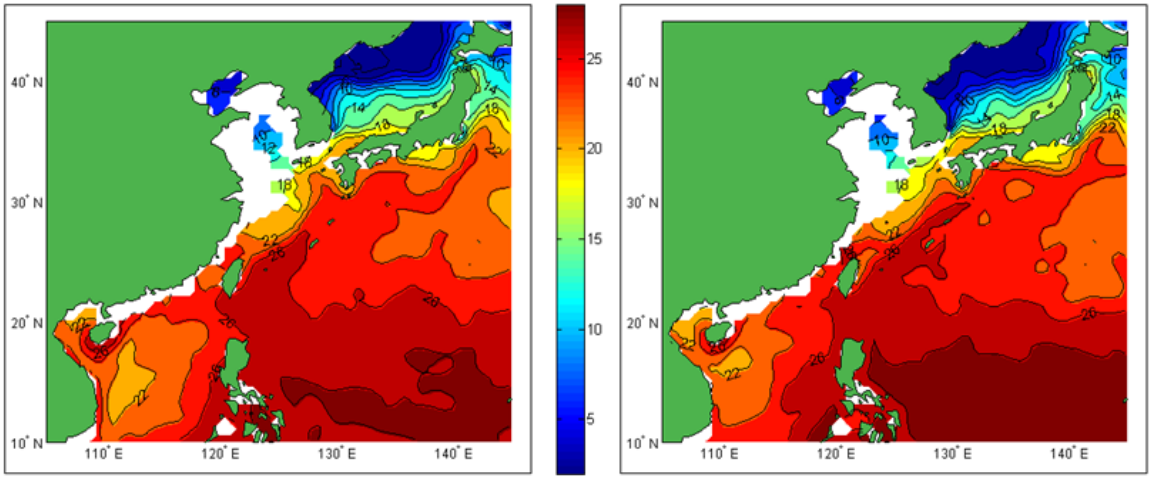

Figure 30. SODA ocean temperatures (deg C) at 70 meters depth for: (left) composites of five highest meridional wind speed Octobers, and (right) five lowest meridional wind speed Octobers. See Chapter II, section B, for details on how these composites were constructed. White shading indicates areas in which sea floor depth is 70 meters or less.

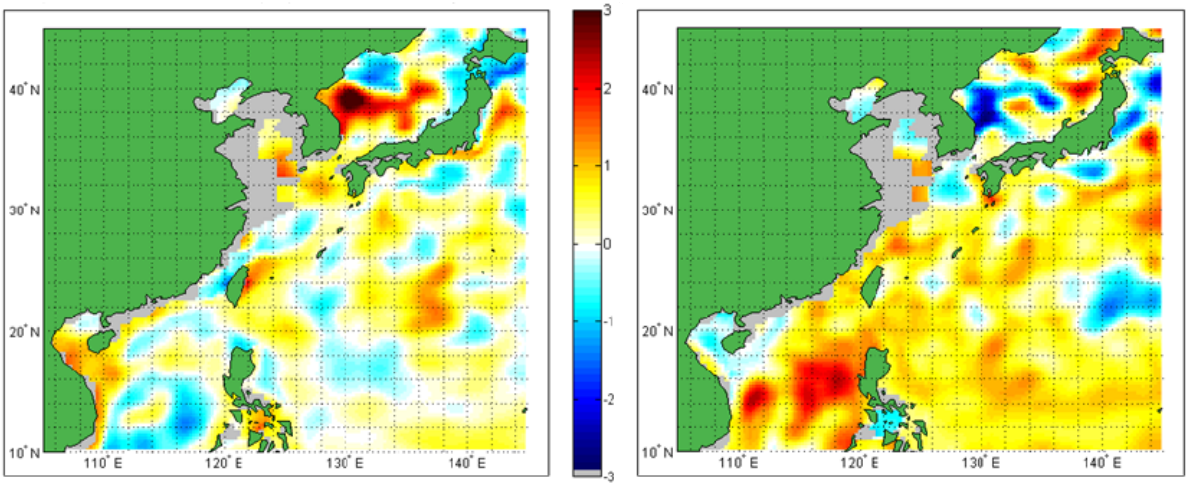

Figure 31. SODA ocean temperature anomalies (deg C) at 70 meters depth for: (left) composites of five highest meridional wind speed Octobers, and (right) five lowest meridional wind speed Octobers. See Chapter II, section B, for details on how these composites were constructed. Grey shading indicates areas in which sea floor depth is 70 meters or less.

3. Upwelling and Downwelling

The SODA ocean re-analysis is fundamentally different from the GDEM ocean climatology in its assimilation of wind data. The incorporation of this data along with the dynamics of the POP ocean general circulation model used in SODA allows the representation of physical processes, such as wind forced circulations and Ekman transport (Figure 32).

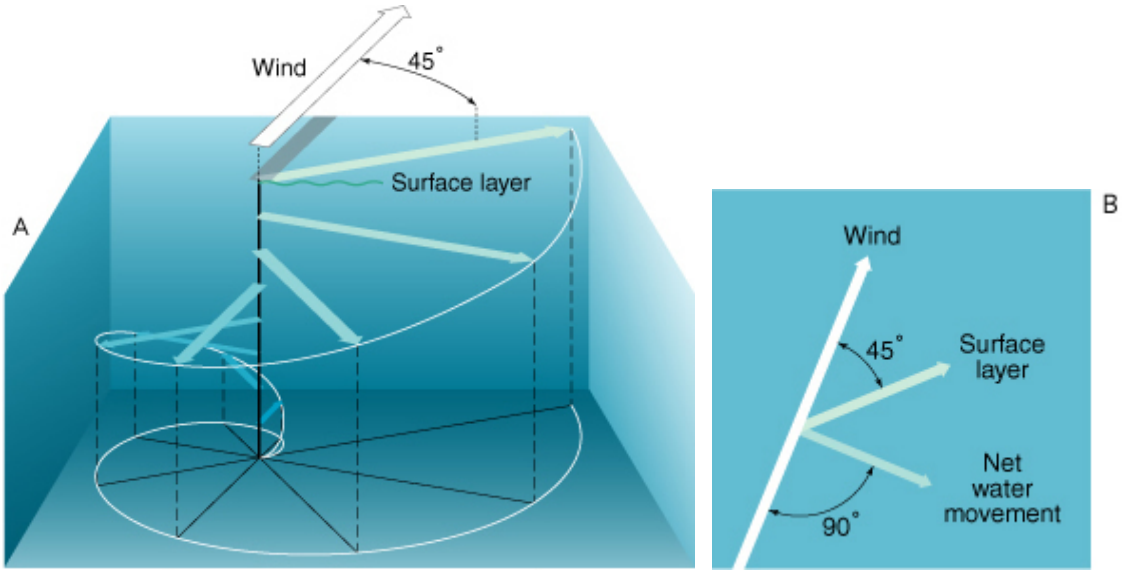

Figure 32. Schematic depiction of surface wind stress and Ekman transport in the upper ocean. (A) Horizontal wind sets the water column in motion as each moving layer is deflected to the right of the overlying layer's movement. (B) The result is net water movement 90 degrees to the right of the wind motion. Accessed on September 2008, at http://oceanmotion.org/html/background/ocean-in-motion.htm.

Ekman transport of near surface waters in coastal areas can lead to upwelling and downwelling as shown in Figure 33. SODA conditional climatologies contain evidence of these processes in areas such as the Yellow Sea and South China Sea. A vertical cross section from the central Yellow Sea (Figure 34) shows evidence of both upwelling and downwelling in the high wind composite. The cool anomaly along the western coast of Korea (125E-126E) is consistent with cold deeper water moving to the surface as northerly winds

create offshore (westward) Ekman transport. Conversely, continued westward transport of surface waters by the strong northerly winds causes surface waters to pile up along the western side of the Yellow Sea. Some of this warm surface water is forced downward, displacing cooler deeper waters, creating a warm anomaly. The low wind case has a very different pattern, with a thin layer of warmer surface water extending across the entire Yellow Sea, consistent with anomalously low turbulent mixing and surface heat flux from the ocean due to reduced wind forcing. A similar case of downwelling can be seen in the South China Sea (Figure 35).

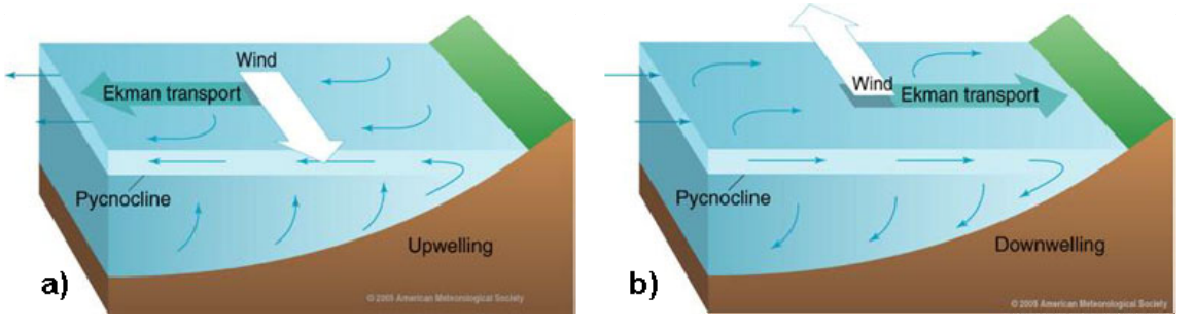

Figure 33. Schematic representation of coastal upwelling and downwelling in the northern hemisphere induced by surface wind stress and Ekman transport. (a) Northerly wind along an eastern ocean boundary produces offshore transport of water and upwelling. (b) Southerly wind along an eastern ocean boundary produces onshore transport of water and downwelling. http://oceanmotion.org/html/background/upwelling-and-downwelling.htm.

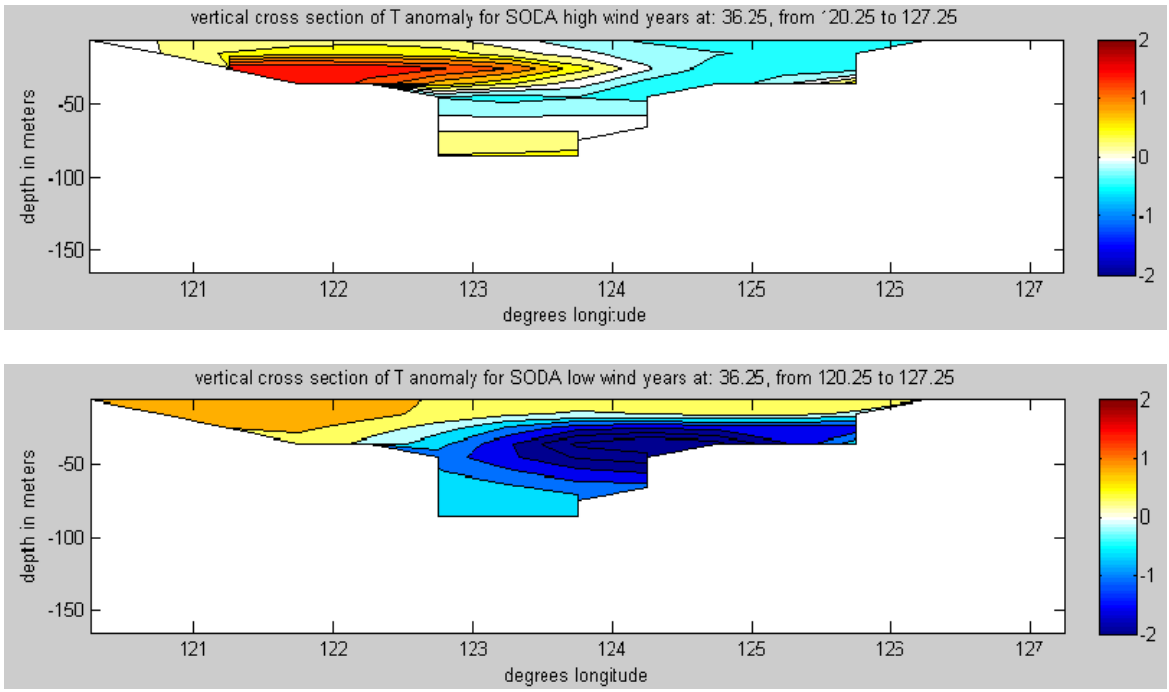

Figure 34. Vertical cross section (west to east) of upper ocean temperature for the Yellow Sea from SODA conditional climatologies for: (top) Octobers with 5 highest meridional wind speeds, (bottom) Octobers with 5 lowest wind speeds. See Chapter II, section B, for details on how these composites were constructed.

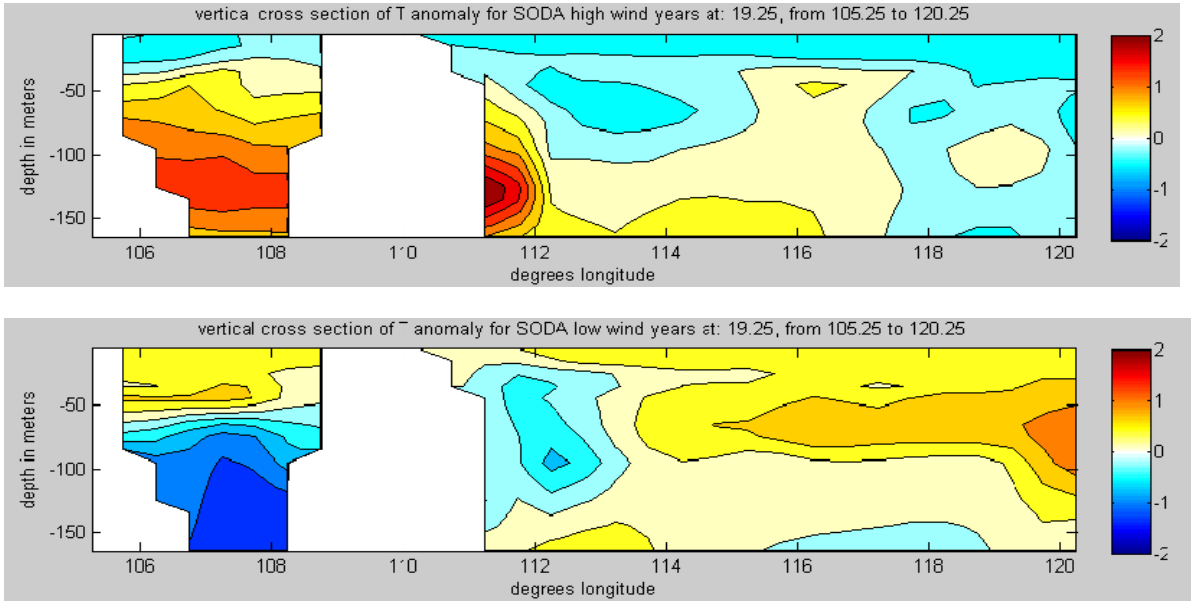

Figure 35. Vertical cross section (west to east) of upper ocean temperature for the South China Sea from SODA conditional climatologies for: Octobers with 5 highest meridional wind speeds, (bottom) Octobers with 5 lowest wind speeds. See Chapter II, section B, for details on how these composites were constructed.

4. Sonic Layer Depth and Conditional Climatologies

We have seen in the previous sections how variations in wind speed can have a pronounced effect on upper ocean temperature structure. Sonic layer depth is the near surface level of maximum sound speed, and is highly dependent on temperature. Therefore, variations in wind speed affect derived acoustically relevant quantities, such as sonic layer depth.

Having a sonic layer depth at any level below the surface requires a neutral or positive temperature gradient, which is often the product of turbulent mixing by winds. A deep sonic layer depth requires deep mixing. Therefore, it is reasonable to assume a connection among high (low) wind speeds, deep (shallow) mixing, and deep (shallow) sonic layer depths.

Figure 36 shows the sonic layer depths for the high and low wind speed SODA conditional climatologies. The deeper sonic layer depths between Japan and Taiwan in the high wind composite appear directly related to the stronger winds. In contrast, the deeper sonic layer depths in the low wind composite east of the Philippines appear related to the stronger trade winds in that area in the low wind composite. The difference in sonic layer depths between the high and low wind composites in the northern South China Sea also appears to reflect the differences in wind speed between the two composites. These strong relationships between wind speed and sonic layer depth are further evidence of the impact of wind on ocean variability and, by implication, on ocean acoustics.

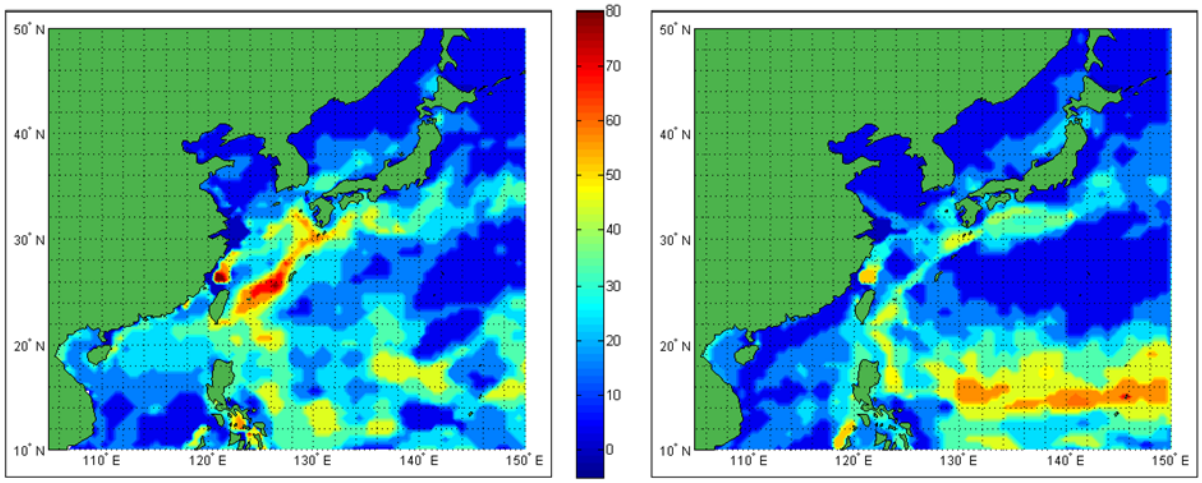

Figure 36. SODA conditional climatologies of sonic layer depth for: (left) Octobers with 5 highest meridional wind speeds, (right) Octobers with 5 lowest wind speeds. See Chapter II, section B, for details on how these composites were constructed.

D. TACTICAL SIGNIFICANCE OF CLIMATOLOGY DIFFERENCES

1. Overview

The previous sections demonstrate that variations in wind speed and direction have a significant impact on ocean structure. Even small changes in the ocean environment can have large impacts on sound propagation and therefore sonar sensor performance. In the following sections we will attempt to answer the question as to whether these changes in the ocean environment are tactically significant.

The U.S. Navy currently uses the GDEM LTM climatology in TDAs fielded by operational forces. Therefore, in the following sections we will endeavor to illuminate the differences between the SODA conditional climatologies and demonstrate the tactically significant environmental variability that is being overlooked by LTM climatologies such as GDEM.

a. Deep SLDs and Strong Surface Duct

A deep sonic layer depth is tactically significant for two reasons: first, it signifies the existence of a surface duct that may be of adequate depth to trap or duct a certain range of frequencies; and second, it creates a shadow zone below the SLD into which sound has trouble propagating (Figure 37). The surface duct can be beneficial in that it can produce longer ranges for a specific range of frequencies, particularly active sonar frequencies. The down side is that the very qualities that allow the surface duct to trap sound also make it difficult for sound to enter the SLD from below. Therefore, a signal emanating from below the SLD may go undetected by a sensor above the SLD.

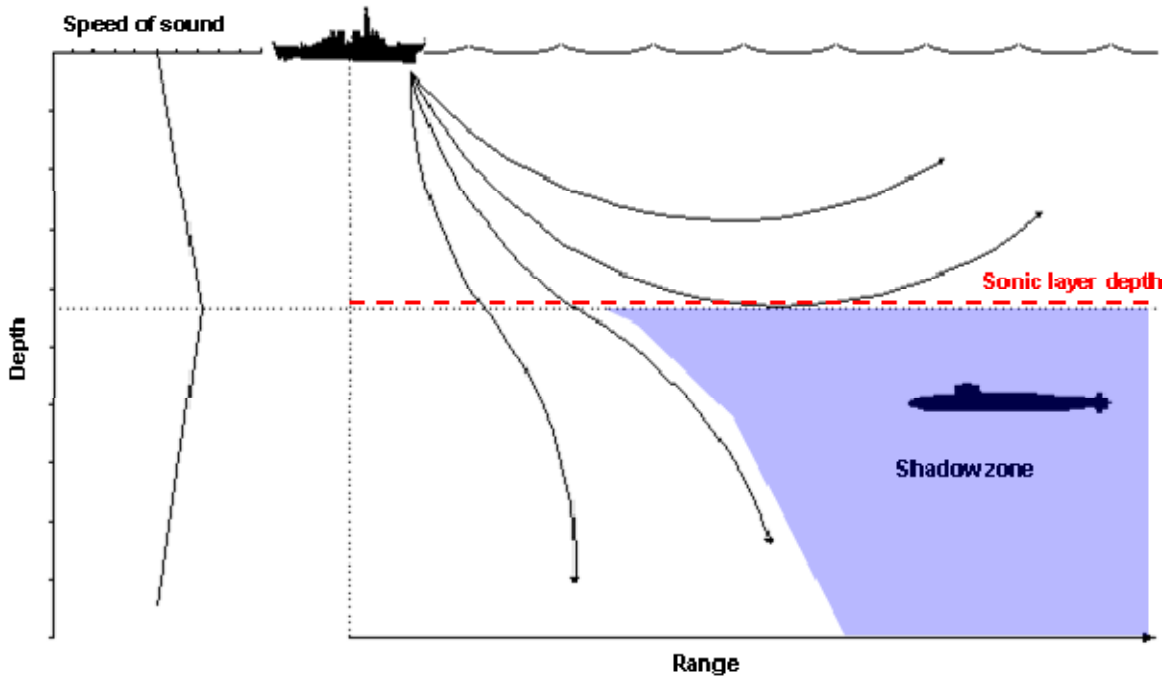

Figure 37. Propagation of sound in an ocean environment with a positive over negative vertical sound speed gradient. The depth of maximum sound speed is called the sonic layer depth (red dashed line), which produces a shadow zone (shaded area). Image from http://www.fas.org/ man/dod-101/navy/docs/es310/SNR_PROP/snr_prop.htm accessed September 2008.

The depth of the sonic layer is critical to the range of frequencies that can be trapped within the duct. A deep sonic layer can normally duct a lower frequency than a shallow duct. A very shallow SLD will likely only duct high, active sonar frequencies, and a deep SLD will duct active frequencies as well as lower passive broadband frequencies. Tactically significant changes in SLD can be induced by wind variations. Figure 38 shows examples of SLD variations associated with wind variations in the Okinawa area. Note that the deepest (shallowest) SLD is associated with the high (low) case, and that SLD variations are relatively large, from 15 m in the low wind case to 50 m in the high wind case.

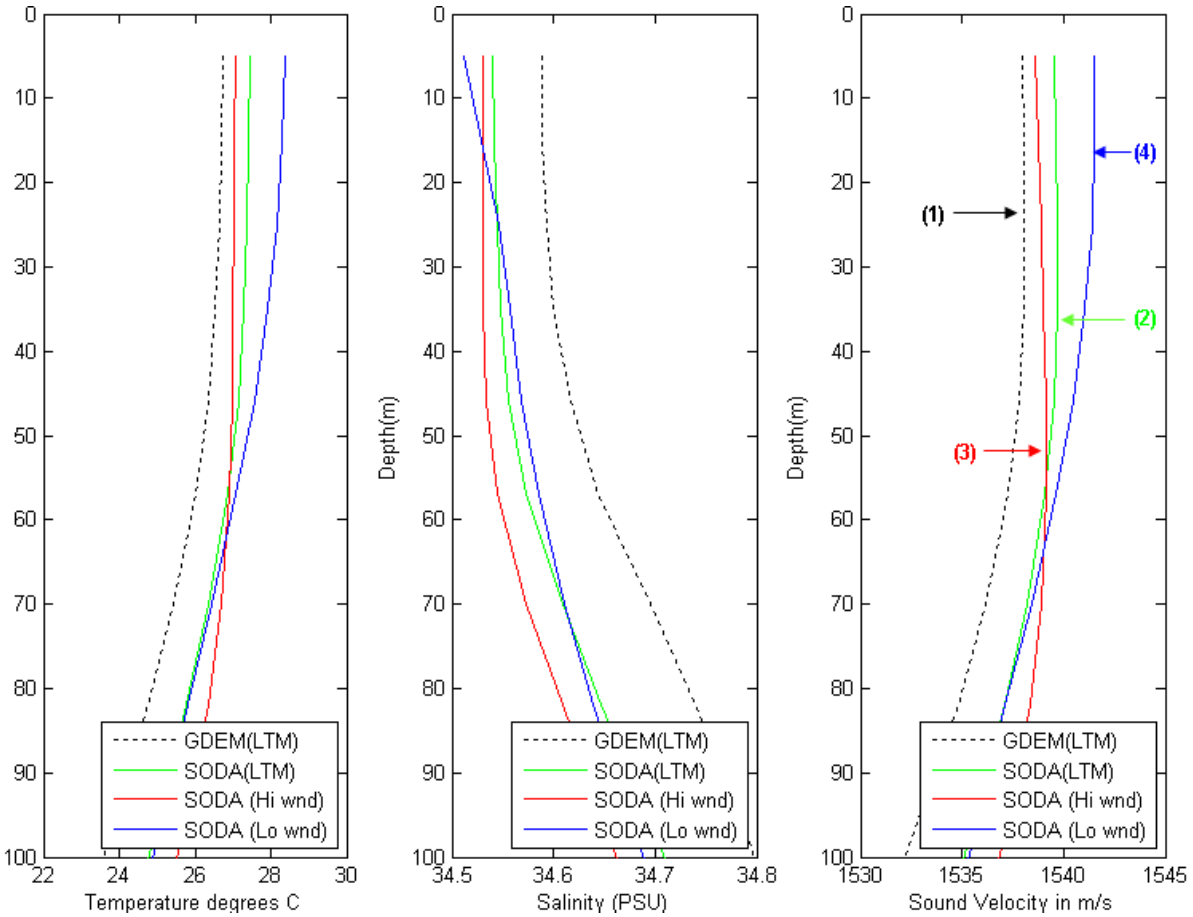

Figure 38. Temperature, salinity, and sound speed profiles for the area near Okinawa, depicting ocean variability for GDEM and SODA long-term means and SODA conditional climatologies for Octobers with 5 highest and 5 lowest meridional wind speeds. The SLD for each climatology is indicated by the numerals 1-4 in the right panel. See Chapter II, section B, for details on how these composites were constructed.

b. No Surface Duct

Formation of a surface duct is not possible when the maximum of near surface sound speed is at the surface. In this situation, there is a negative vertical gradient in sound speed, and the SLD is at zero depth. A negative sound speed gradient is normally due to decreasing temperature with depth, which occurs mainly in the summer when winds are calm and turbulent mixing is at a

minimum. Sound will always refract or bend towards regions of slower sound speed, so in a negative sound speed gradient sound refracts downward, as shown in Figure 39.

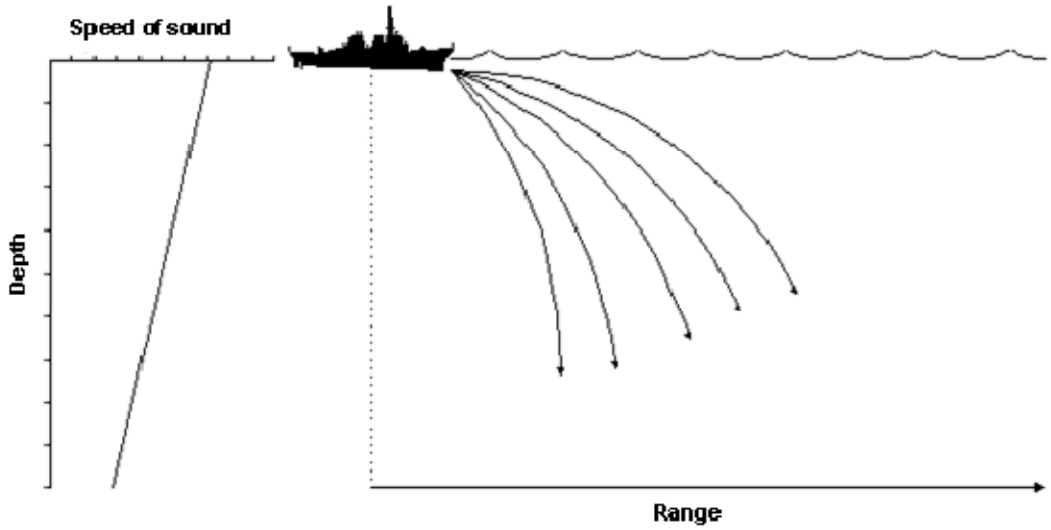

Figure 39. Propagation of sound in an ocean environment, with a negative vertical sound speed gradient. Image from http://www.fas.org/ man/dod-101/navy/docs/es310/SNR_PROP/snr_prop.htm accessed September 2008.

In this case, sound will tend to propagate downward until temperature becomes isothermal and increasing pressure acts to raise sound speed and thus refract sound upward again (Figure 40). This results in what is called a deep sound channel, which behaves like a duct.

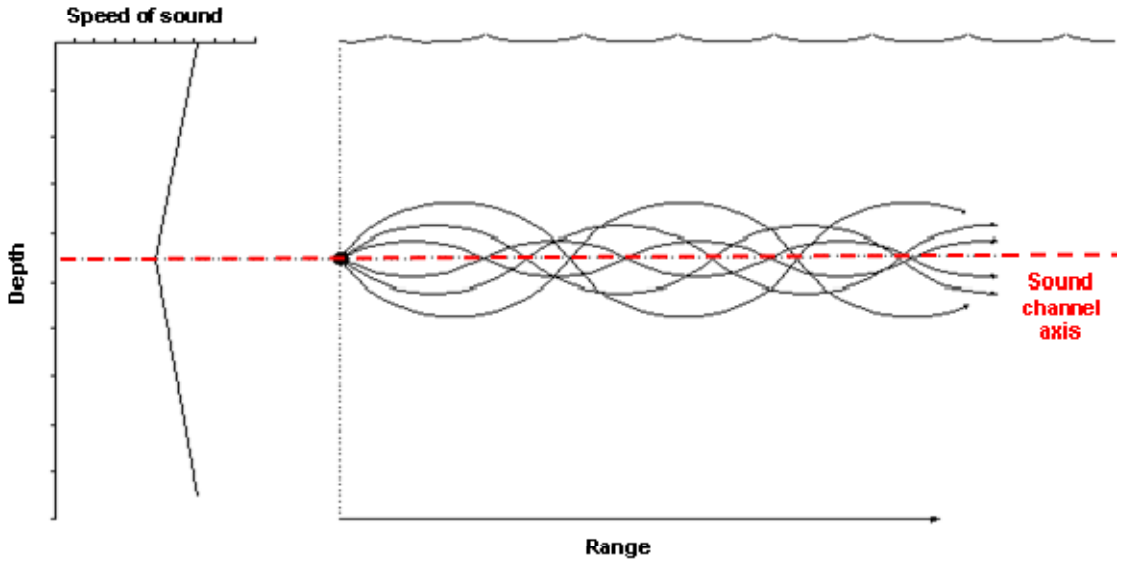

Figure 40. Propagation of sound in an ocean environment, with a negative vertical sound speed gradient over a positive vertical sound speed gradient. Image from http://www.fas.org/ man/dod-101/navy/docs/es310/SNR_PROP/ snr_prop.htm accessed September 2008.

c. SSP Variation and Acoustic Propagation

The speed of sound in seawater is highly dependent on temperature and to a lesser extent on salinity. Therefore, variations in these parameters lead to changes in sound speed. These changes in sound speed cause sound to refract when moving between areas of differing sound speed, bending or refracting toward the region of lower sound speed. The larger the sound speed gradient between regions, the larger the amount of refraction.

The refraction of sound in seawater is an important aspect of acoustic propagation, because certain refraction patterns lead to characteristic propagation paths. For example, a slight increase in sound speed from the surface to 35 meters below the surface can lead to a surface duct. This slight increase in sound speed could be due to a combination of isothermal conditions in a well-mixed surface layer combined with increasing pressure with depth. In this case, the surface duct is very sensitive to slight temperature changes (e.g., a

few tenths of a degree C) in the duct. For example, slight warming at the surface and/or slight cooling at the bottom of the surface duct could cause the surface duct to disappear.

An abrupt change in refraction can also cause an abrupt change in the path of acoustic propagation. As seen in Figure 37, a positive sound speed gradient over a negative gradient leads to the formation of a surface duct, with sound below the layer refracting downward. If the negative sound speed gradient were to increase, then sound would be refracted downward at a greater angle and would lead to reduced direct path ranges to a target below the surface layer.

The changes in sound speed mentioned above are often visible as abrupt changes in sound speed profiles. An individual sound speed profile created from an in situ observation, such as an XBT, may have a few abrupt changes that relate to observed propagation paths. A sound speed profile derived from a climatology may have less abrupt changes and a smoother appearance. If the profile is based on a LTM climatology, that is averaging a vast number of profiles for a period of several decades, the resulting profile is likely to be very smooth. A smart climatology that focuses on a specific climate pattern or process may provide a profile that more closely represents the actual environment. Heidt (2008) offers a good example of this via a comparison of ocean temperature profiles for four Januarys based on GDEM LTM climatology, SODA re-analysis, and in situ measurements from a moored buoy (Figure 41). Note that the GDEM profile is the same for all four Januarys while the observed profile and the SODA profiles all show considerable interannual variation. The observed and SODA profile variations are very similar to each other, while the GDEM profiles show no variation, of course. These differences illustrate the importance of the high temporal resolution in the SODA re-analysis data. This resolution allows SODA profiles to represent significant temporal variability that cannot be represented in the LTM profiles (e.g., GDEM profiles).

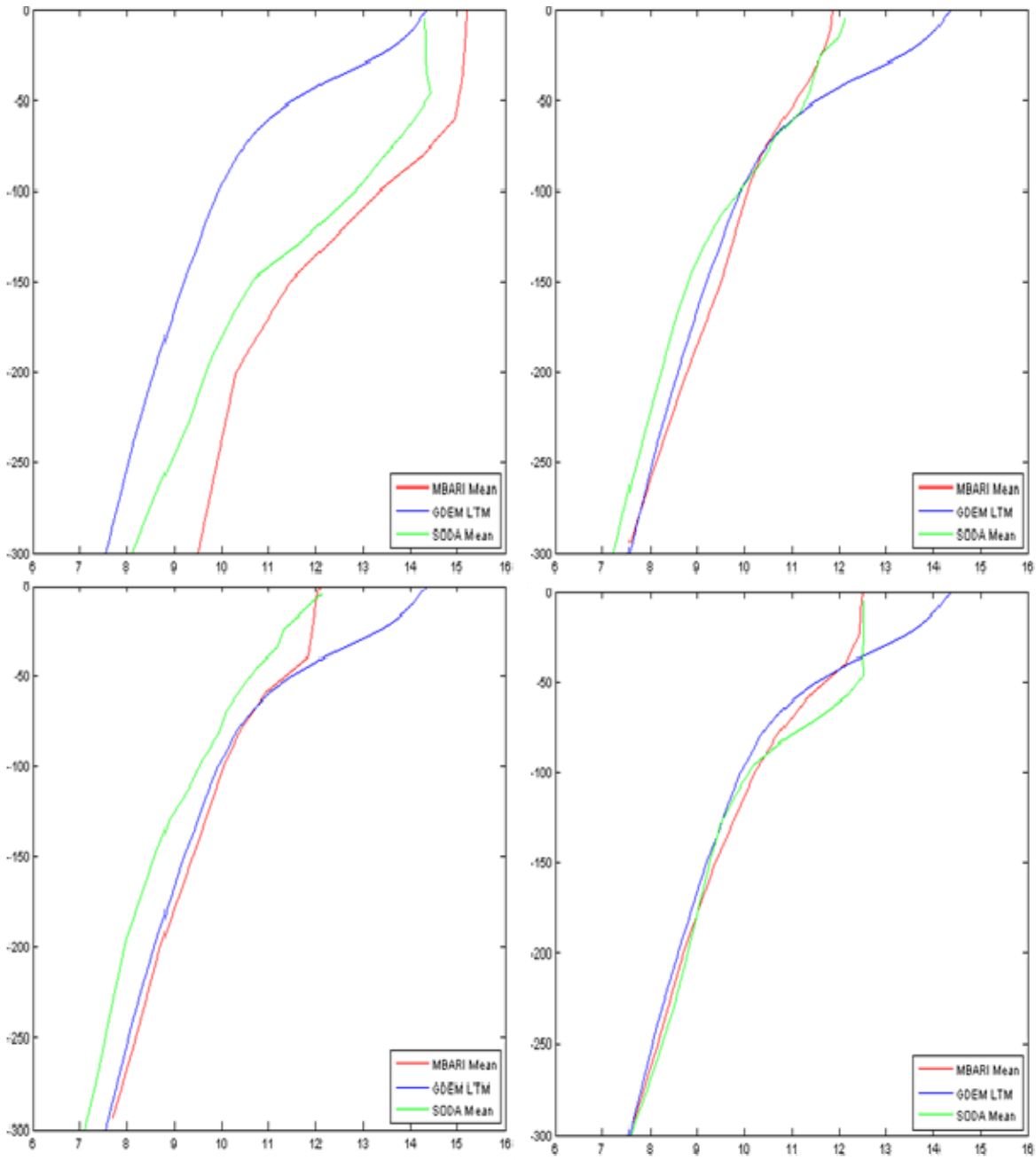

Figure 41. Vertical profiles of observed and SODA re-analysis January mean ocean temperatures (deg C) at 36.70N 122.39W from four years: (top, left) 1998, (top, right) 1999, (bottom, left) 2000, and (bottom, right) 2001. The observed (red curve) and SODA (green curve) temperatures are compared to GDEM LTM temperatures (blue curve). Observed temperatures from the Monterey Bay Aquarium Research Institute (MBARI) 2 buoy located near Monterey, California. From Heidt (2008).

2. Location Case Studies

a. Sea of Japan

The Sea of Japan is a unique basin in the WESTPAC. It is largely contained by geography, yet is strongly influenced by warm currents entering from the south and cold currents entering from the north. The large temperature difference between these two dissimilar water masses entering the basin results in a frontal boundary that bisects this sea.

The conditional climatologies of high and low wind years chosen for this study do not appear to have large variations of wind over the Sea of Japan (Figure 21). Even though winds over this basin do not vary considerably, there still exists a large degree of variability in ocean structure between the conditional climatologies, as seen in Figures 42-46.

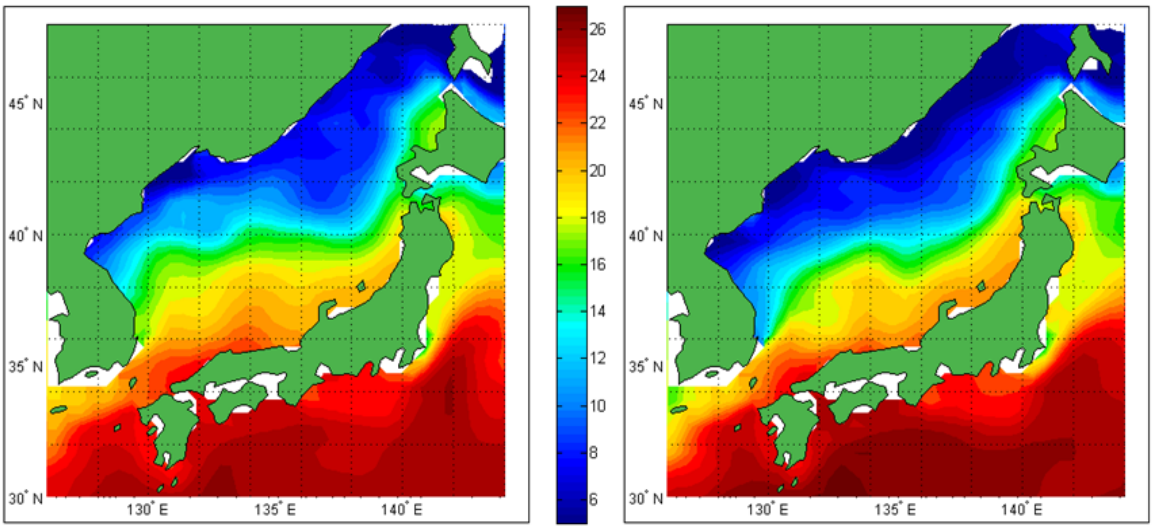

Figure 42. SODA ocean temperatures (deg C) at 35 meters depth for: (left) composites of five highest meridional wind speed Octobers, and (right) five lowest meridional wind speed Octobers. See Chapter II, section B, for details on how these composites were constructed. White shading indicates areas in which sea floor depth is 35 meters or less.

The temperature gradients in the high and low wind composites (Figure 42) suggest that poleward warm water advection by the Tsushima Current flow is enhanced during the high wind cases leading to anomalously high ocean temperatures in the western Sea of Japan (Figure 43). In the low wind case, equatorward cold water advection by the Liman Current is enhanced, leading to anomalously cold conditions in the western Sea of Japan.

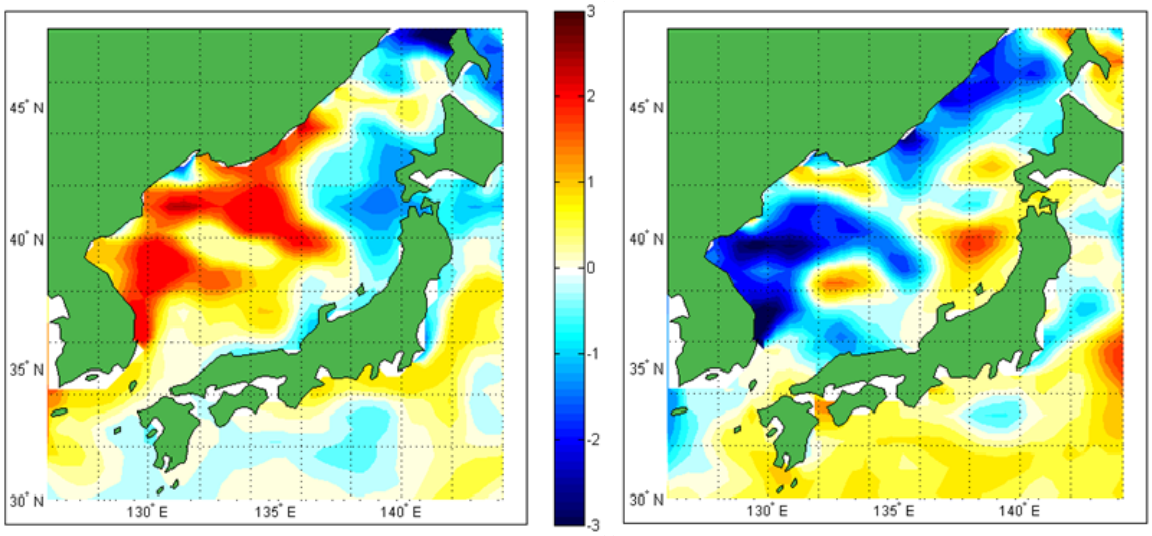

Figure 43. SODA ocean temperature anomalies (deg C) at 35 meters depth for: (left) composites of five highest meridional wind speed Octobers, and (right) five lowest meridional wind speed Octobers. See Chapter II, section B, for details on how these composites were constructed. Grey shading indicates areas in which sea floor depth is 35 meters or less.

A north-south vertical cross section taken just off the east coast of Korea (Figure 44) reveals large differences in the polar front structure between the high and low wind conditional climatologies. These are much greater differences in ocean structure than those between the SODA LTM and GDEM LTM climatologies (Figure 15). Variations in the position of the polar front between the high and low wind cases lead to temperature differences of close to 7 degrees C in some areas (Figure 45). Comparison of Figures 44 and 45 show that the large anomalies seen in Figure 45 are the result of anomalous vertical displacements of the main thermocline in the central Sea of Japan (deeper in the high wind case and shallower in the low wind case).

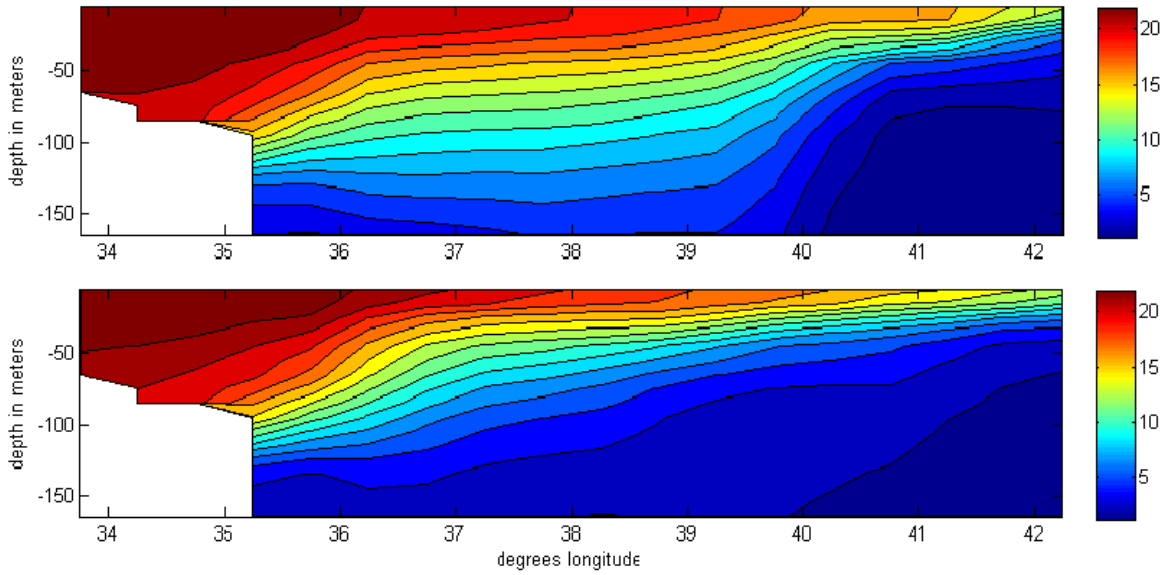

Figure 44. Vertical cross sections (south to north) of SODA ocean temperature (deg. C) versus depth (m) in the Sea of Japan along 130.25E for: (top) composites of five highest meridional wind speed Octobers, and (bottom) five lowest meridional wind speed Octobers. See Chapter II, section B, for details on how these composites were constructed.

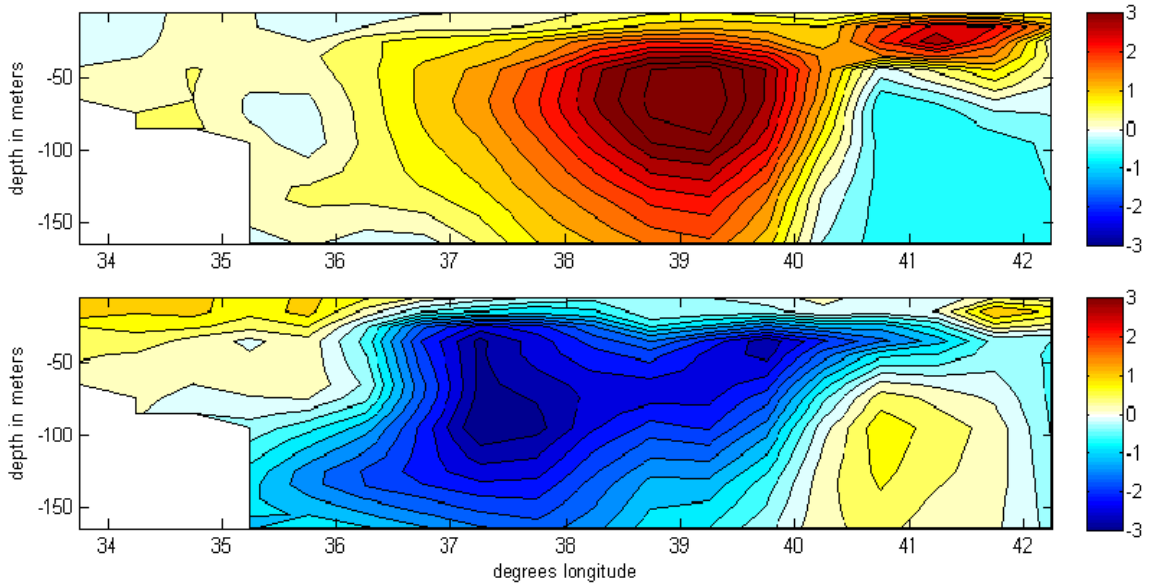

Figure 45. Vertical cross section (south to north) of SODA ocean temperature anomalies (deg. C) versus depth (m) in the Sea of Japan along 130.25E for: (top) composites of five highest meridional wind speed Octobers, and (bottom) five lowest meridional wind speed Octobers. See Chapter II, section B, for details on how these composites were constructed.

Figure 46 compares temperature, salinity, and sound speed profiles for the GDEM and SODA LTMs, as well as the SODA conditional climatologies. The similarities between the LTM climatologies are striking in light of large the differences between the SODA conditional climatologies. This also serves as an another example of how ocean variability can be obscured by long-term means.

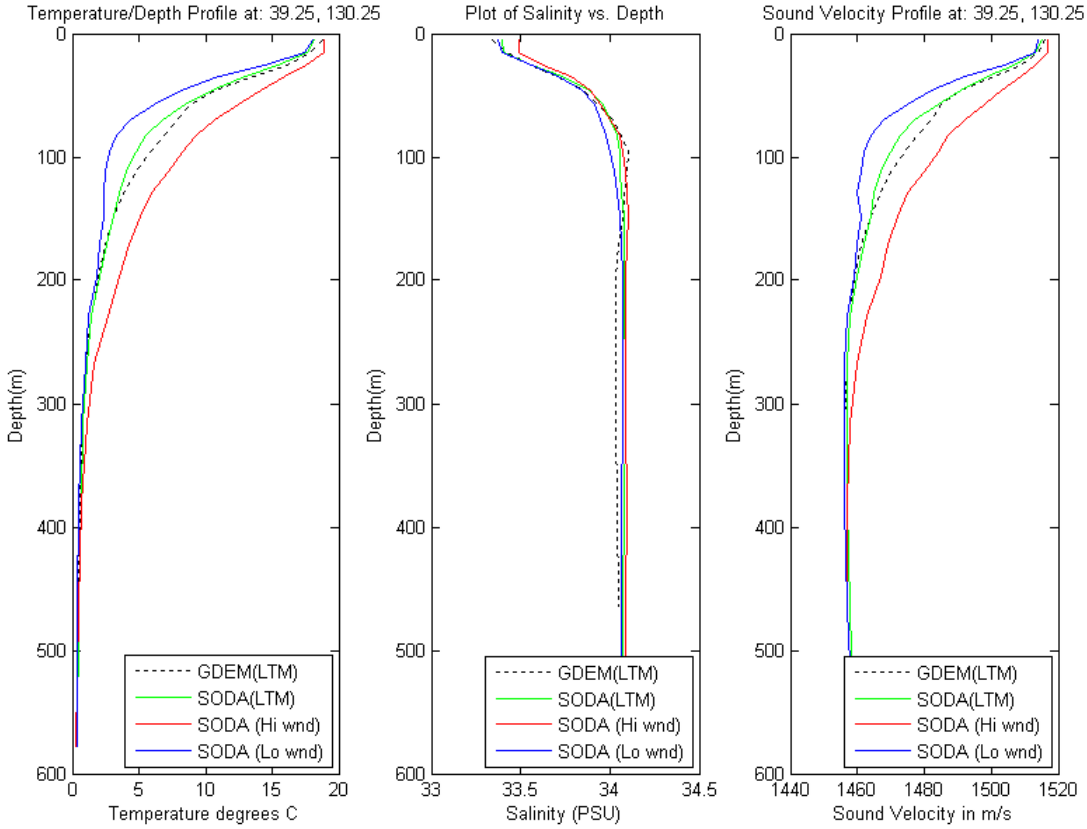

Figure 46. Temperature (left), salinity (center), and sound speed profiles (right) for October in the Sea of Japan at 39.25N 130.25E for: GDEM LTM (black, dashed), SODA LTM (green, solid), SODA conditional climatologies for Octobers of the 5 highest wind years (red, solid), and SODA conditional climatologies for Octobers of the 5 lowest wind years (blue, solid). Sound speed values were computed using the nine-term Mackenzie Equation as described in Chapter II, section B, sub-section 7.

b. Yellow Sea

The Yellow Sea experiences a larger variation in surface wind speed between the conditional climatologies than the Sea of Japan, and the relationships between wind speed and ocean structure are more obvious,

particularly in the southern Yellow Sea. SST and 5-meter temperatures both show cool anomalies during the high wind composite and warm anomalies in the low wind composite, as seen in Figure 22 and Figure 25. The stronger northeasterly winds appear to enhance the flow of cooler surface waters south along the coast of China and into the South China Sea in the high wind composite (Figure 24). At deeper depths, the trend reverses and warmer waters are seen moving further north in the Yellow Sea basin in the high wind composite than in the low wind composite, as shown in Figure 47. This evidence for a sub-surface flow into the Yellow Sea fits dynamically (via conservation of mass) with the evidence for near surface outflow from the Yellow Sea.

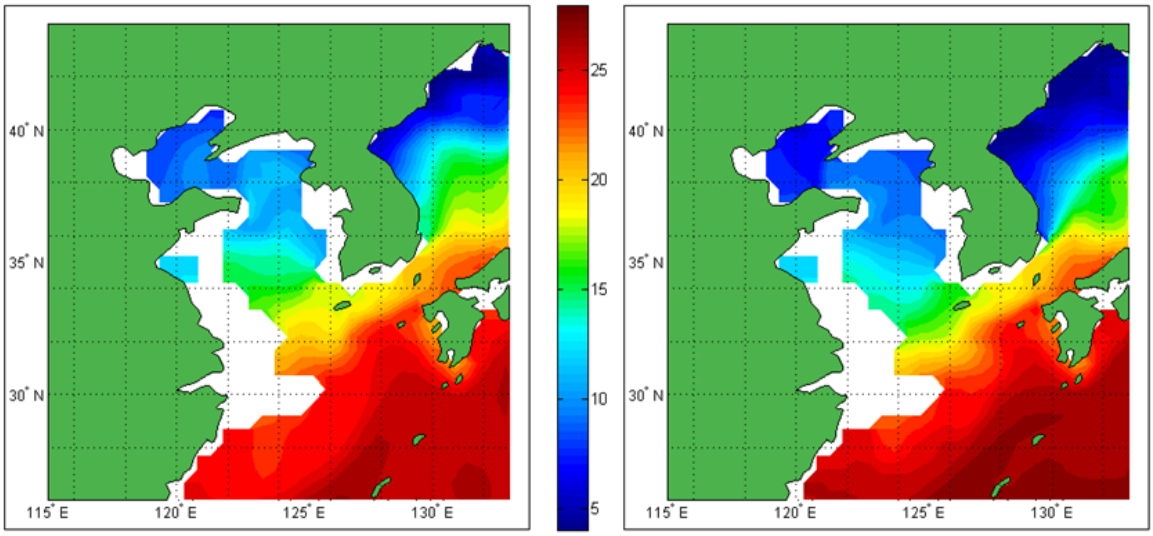

Figure 47. SODA ocean temperatures (deg C) at 45 meters depth for: (left) composites of five highest meridional wind speed Octobers, and (right) five lowest meridional wind speed Octobers. See Chapter II, section B, for details on how these composites were constructed. White shading indicates areas in which sea floor depth is 45 meters or less.

Comparisons of SODA ocean temperature anomalies for the conditional composites at 45 meters depth (Figure 48) reveal a strong north-south dipole pattern in the temperature anomalies. Coastal upwelling and downwelling may explain some of the pattern as described in Chapter III, part C, section 3. However, the shallow depth of the basin may limit Ekman transport and result in a more direct relationship between wind stress and transport of near

surface waters. Another possible explanation for the contrasting high wind and low wind anomalies at 35 m is that: (a) warm water advection from the south warms the yellow Sea in the high wind case; and (b) low mixing in the Yellow Sea prevents the mixing downward of warm surface waters in the low wind case.

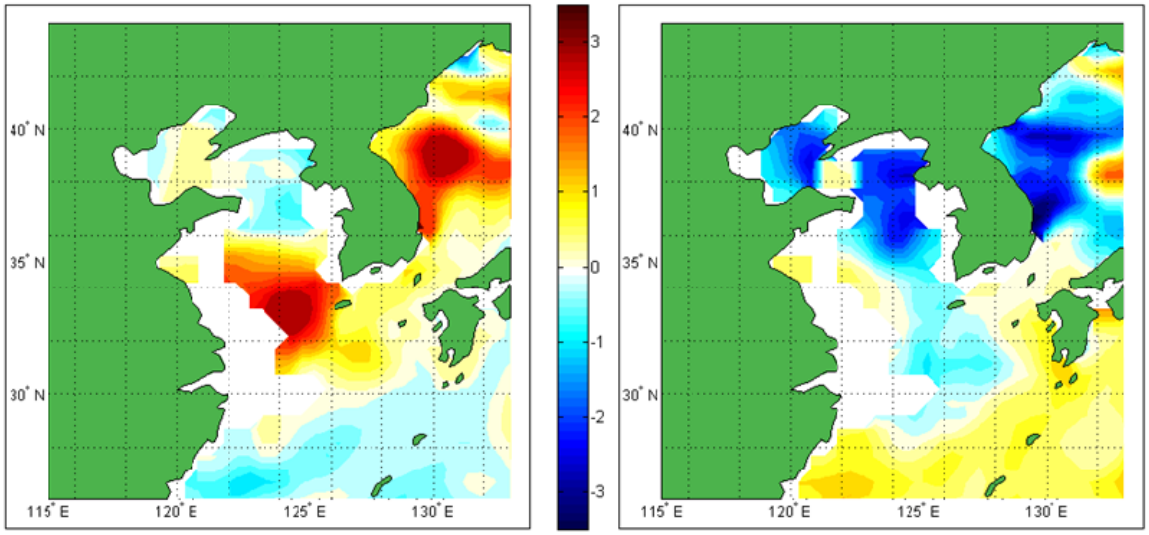

Figure 48. SODA ocean temperature anomalies (deg C) at 45 meters depth for: (left) composites of five highest meridional wind speed Octobers, and (right) five lowest meridional wind speed Octobers. See Chapter II, section B, for details on how these composites were constructed. Grey shading indicates areas in which sea floor depth is 45 meters or less.

North-south vertical cross sections through the Yellow Sea for the high and low wind cases (Figure 49 and Figure 50) support these interpretations. For example, Figure 49 shows: (a) a much deeper thermocline in the high wind case, consistent with greater vertical mixing and an early onset of winter conditions in the high wind case; and (b) a thin warm layer underlain by a well developed cold layer consistent with reduced vertical mixing and a late transition out of summer conditions in the low wind case. The warm anomaly, shown in the top panel of Figure 50, may be due to downwelling. However, the complex interaction of local currents (Figure 51) may also have an effect. According to Tomczak and Godfrey (1994), the Taiwan Warm Current submerges when it flows against the wind during the winter monsoon and is overlapped by the cooler low salinity waters of the China Coastal Current. The cool anomaly is

likely the result of reduced mixing of deeper waters due to decreased wind speed in the low wind composite.

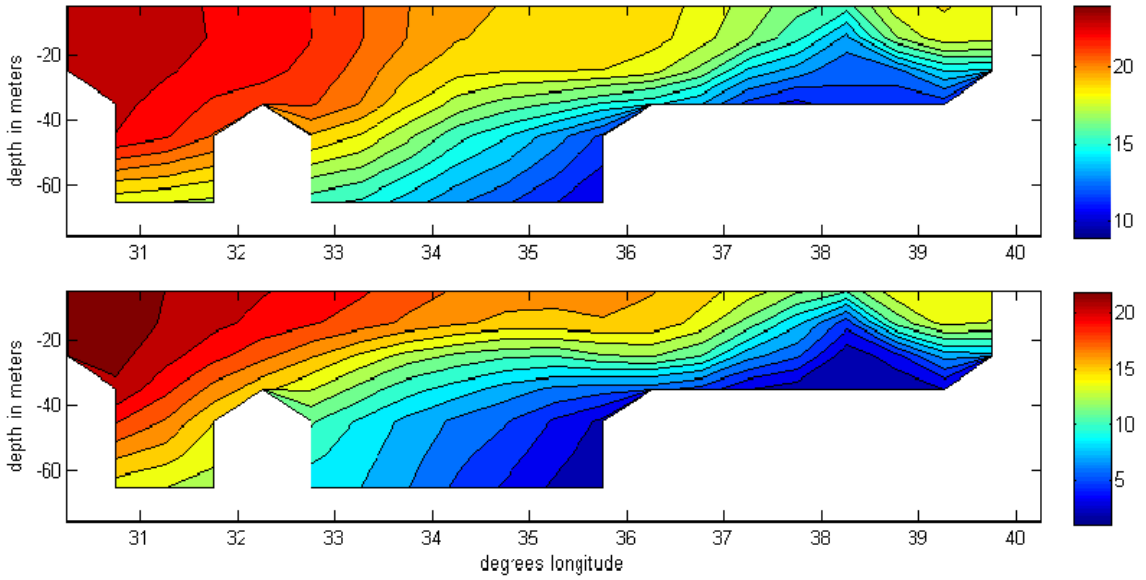

Figure 49. Vertical cross sections (south to north) of SODA ocean temperature (deg. C) versus depth (m) in the Yellow Sea at 124.75E for: (top) composites of five highest meridional wind speed Octobers, and (bottom) five lowest meridional wind speed Octobers. See Chapter II, section B, for details on how these composites were constructed.

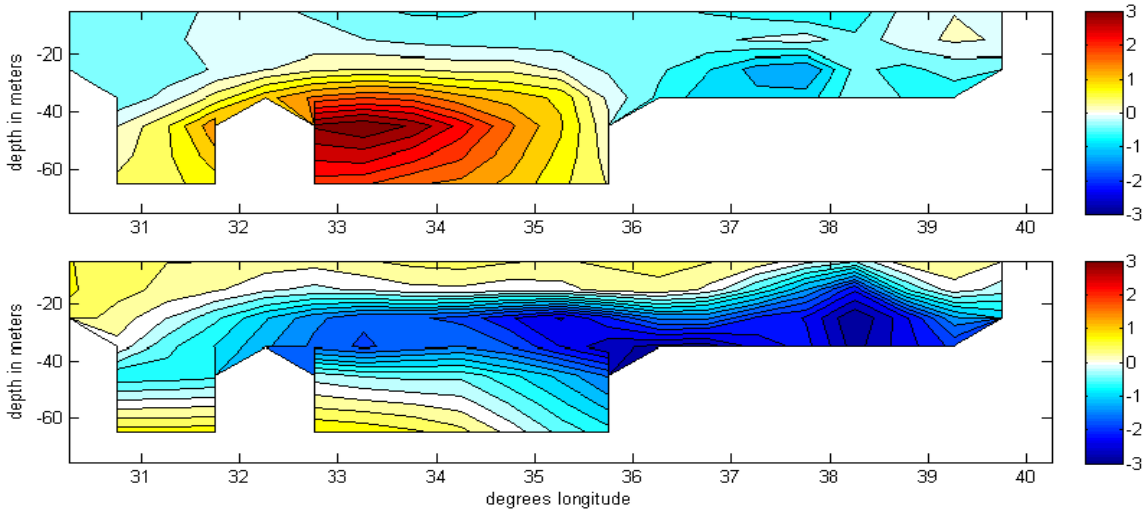

Figure 50. Vertical cross sections (south to north) of SODA ocean temperature anomalies (deg. C) versus depth (m) in the Yellow Sea at 124.75E for: (top) composites of five highest meridional wind speed Octobers, and (bottom) five lowest meridional wind speed Octobers. See Chapter II, section B, for details on how these composites were constructed.

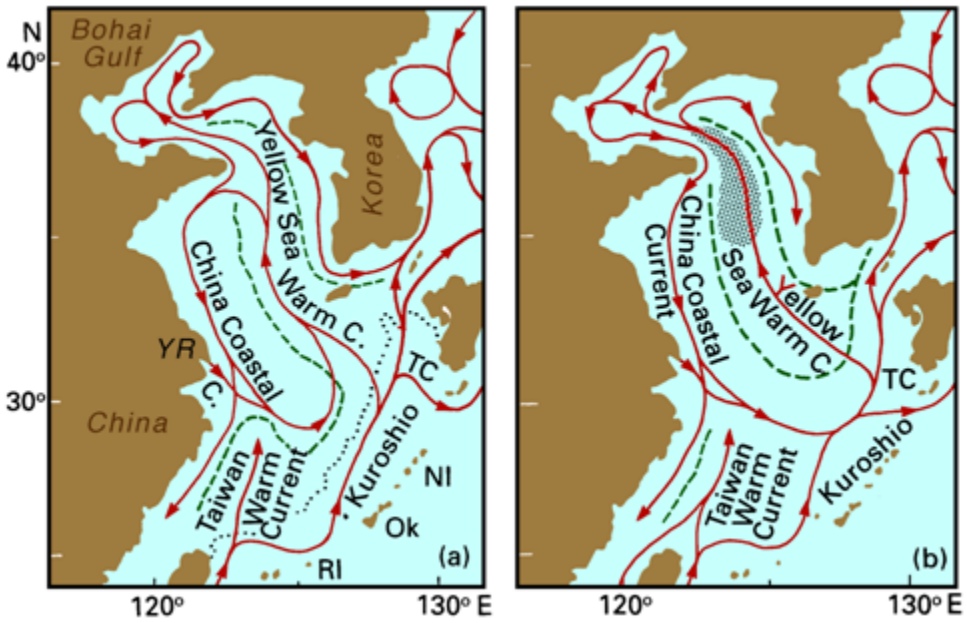

Figure 51. Schematic illustrations of the circulations of the East China and Yellow Seas. (a) During the winter monsoon, (b) during the summer monsoon. TC: Tsushima Current, Ky: Kyushu, NI: Nansei Islands, Ok: Okinawa, RI: Ryukyu Islands, YR: Yangtze River. The shaded area in (b) indicates the region of the Yellow Sea Bottom Cold Water. From Tomczak and Godfrey (1994).

The comparison of temperature, salinity, and sound speed profiles in Figure 51 reveals that the GDEM LTM climatology and the SODA low wind conditional climatology are relatively similar, with little mixing and no surface duct. The high wind conditional climatology has a notable deeper mixed layer and SLD, due to the increased mixing and wind speed. The SODA LTM exhibits a profile that appears to trace the mean of the high and low wind composites in the upper levels, then rapidly becomes cooler than the other profiles at lower levels. This indicates that the ten years of data from the conditional composites does not entirely explain all the variability of the SODA data set, particularly for the lower levels at this location.

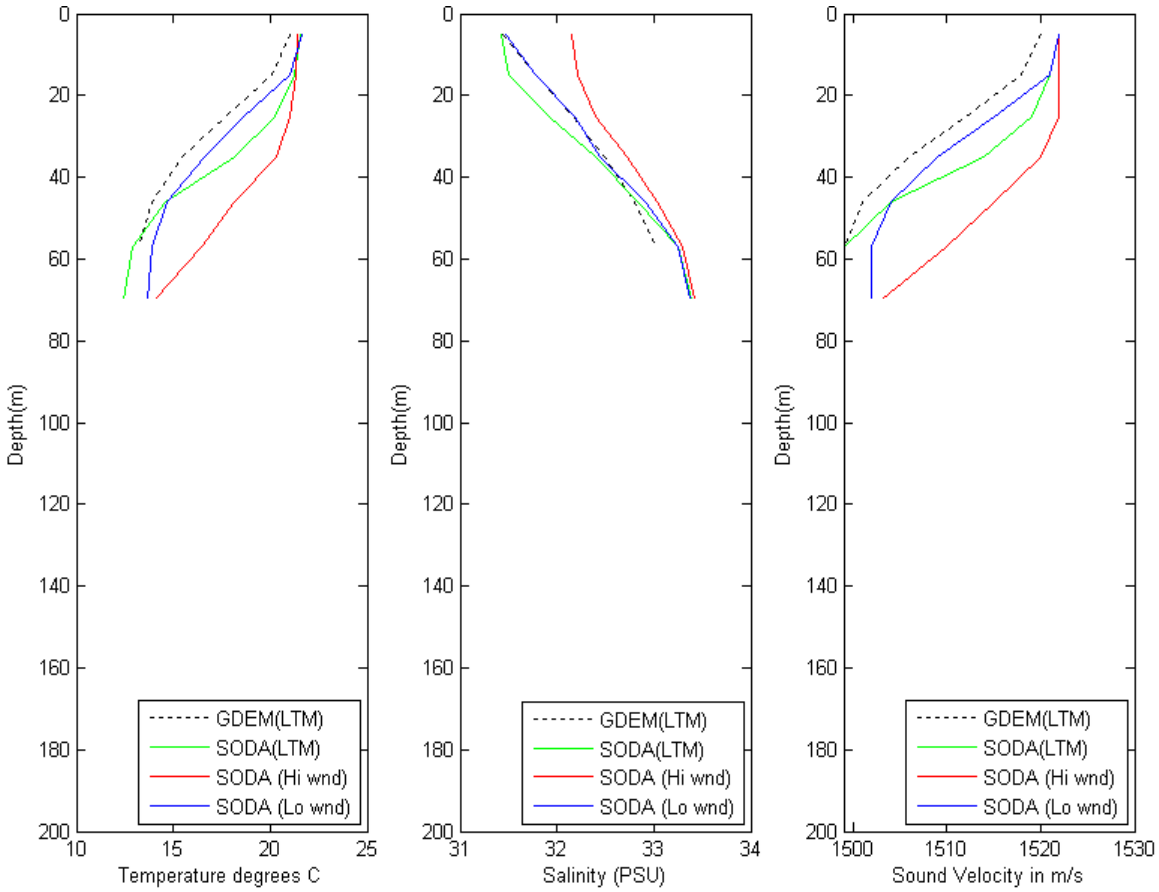

Figure 52. Temperature (left), salinity (center), and sound speed profiles (right) for October in the Yellow Sea at 33.25N 124.25E for: GDEM LTM (black, dashed), SODA LTM (green, solid), SODA conditional climatologies for Octobers of the 5 highest wind speed years (red, solid), and SODA conditional climatologies for Octobers of the 5 lowest wind speed years (blue, solid). Sound speed values were computed using the Nine-term Mackenzie Equation as described in Chapter II, section B, sub-section 7.

c. East China Sea Southwest of Okinawa

The East China Sea has a significant amount of variability in wind speed between the conditional climatologies for high and low wind years, as seen in Figure 21. The Kuroshio also runs through this area (Figure 18), providing additional spatial variability in ocean structure. The most obvious differences between the high and low wind cases are in upper ocean temperatures, which are lower in the high wind case than the low wind case

(Figures 53-56). This is consistent with higher wind speeds causing increased mixing and larger surface heat fluxes out of the ocean, resulting in lower near surface temperatures.

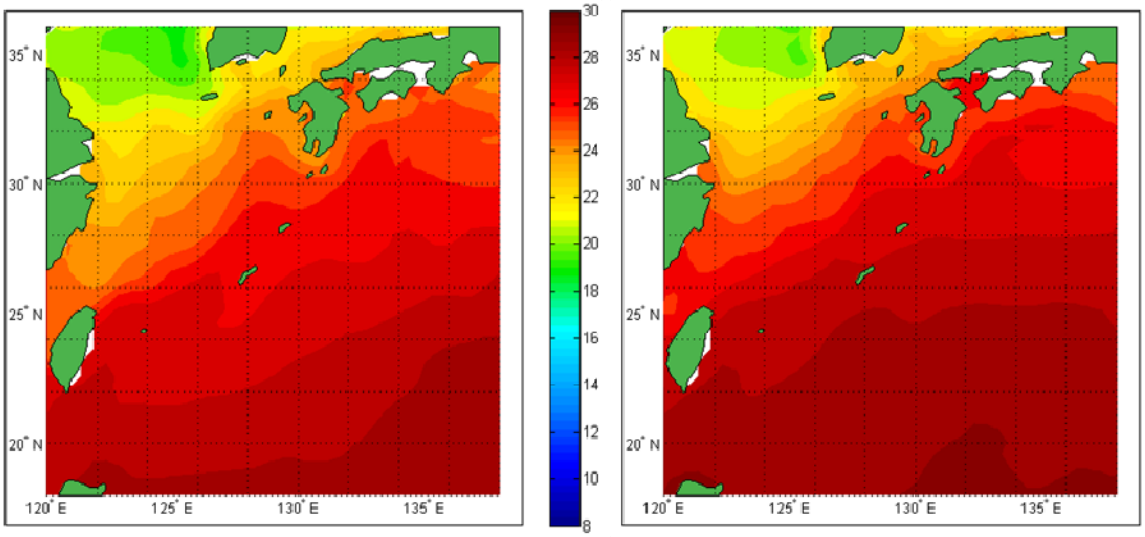

Figure 53. SODA ocean temperatures (deg C) at 5 meters depth for: (left) composites of five highest meridional wind speed Octobers, and (right) five lowest meridional wind speed Octobers. See Chapter II, section B, for details on how these composites were constructed. White shading indicates areas in which sea floor depth is 5 meters or less.

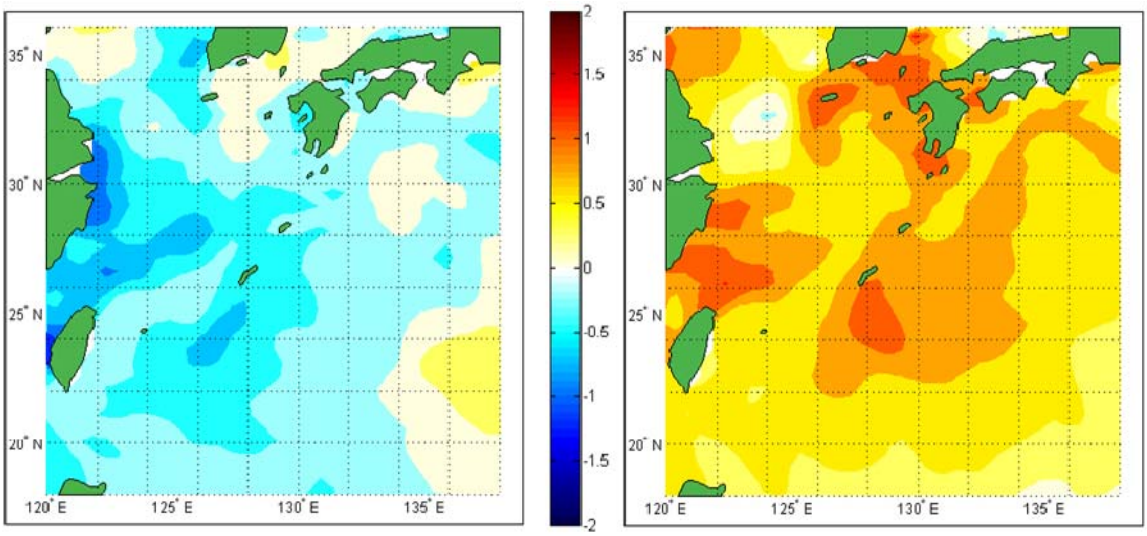

Figure 54. SODA ocean temperature anomalies (deg C) at 5 meters depth for: (left) composites of five highest meridional wind speed Octobers, and (right) five lowest meridional wind speed Octobers. See Chapter II, section B, for details on how these composites were constructed. Grey shading indicates areas in which sea floor depth is 5 meters or less.

The strong surface heat fluxes out of the ocean and strong vertical mixing in the high wind composite creates a nearly isothermal layer in the upper 50 m and a deep thermocline, compared to the low wind case (Figure 55). These deep, nearly isothermal conditions allow for the maximum in sound speed to occur lower in the ocean than in the low wind composite, which has a thin warm surface layer. Therefore, SLDs in this area are deeper in the high wind composite than in the low wind composite as depicted in Figure 55 and Figure 56.

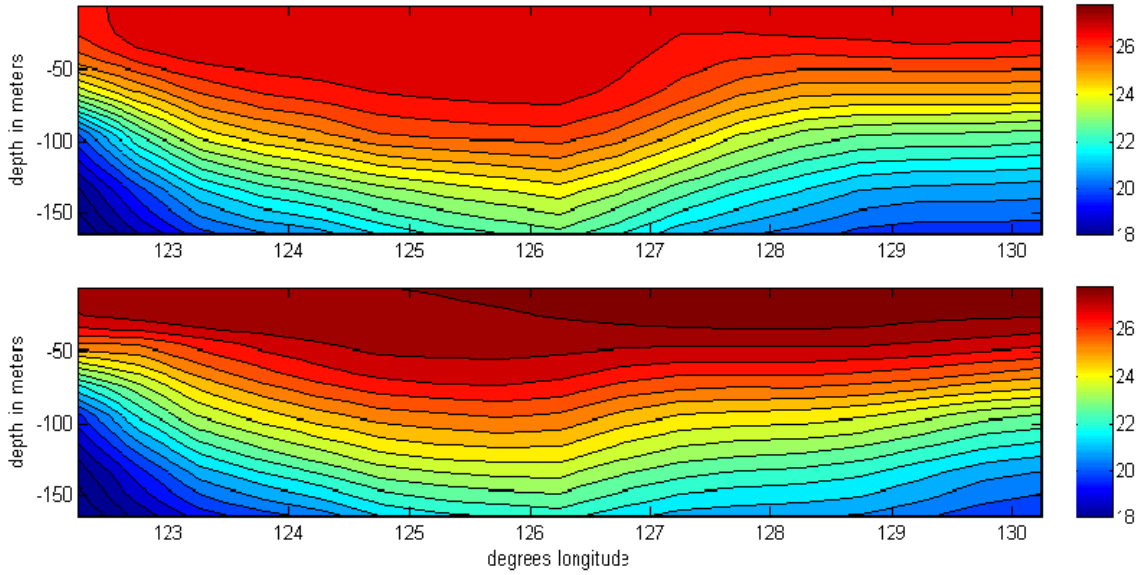

Figure 55. Vertical cross sections (west to east) of SODA ocean temperature (deg. C) versus depth (m) in the East China Sea at 25.25N for: (top) composites of five highest meridional wind speed Octobers, and (bottom) five lowest meridional wind speed Octobers. See Chapter II, section B, for details on how these composites were constructed.

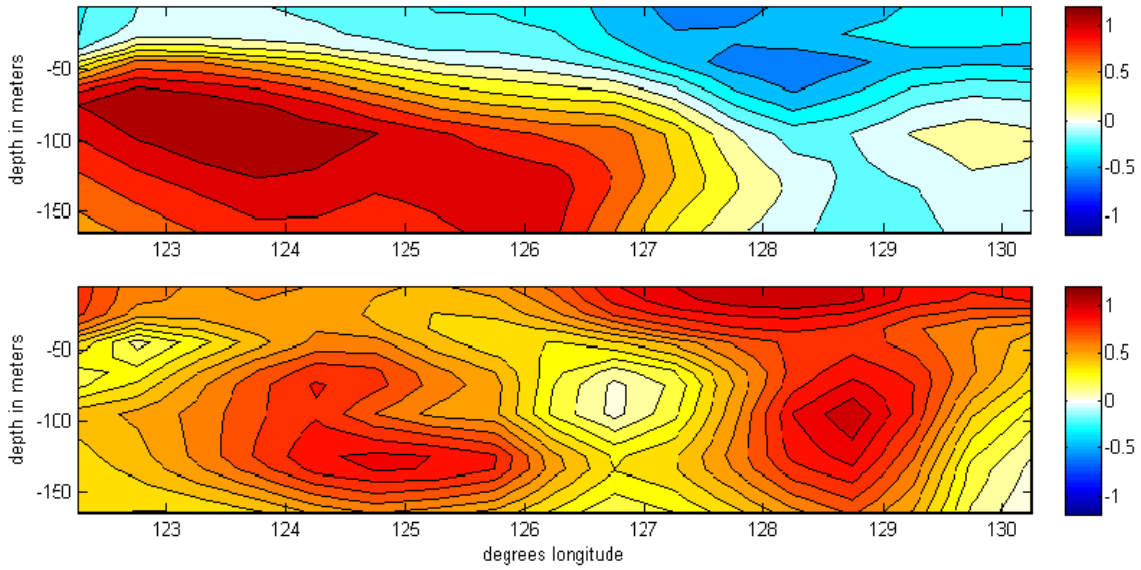

Figure 56. Vertical cross sections (west to east) of SODA ocean temperature anomalies (deg. C) versus depth (m) in the East China Sea at 25.25N for: (top) composites of five highest meridional wind speed Octobers, and (bottom) five lowest meridional wind speed Octobers. See Chapter II, section B, for details on how these composites were constructed.

These differences in ocean temperature and SLD are represented in the temperature and sound speed profiles for this area. Figure 57 illustrates the differences in SLD between the SODA high and low wind composites. Although there is a fair degree of similarity between the temperature and salinity profiles for all the climatologies, the relatively subtle differences in these profiles lead to pronounced differences in SLD (deeper in the high wind case, lower in the low wind case). This supports the concept that surface wind variations can cause relatively small changes in ocean structure that lead to tactically significant differences in SLD and other ocean parameters (e.g., below layer gradient).

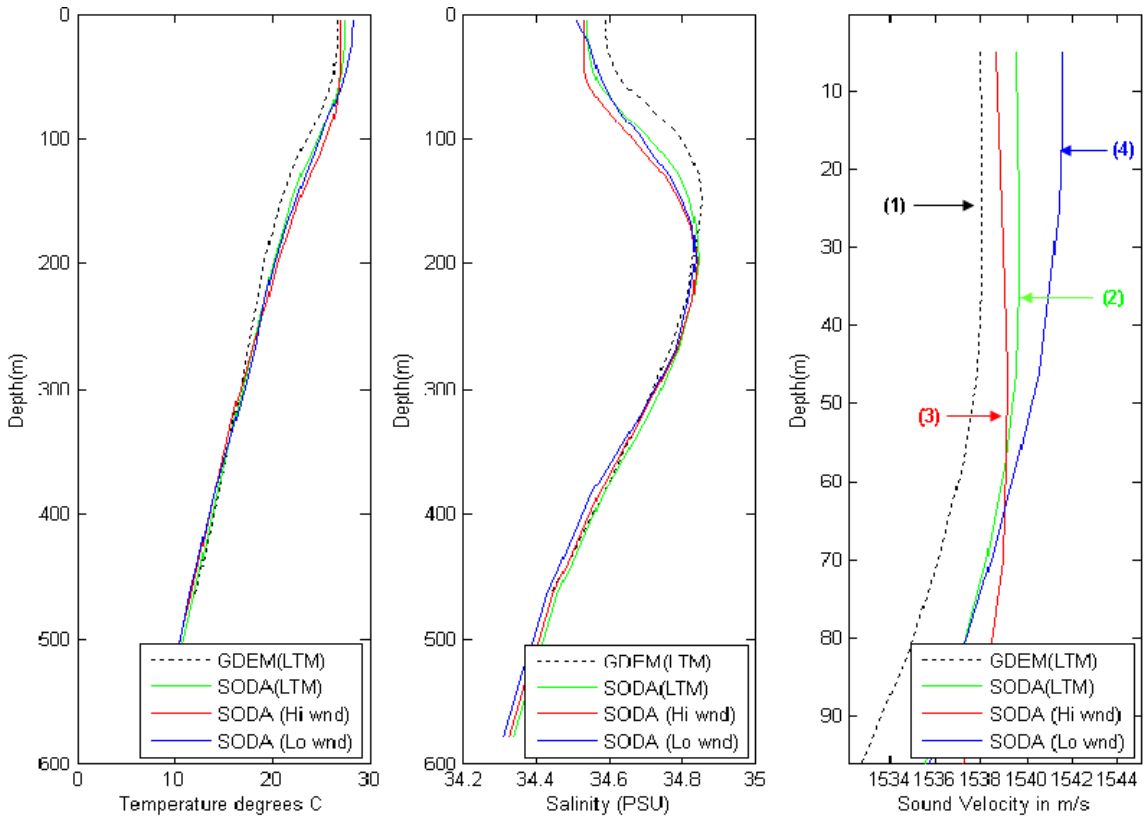

Figure 57. Temperature (left), salinity (center), and sound speed profiles (right) for October in the East China Sea at 25.25N 126.75E for: GDEM LTM (black, dashed), SODA LTM (green, solid), SODA conditional climatologies for Octobers of the 5 highest wind speed years (red, solid), and SODA conditional climatologies for Octobers of the 5 lowest speed wind years (blue, solid). Sonic layer depth for each climatology is indicated by arrows: (1) GDEM LTM, (2) SODA LTM, (3) SODA conditional climatologies for Octobers of the 5 highest wind speed years, and (4) SODA conditional climatologies for Octobers of the 5 lowest wind speed years. Sound speed values were computed using the Nine-term Mackenzie Equation as described in Chapter II, section B, sub-section 7.

d. Taiwan Strait

The geography of the Taiwan Strait causes funneling of winds and constrains the flow of ocean currents. Therefore, we might expect relatively large differences between the high and low wind cases. Such differences in ocean near surface temperature are apparent in Figure 58 and Figure 59. Relatively cool near surface waters occur further southward along the Chinese coast in the high wind composite, with the largest anomalies occurring in and near the Taiwan Strait.

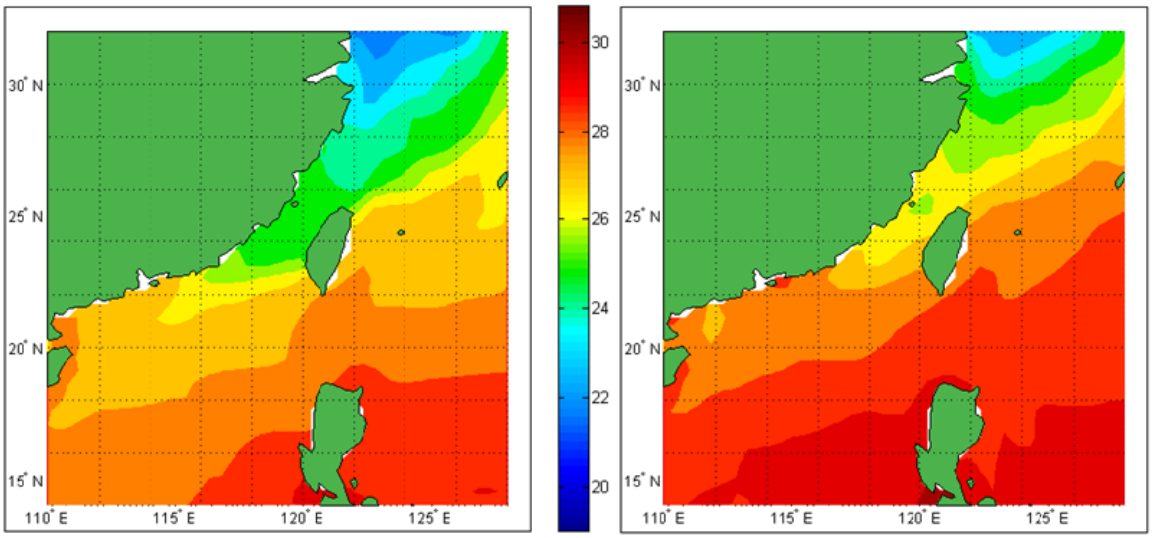

Figure 58. SODA ocean temperatures (deg C) at 5 meters depth for: (left) composites of five highest meridional wind speed Octobers, and (right) five lowest meridional wind speed Octobers. See Chapter II, section B, for details on how these composites were constructed. White shading indicates areas in which sea floor depth is 5 meters or less.

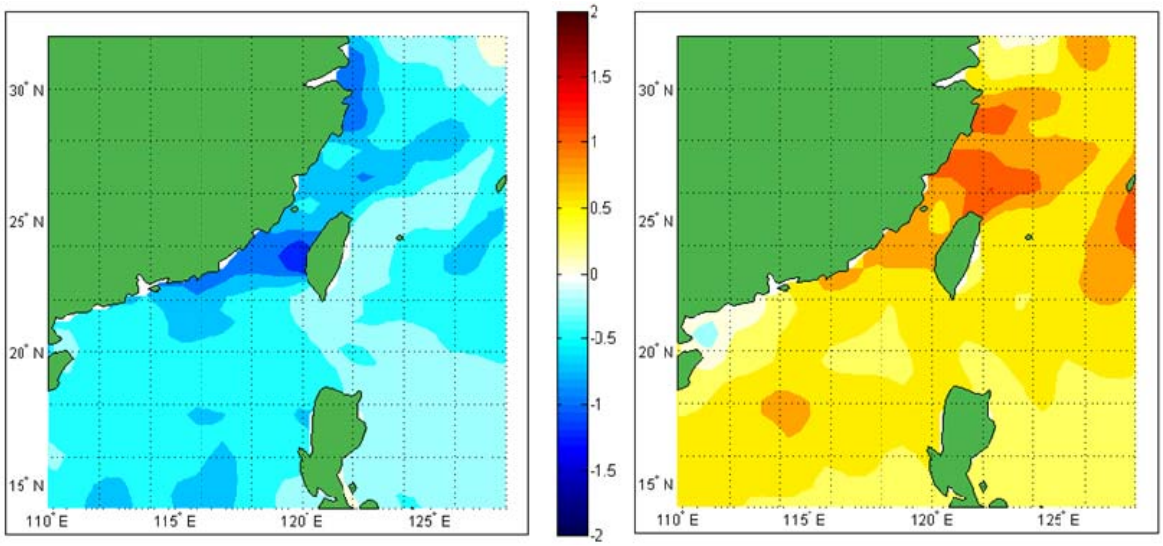

Figure 59. SODA ocean temperature anomalies (deg C) at 5 meters depth for: (left) composites of five highest meridional wind speed Octobers, and (right) five lowest meridional wind speed Octobers. See Chapter II, section B, for details on how these composites were constructed. Grey shading indicates areas in which sea floor depth is 5 meters or less.

The overall patterns in the vertical structure of the Taiwan Strait are similar for the high and low wind conditional climatologies (Figure 60 and Figure 61). However, the temperatures in the high wind case are cooler at all depths, with much stronger vertical gradients (e.g., at 100 m depth), in the high wind composite.

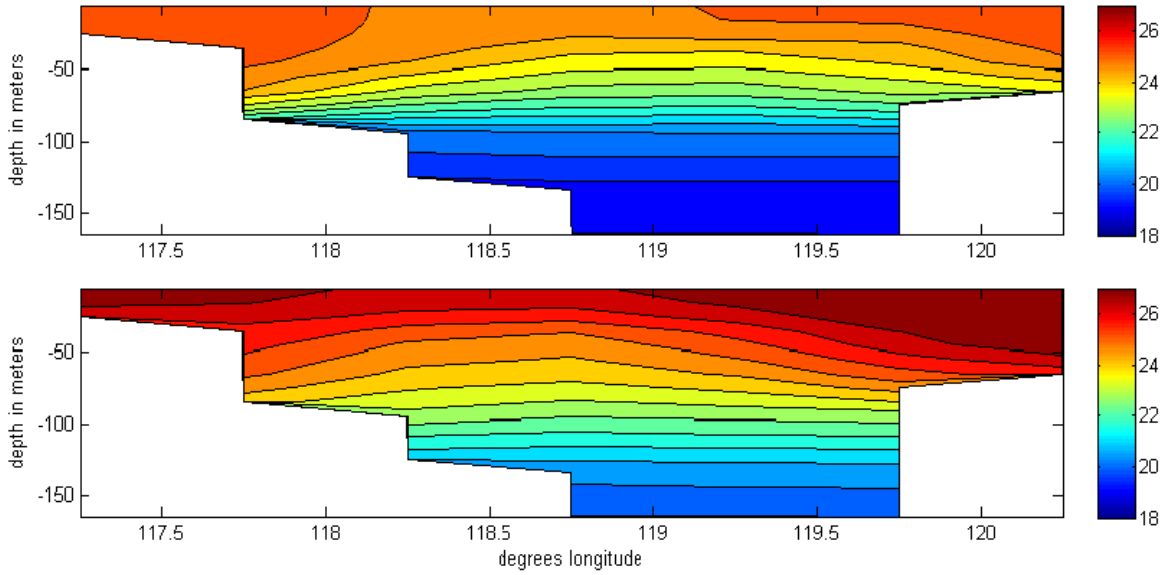

Figure 60. Vertical cross sections (west to east) of SODA ocean temperature (deg. C) versus depth (m) in the Taiwan Strait at 23.75N for: (top) composites of five highest meridional wind speed Octobers, and (bottom) five lowest meridional wind speed Octobers. See Chapter II, section B, for details on how these composites were constructed.

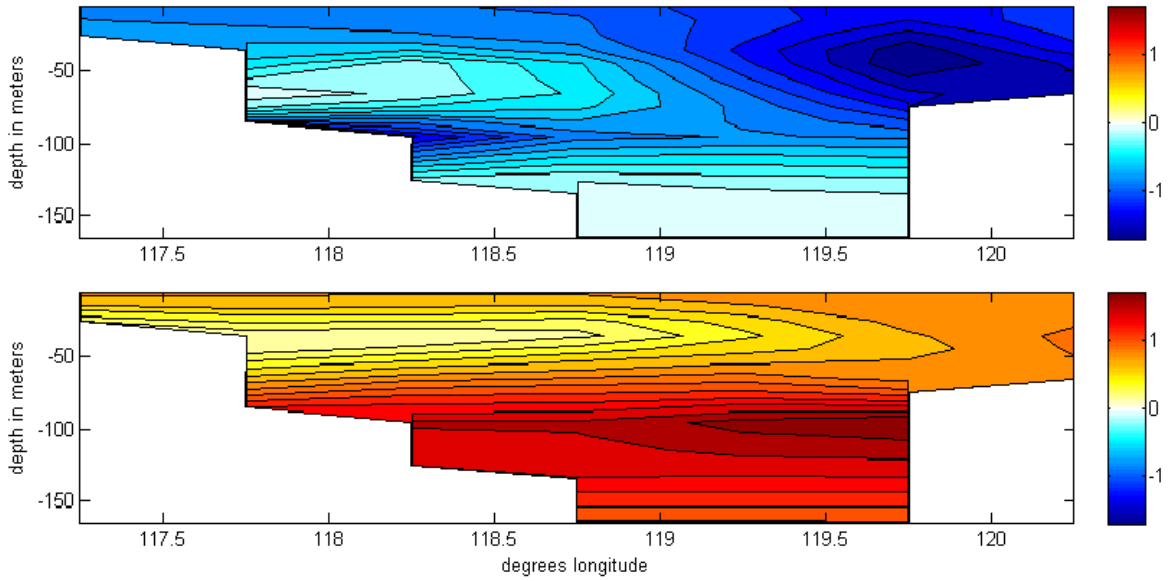

Figure 61. Vertical cross sections (west to east) of SODA ocean temperature anomalies (deg. C) versus depth (m) in the Taiwan Strait at 23.75N for: (top) composites of five highest meridional wind speed Octobers, and (bottom) five lowest meridional wind speed Octobers. See Chapter II, section B, for details on how these composites were constructed.

The similarities in overall vertical structure patterns are also apparent in the temperature, salinity, and sound speed profiles (Figure 62). The temperature, salinity, and sound speed profiles for the SODA LTM climatology and both SODA conditional climatologies all have very similar shapes. However, as expected, the high (low) wind climatology has lower (higher) temperatures and sound speeds than the LTM.

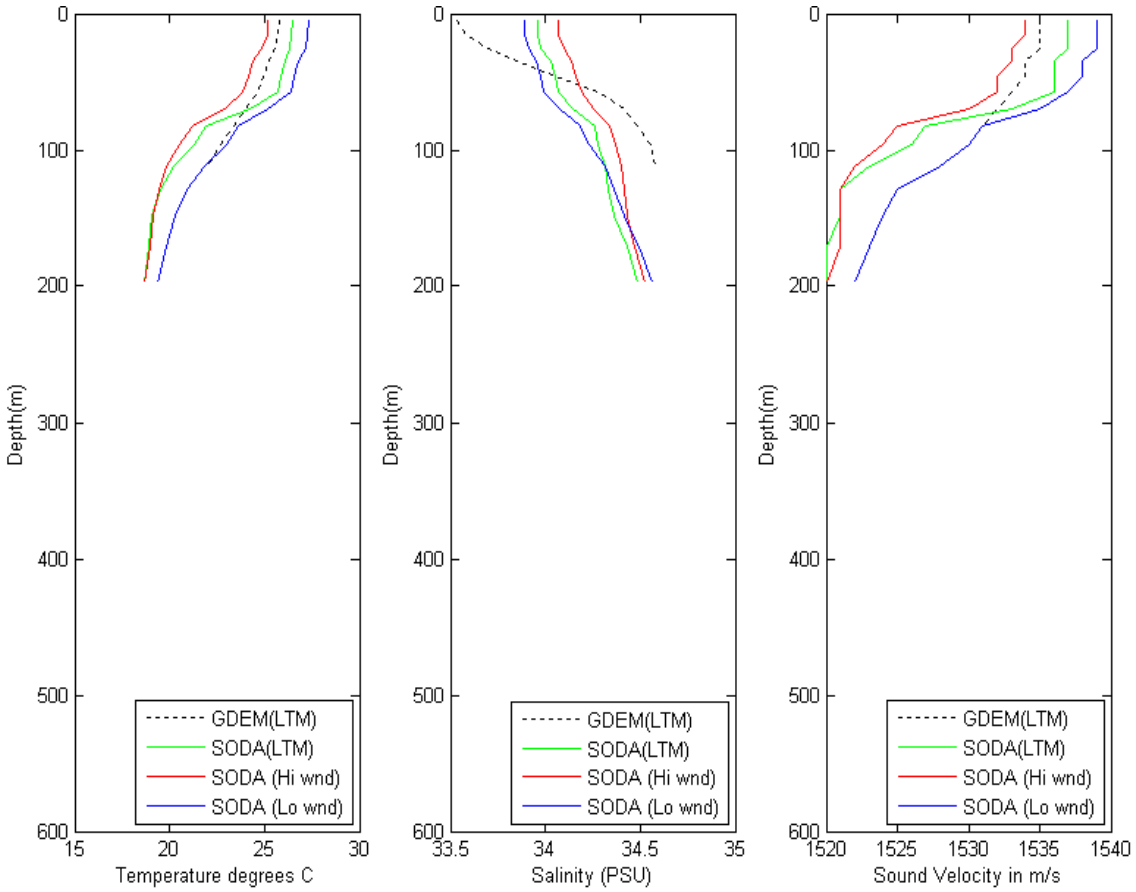

Figure 62. Temperature (left), salinity (center), and sound speed profiles (right) for October in the Taiwan Strait at 23.75N 119.75E for: GDEM LTM (black, dashed), SODA LTM (green, solid), SODA conditional climatologies for Octobers of the 5 highest wind speed years (red, solid), and SODA conditional climatologies for Octobers of the 5 lowest wind speed years (blue, solid). Sound speed values were computed using the Nine-term Mackenzie Equation as described in Chapter II, section B, sub-section 7.

e. South China Sea

Figure 63 shows the temperature at 130 m for the high and low wind composites. Note the generally lower temperatures in the high wind case, with the notable exception of the region to the south and west of Hainan where the high wind composite temperatures are higher than in the low wind composite. These differences are especially apparent in the temperature anomalies at 130 m (Figure 64).

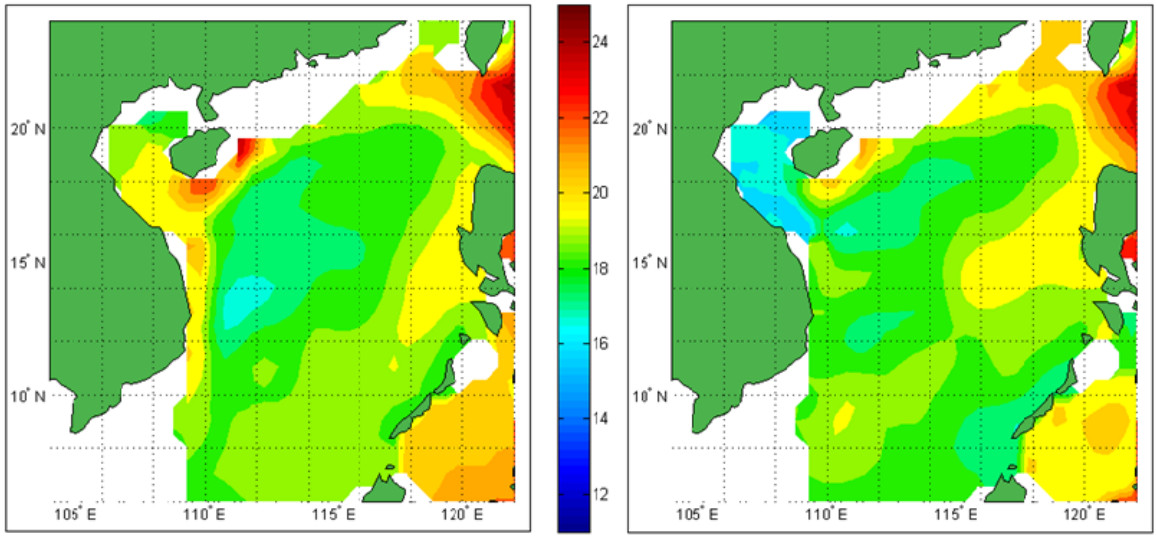

Figure 63. SODA ocean temperatures (deg C) at 130 meters depth for: (left) composites of five highest meridional wind speed Octobers, and (right) five lowest meridional wind speed Octobers. See Chapter II, section B, for details on how these composites were constructed. White shading indicates areas in which sea floor depth is 130 meters or less.

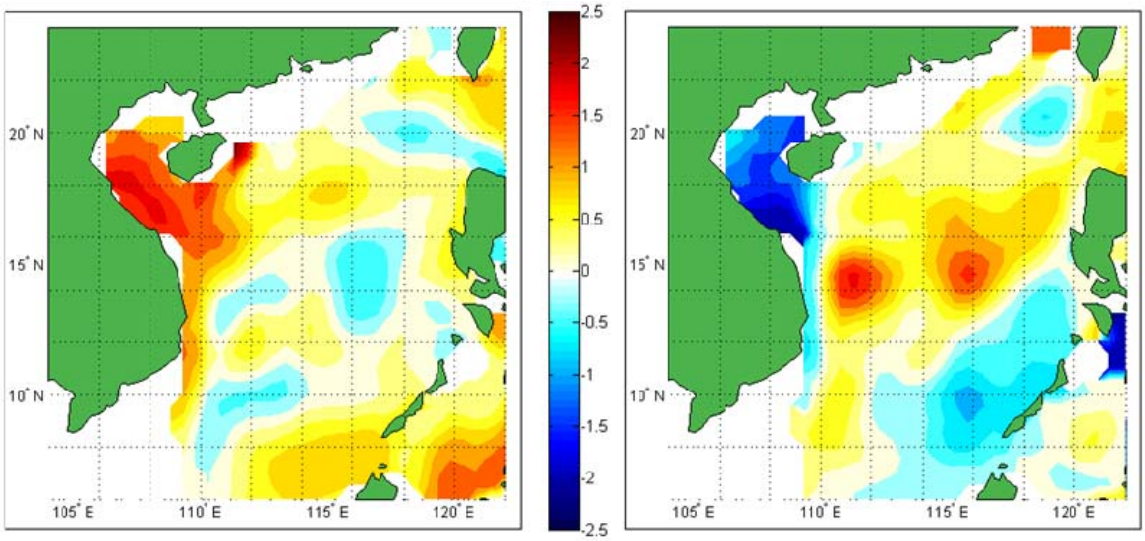

Figure 64. SODA ocean temperature anomalies (deg C) at 130 meters depth for: (left) composites of five highest meridional wind speed Octobers, and (right) five lowest meridional wind speed Octobers. See Chapter II, section B, for details on how these composites were constructed. Grey shading indicates areas in which sea floor depth is 130 meters or less.

The west to east vertical cross sections of temperature for the high and low wind composites (Figure 65), show that in the high wind composite there is a cooler, deeper, and more well mixed surface layer than in the low wind composite. Warmer waters also appear to extend deeper in the high wind composite. One possible explanation for these differences is that — in addition to the impacts of the wind differences on surface heat fluxes and upper ocean mixing — the wind differences may also lead to differences in Ekman transports that then alter the deeper temperatures. For example, along the east coast of Hainan and in the Gulf of Tonkin, the high winds may induce costal downwelling and the subsidence of relatively warm surface water. This would be consistent with the negative (positive) temperature anomalies above (below) 50 m in these locations. Such temporal variability in atmospheric forcing and oceanic responses to that forcing will, of course, not be discernible in LTM ocean climatologies, such as GDEM.

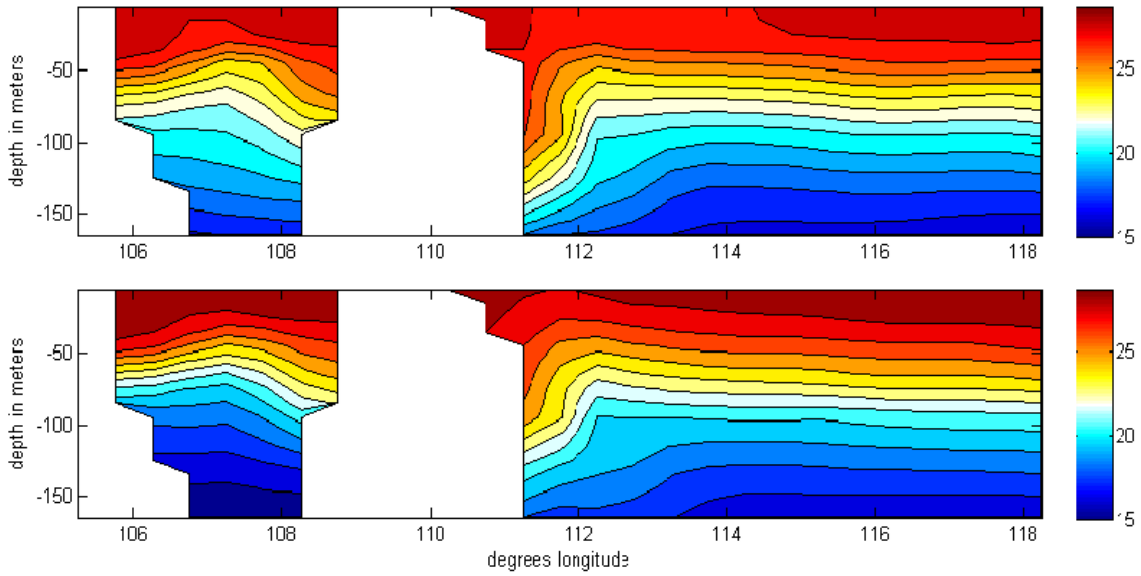

Figure 65. Vertical cross sections (west to east) of SODA ocean temperature (deg. C) versus depth (m) in the South China Sea at 19.75N for: (top) composites of five highest meridional wind speed Octobers, and (bottom) five lowest meridional wind speed Octobers. See Chapter II, section B, for details on how these composites were constructed.

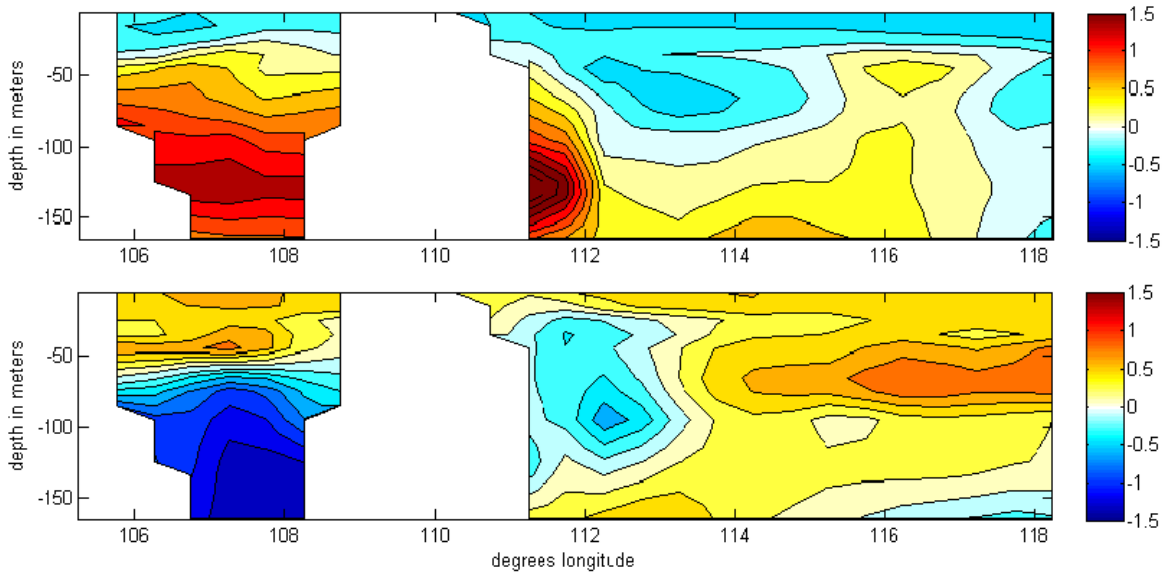

Figure 66. Vertical cross sections (west to east) of SODA ocean temperature anomalies (deg. C) versus depth (m) in the South China Sea at 19.75N for: (top) composites of five highest meridional wind speed Octobers, and (bottom) five lowest meridional wind speed Octobers. See Chapter II, section B, for details on how these composites were constructed.

The temperature, salinity, and sound speed profiles shown in Figure 67 depict the similarities (differences) in the SODA conditional climatologies in the upper (lower) levels. The high wind composite sound speed profile is more nearly neutral than the other profiles. This is due to the cooling in the upper layer and warming in the lower layer shown in Figures 65-66. It is interesting to note that the GDEM profiles do not resemble any of the SODA profiles in this case. The GDEM profiles are also highly smoothed curves, whereas the SODA profiles have some pronounced irregularities. Note too that the SODA LTM and the SODA low wind composite profiles are very similar, while the high wind composite is quite different. This is additional evidence for the idea that the high and low wind composite represent only a part of the October variability in this region.

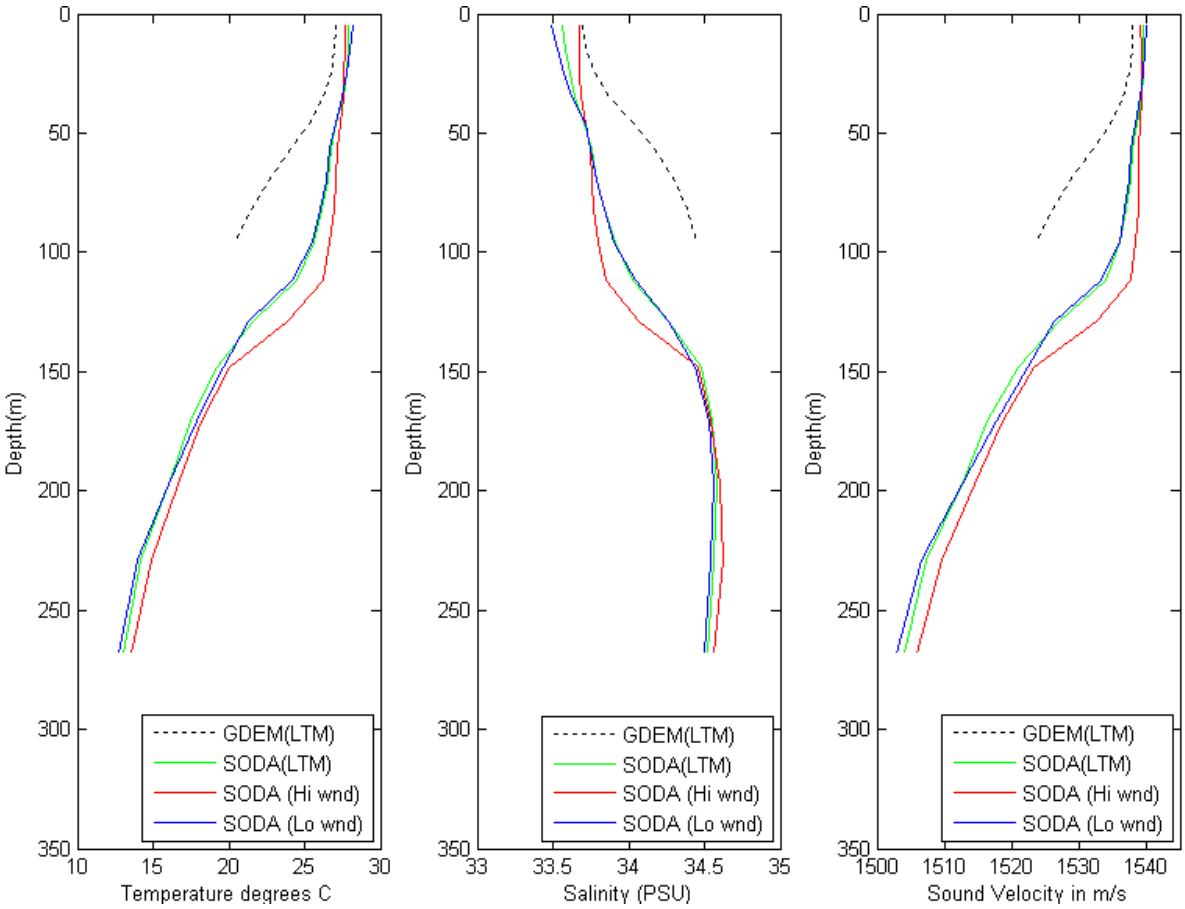

Figure 67. Temperature (left), salinity (center), and sound speed profiles (right) for October in the South China Sea at 19.25N 111.25E for: GDEM LTM (black, dashed), SODA LTM (green, solid), SODA conditional climatologies for Octobers of the 5 highest wind speed years (red, solid), and SODA conditional climatologies for Octobers of the 5 lowest wind speed years (blue, solid). Sound speed values were computed using the Nine-term Mackenzie Equation as described in Chapter II, section B, sub-section 7.

IV. CONCLUSIONS AND RECOMMENDATIONS

A. SUMMARY OF KEY RESULTS

In this study, we compared a traditional LTM ocean climatology with a prototype smart ocean climatology and assessed the tactical significance in undersea warfare of the differences between these two types of climatologies. GDEM was the LTM climatology used in our study and is currently employed in TDAs used by the U.S. Navy. The SODA ocean re-analysis was used to construct both: (a) a LTM climatology for direct comparison with GDEM; and (b) conditional climatologies based on variations in wind forcing of the upper ocean. to assess the ability of smart climatology to provide more realistic representations of the ocean environment than those available from LTMs.

Our initial comparisons identified that many general similarities exist between the GDEM and SODA LTM climatologies. However, many differences also exist. GDEM proved to be generally cooler in the near surface levels of the ocean for our area of interest. Bull's eye patterns were evident in maps of GDEM temperature and sonic layer depth (SLD), which we attribute to the interpolation scheme used in GDEM.

Comparisons between the high and low wind conditional climatologies indicated that SODA is capable of producing realistic responses to wind forcing variations, and that these responses lead to tactically significant sound speed variations. Large temperature differences exist between the two composites and between the composites and SODA LTM values. These differences occurred over most of the western North Pacific, including in areas of interest for US Navy operations. These temperature differences were very consistent with the changes in surface heat fluxes, vertical mixing, and Ekman transport that would be expected from the wind variations represented by the composites.

One of the goals of this study was to determine if differences between the LTM climatology and smart climatology were tactically significant. The propagation loss graphics and range predictions produced in PC-IMAT show that even small changes in the shape of sound speed profiles, including changes to SLD, could have significant impacts on sound propagation and sonar sensor performance. For example, propagation paths that occurred when using one LTM climatology were often absent when using the other LTM climatology. These propagation differences often involved clear differences in sonic layer depth, but often also involved relatively subtle differences in the shapes of sound speed profiles. Our acoustic propagation results are contained in a classified appendix to this thesis.

B. CONCLUSIONS

The numerous examples of large differences between GDEM and SODA LTMs, and the physically realistic depictions of LTM conditions by SODA LTMs, and of ocean variability by the SODA conditional climatologies, indicate that SODA is a very viable alternative to GDEM.

The consistent differences between the high and low wind composite climatologies, and their clear relationships to known dynamical processes in indicate that well designed conditional climatologies are capable of capturing tactically significant variations in the ocean. Our results indicate that the use of a smart climatology process, including the use of state-of-the-science data sets and methods, can provide characterizations of the ocean that are physically reasonable and representative of ocean variability that cannot be captured by existing Navy climatology data sets and methods.

Smart climatology provides an additional advantage over long-term mean climatologies by providing the ability to forecast the future environment and assess environmental probabilities and uncertainties. Previous studies (Hanson, 2007; Moss, 2007; LaJoie, 2006; Vorhees, 2006) have proven the capability of smart climatology to provide long-range outlooks of atmospheric variables.

Using smart climatology to create such long-range forecasts of the ocean environment would provide a competitive advantage to war fighters in undersea warfare.

This study was created without the expenditure of funds for material, data, or travel. The latest state-of-the-science civilian oceanic and atmospheric re-analysis data sets were not only acquired free of charge but were also available open source via down loads from the World Wide Web. Commercial off-the-shelf software was used for processing and graphical representation of the data. Most importantly, the skills required for processing and analyzing the data were acquired through the METOC curriculum at NPS. These facts illustrate the availability and accessibility intrinsic to smart climatology, and are line with the concept of efficiently providing the capabilities of Battlespace on Demand (Titley, 2008).

C. RECOMMENDATIONS

Based on the results and conclusions of this study, it is evident that smart climatology can provide an immediate means of improving long lead descriptions of the ocean environment that have a multitude of military applications. Therefore, we recommend the following actions by the Naval Oceanography Program:

1) Operationalize long lead-time ocean environmental outlooks, by applying the NPS smart climatology process, including the use of state-of-the-science, civilian, oceanic and atmospheric re-analysis data sets.

2) Create and institute education and training on smart ocean climatology. A good model for this training is the online training program initiated by the National Weather Service for creating local climate products. Additional training can be leveraged from the NPS Smart Climatology website, the NPS climatology courses, and the MetEd website.

3) Educate and sell customers on the capabilities and advantages of smart ocean climatology using real world case studies and examples.

4) Create a multi-faceted approach to environmental information dominance supported by smart climatology. By bringing together smart climatology forecasts of the ocean environment, weather, radar range/evaporative duct heights, and ambient noise, a complete environmental picture can be created that enables planning and decision making.

D. FUTURE RESEARCH

This study explored the feasibility of applying the NPS smart climatology process to the ocean. The results indicate that smart climatology process can indeed improve upon traditional long-term mean ocean climatologies. However, more research would help to refine the process and potentially improve application of the results.

The SODA high and low wind composites of smart ocean climatology represented the wind related variations in ocean temperature quite well, however variability of the near surface layers is harder to predict due to shorter time scale forcing, such as diurnal effects. The issue of near surface variability is apparent in the study by Heidt (2008), where we can see that the MBARI buoy temperature profiles sometimes have abrupt changes in the upper 50 meters that are not represented well in SODA. Below 50 meters, the profiles are very similar, although sometimes offset. Further research into how environmental variables and physical processes impact the near surface layers, may lead to greater predictability of upper ocean temperature profiles. Research could focus on how atmospheric variables such as wind, atmospheric temperature, OLR, and precipitation affect these profiles. In addition, the impacts of atmospheric factors that affect ambient noise should be investigated from a smart climatology perspective (e.g., a smart climatology study similar to ours that focuses on the impacts of wind and precipitation on ocean ambient noise).

The construction of propagation loss graphics and range predictions in PC-IMAT was a time consuming process that required sound speed profiles for each location to be individually entered by hand through the XBT application.

The ocean at each station was assumed to be horizontally homogeneous, as entering a large number of profiles was prohibitively time consuming. A solution would be to convert SODA data to the MODAS-lite format and import the data via the MODAS-lite input interface. This would allow users to create an environment within PC-IMAT with horizontal variability in temperature, salinity, and sound speed. Additionally, this capability would allow the creation of acoustic performance surfaces based on SODA data.

A comparison of the SODA and GDEM LTM, and SODA conditional climatologies to in situ observations for a variety of locations and seasons would be helpful in determining whether climatological variability shown in these data sets reliably represents real world climate variability. Research in this area may also help identify weaknesses in each climatology that might be improved or mitigated.

Finally, strong coordination and collaboration between the climate research and development community (e.g., Naval Postgraduate School) and METOC support centers (e.g., Naval Oceanographic Office) should be developed to allow optimal transitioning of research results to operational use.

THIS PAGE INTENTIONALLY LEFT BLANK

APPENDIX CLIMATOLOGICAL ACOUSTIC PROPAGATION LOSSES

Note: The contents of this appendix are CLASSIFIED. A copy of this appendix is located in the Dudley Knox Library, at the Naval Postgraduate School, Monterey, CA. Requests for this document must be referred to President, Code 261, Naval Postgraduate School, Monterey, CA 93943-5000.

THIS PAGE INTENTIONALLY LEFT BLANK

LIST OF REFERENCES

Carnes, M. R., 2003: Description and Evaluation of GDEM-V 3.0, OAML CIDREP review, 24 pp.

Carton, J.A., and B. Giese, 2008: A Re-analysis of ocean climate using Simple Ocean Data Assimilation. Mon. Weather Rev., **136,** 2999–3017.

___, G. Chepurin, X. Cao, and B. Giese, 2000a: A Simple Ocean Data Assimilation analysis of the global upper ocean 1950–95. Part I: Methodology. J. Phys. Oceanogr., **30,** 294–309.

___, G. Chepurin, and X. Cao, 2000b: A Simple Ocean Data Assimilation Analysis of the global upper ocean 1950–95. Part II: Results. J. Phys. Oceanogr., **30,** 311–326.

Chen, C-T. , and Millero, F.J., 1977: Speed of sound in seawater at high pressures. J. Acoust. Soc. Am. **62(5),** 1129-1135.

CPC, cited 2008: Climate glossary. [Available online at http://www.cpc.ncep.noaa.gov/products/outreach/glossary.shtml.]

CCSP. cited 2008: Climate glossary. [Available online at http://www.climatescience.gov/Library/sap/sap1-3/public-review-draft/sap1-3-prd-glossary.pdf.]

Daubin, S. C., Hashimoto, E.,1981: Comparison of Observed Data and GDEM/standard Ocean Data. part 1. Vertical Temperature, Salinity, and Sound Speed Profiles at Six Selected Site Locations in the Mediterranean sea. NORDA tech. note ADA121468, 129 pp.

Del Grosso, V.A., 1974: New equation for the speed of sound in natural waters (with comparisons to other equations). J. Acoust. Soc. Am **56(4),** 1084-1091.

ENSEMBLES, cited 2008: Ocean re-analysis within the European ENSEMBLES project. [Available online at http://www.clivar.org/organization/gsop/synthesis/mit/talks/weaver_ensembles.ppt#343,1,Ocean Re-analysis within the European ENSEMBLES project.]

Feldmeier, J., 2005: Climatic variations of the California Current System: application of smart climatology to the coastal ocean. M.S. thesis, Naval Postgraduate School, 168 pp.

Ford, B., 2000: El Nino and La Nina Events, and tropical cyclones: impacts and mechanisms. M.S. thesis, Department of Meteorology, Naval Postgraduate School, 120 pp.

Gove, D. A., 2008: Naval Oceanography 2025. Naval oceanography program future vision.

Hanson, C. M., 2007: Long-range operational military forecasts for Iraq. M.S. thesis, Department of Meteorology, Naval Postgraduate School, 77 pp.

Heidt, S., 2008: A Comparison of MBARI II Buoy Temperature and Salinity Measurements to SODA and GDEM Climatology. Report prepared for Operational Oceanography course, Department of Oceanography, Naval Postgraduate School, 34 pp. [Available online at http://met.nps.edu/smart-climo/reports.php]

JPL, California Institute of Technology, cited 2008: Spaceship-to-Shore: Society Benefits from Ocean Altimetry Data. [Available online at http://sealevel.jpl.nasa.gov/science/soc-benefits.html.]

Kalnay, E., M. Kanamitsu, R. Kistler, W. Collins, D. Deaven, L. Gandin, M. Iredell, S. Saha, G. White, J. Woollen, Y. Zhu, M. Chelliah, W. Ebisuzaki, W. Higgins, J. Janowiak, K. C. Mo, C. Ropelewski, J. Wang, A. Leetmaa, R. Reynolds, R. Jenne, and D. Joseph, 1996: The NCEP/NCAR 40-year re-analysis project. *Bull. Am. Meteorol. Soc.,* **77**, 437-471.

Kistler, R., and Co-authors, 2001: The NCEP/NCAR 50-year reanalysis: monthly means CD-ROM and documentation. *Bull. Amer. Meteor. Soc.*, **82**, 247-267.

LaJoie, M., 2006: The impact of climate variations on military operations in the Horn of Africa. M.S. thesis, Dept. of Meteorology, Naval Postgraduate School, 153 pp.

Levitus, S., 1982: Climatological Atlas of the World Ocean, *NOAA Prof. Pap.*, 13, U.S. Govt. Printing Office, Washington, D.C., 173 pp.

Levitus, S., and Boyer, T. 1994: Temperature. Vol. 4, World Ocean Atlas 1994, NOAA Atlas NESDIS 4, 150 pp.

Lozier, M. S., Owens, W. B., and Curry, R. G. 1995: The climatology of the North Atlantic, Progress in Oceanography **36**, 1–44.

Mathworks, 2005: MATLAB 7.1, The MathWorks, Inc.

Mackenzie, K. V., 1981: Nine-term equation for the sound speed in the oceans. J. Acoust. Soc. Am. **70(3),** 807-812.

Montgomery, C., LCDR, USN, 2008. Climate variations in tropical West Africa and their implications for military planners. M.S. thesis, Dept. of Meteorology, Naval Postgraduate School, 89 pp.

Moss, S. M., 2007: Long-range operational military forecasts for Afghanistan. M.S. thesis, Department of Meteorology, Naval Postgraduate School, 99 pp.

Murphree, T., 2008: Naval Smart Climatology: Data, Methods, Products, and Operational Implementation. Smart Climatology Meeting, FNMOC, Monterey, CA, 105 pp.

_____ and Ford, B. W., 2007, Smart Climatology for ASW: Initial Assessments and Recommendations. Department of Meteorology, Naval Postgraduate School, Monterey, CA, 88 pp. Available at: http://met.nps.edu/smart-climo/ reports.php (accessed Sep 2008).

NAVO, 2003: Database Description for the Generalized Digital Environmental Model (GDEM-V) (U) Version 3.0, Oceanographic Databases Division, Naval Oceanographic Office, 39 pp.

Teague, W. J., Carron, M. J., & Hogan, P. J. 1990: A comparison between the generalized digital environmental model and Levitus climatologies. *J. Geophys. Res.*, **95(C5),** 7167-7183.

Titley, D. W., 2008: Battlespace on Demand, Commander's Intent. CNMOC, Stennis Space Center, MS, 14 pp.

Tomczak, M., and Godfrey, J. S., 1994: *Regional Oceanography: an Introduction.* Pergamon, 422 pp. [Available online at http://gyre.umeoce.maine.edu/physicalocean/Tomczak/regoc/index.html.]

Vorhees, D., Capt, USAF, 2006: The impacts of global scale climate variations on Southwest Asia. M.S. thesis, Naval Postgraduate School, 175 pp.

THIS PAGE INTENTIONALLY LEFT BLANK

INITIAL DISTRIBUTION LIST

1. Defense Technical Information Center
   Ft. Belvoir, Virginia

2. Dudley Knox Library
   Naval Postgraduate School
   Monterey, California

3. Dr. Tom Murphree
   Naval Postgraduate School
   Monterey, California

4. CAPT Robert Kiser
   Naval Oceanography Operations Command
   Stennis Space Center, Mississippi

5. CAPT James Berdeguez
   Naval Oceanographic Office
   Stennis Space Center, Mississippi

6. CDR Rebecca Stone
   Naval Postgraduate School
   Monterey, California

7. CDR Tony A Miller
   Naval Oceanography ASW Center
   Stennis Space Center, Mississippi

8. CDR Eric Trehubenko
   Naval Oceanography ASW Center
   Yokosuka, Japan

9. LT Tim Campo
   Naval Oceanography Operations Command
   Stennis Space Center, Mississippi